5-1-2013

Regulation of hydraulic function and consequences for drought-related mortality in mature woody plants

Jennifer Plaut

Jennifer A. Plaut
Candidate

Biology
Department

This dissertation is approved, and it is acceptable in quality and form for publication:

Approved by the Dissertation Committee:

William T. Pockman , Chairperson

Marcy E. Litvak

Nathan G. McDowell

John S. Sperry

REGULATION OF HYDRAULIC FUNCTION AND CONSEQUENCES FOR DROUGHT-RELATED MORTALITY IN MATURE WOODY PLANTS

by

JENNIFER ABBETT PLAUT

Sc.B., Environmental Science, Brown University, 2002

DISSERTATION

Submitted in Partial Fulfillment of the
Requirements for the Degree of

Doctor of Philosophy
Biology

The University of New Mexico
Albuquerque, New Mexico

May 2013

ACKNOWLEDGEMENTS

I am enormously grateful to everyone who has supported an encouraged me during this journey. Will Pockman was always patient with my time frames and calm when I was panicking. He probably deleted a quarter of the text I generated in graduate school, and my writing is the better for it. He also taught me the value of backing up from the immediate question to take in the larger significance and wider possibilities, which often brought better logical reasoning to the problem at hand. Thanks to Marcy Litvak, too, for encouraging me to think at a scale greater than the tree, as well as for her advocacy and empathy. Nate McDowell I thank for his positive pressure – for drawing my attention to the barriers to progress and my power to remove them, as well as for helping me learn to think more mechanistically. Thanks to John Sperry for his endless patience in explaining his model and his consistently positive editing style. I thank my entire committee for being supportive of the life choices I have made during graduate school (buying and renovating a house, getting married, having a baby and now expecting a second) – they have all provided examples of how to be a rigorous scientist without losing touch with other valuable aspects of life.

I am incredibly lucky to have been able to participate in a large-scale field experiment as part of my graduate education. The piñon-juniper rainfall manipulation experiment has been a huge undertaking, and I thank everyone who has participated in that and who taught me so many different methods: Enrico Yepez, Jimbob Elliot, Jennifer Johnson, Sandra White, Laura Green, Clif Meyer, Monica Gaylord, Judson Hill, Rob Pangle, Jean-Marc Limousin, Patrick Hudson, Amanda Boutz, Nathan Gehres, Don Natvig, Renee Brown and Julie Glaser. In addition to producing more data than any single individual could have on their own, working in the framework of a group effort has been a learning experience about group ownership of data and collaboration. It has been inspiring to see so many people investigating so many different parts of this system that I am curious about.

Outside of the Pockman/PJ lab group, I want to thank Laura Ladwig and Sally Koerner for their support as friends and scientists. From editing drafts to listening to practice talks to exercising together to direct statements of their belief that I could do this, there are innumerable reasons that I am grateful to them both. The writing group we eventually formed provided both social contact and a framework for setting goals that was integral to my actually finishing graduate school. Thanks also to Duncan Wadsworth for so enthusiastically jumping on board when I asked him rather offhandedly whether he thought mixed effect models would be an appropriate way to analyze our dataset. I am so grateful for all the hours he put in to understanding our experimental design, thinking about how to structure the models, and explaining his reasoning in a way that I could then put into writing.

I would not have made it through this graduate school experience without the love and support of my wonderful family and friends. In particular, my parents, Walter and Suzanne Plaut, have always held education as one of the highest ideals and greatest virtues, and have always valued whatever phase of education I was in. My brother, Ethan Plaut, though we work in very different fields, has demonstrated already that it is possible to actually finish a terminal degree! My mother- and father-in-law, Vicky and Ger Danielson, have also always been supportive of and interested in my work, and made the

effort of coming to New Mexico during the final stages of this process to provide much-needed child care so that I could work.

My son Soren was born while I was working on this dissertation and has so far only known his mother as a student. He has been a source of untold joy and fulfillment for me, and a constant reminder to put my academic life in perspective. Thanks, finally, to my husband LeRoy, for his love, support, and faith in me. His support has run the gamut from household chores (all of them, for weeks at a time, while he was either in medical school or residency) to putting up with my being gone to the field site, to understanding my sometimes-high stress level and all the while never doubting that I would finish this thing that I'd started.

REGULATION OF HYDRAULIC FUNCTION AND CONSEQUENCES FOR DROUGHT-RELATED MORTALITY IN MATURE WOODY PLANTS

by

Jennifer Abbett Plaut

Sc.B., Environmental Science, Brown University, 2002

Ph.D., Biology, University of New Mexico, 2013

ABSTRACT

Precipitation and temperature patterns are expected to shift over at least the next century due to anthropogenic climate change. Effects of these shifts may be felt most acutely in arid and semi-arid regions where water is already the most limiting resource. Vegetation mortality due to drought is a likely outcome of predicted future climate, with consequences for ecosystem structure and function and feedbacks on regional and global climate. Yet, mechanisms and interactions of key plant drought responses and the end-point of mortality remain poorly understood.

In this dissertation I examine the roles of xylem cavitation resistance and stomatal control of water loss in enhancing the susceptibility of species to drought-related mortality. I focused first on *Pinus edulis* (piñon) and *Juniperus monosperma* (juniper) woodlands in Southwestern United States. In Chapter 2, I used a hydraulic model to show that piñon mortality under experimental drought occurred in the absence of complete hydraulic failure, but under conditions of chronically low hydraulic conductance and transpiration. Hydraulic limitations, carbon starvation, and pathogen activity were likely

all involved in this mortality. In Chapter 3, utilizing the same rainfall manipulation experiment, I showed that prolonged drought reduced both species' ability to respond to the pulsed precipitation characteristic of semi-arid ecosystems. Transpiration was lower in the drought treatment than in the controls even after differences in pulse size and soil moisture were taken into account, suggesting physiological changes within the trees over the timescale of the experiment. In Chapter 4, I examined the relationship between leaf water potential regulation strategy and xylem cavitation vulnerability as a driver of drought-related mortality, using a global dataset drawn from the literature. Rather than simple classification as either isohydric or anisohydric, I found species to be evenly distributed along a continuum of leaf water potential regulation. Conifers maintained a lower loss of hydraulic conductance in their branches but a greater proportion had experienced drought-related mortality, relative to angiosperms. Together, this research shows that hydraulic constraints may have an important role in carbon starvation leading to drought-related mortality, while highlighting the need for further research on carbon reserves, mobility, and allocation during drought.

TABLE OF CONTENTS

Chapter 1

Introduction

Water stress, i.e. the risk of desiccation, has been a challenge for photosynthesizing land plants since the Ordovician, and will remain so until a carbon fixation mechanism without concomitant water loss evolves. Meteorological drought occurs at some degree of intensity in every ecosystem occupied by land plants, either seasonally or inter-annually. Anthropogenic climate change, however, appears to be exacerbating drought and heat anomalies in some regions, with corresponding effects on plant function and mortality and related effects on ecosystem function and carbon balance. Currently we lack a mechanistic understanding of how observed plant responses to drought progress to the end-point of mortality. This dissertation addresses the relationship between drought-related mortality and both regulation of water loss and plant function during prolonged drought, with a focus on trees and other woody plants.

Current rates of anthropogenic climate change as well as future projections (Allison *et al.* 2009) provide compelling motivation for understanding plant drought responses and how they lead to both individual plant mortality (McDowell 2011, McDowell *et al.* 2011) and broader-scale changes in ecosystem function. Forest mortality due to heat and drought is a global phenomenon (Allen *et al.* 2010, Royer *et al.* 2011, Brouwer *et al.* 2013, Gustafson & Sturtevant 2013, Rigling 2013) and projected changes in temperature and precipitation regimes indicate that many regions of the world will experience greater drought stress in the coming century due to anthropogenic climate forcing (Allison *et al.* 2009, Dai 2012, Seager *et al.* 2012). These climate changes are projected to result in even more mortality of woody species (e.g. Williams *et al.* 2012).

Loss of woody cover has significant implications for local, regional, and global ecosystem function and services. In addition, the mechanisms of and climate feedbacks from forest mortality (Bonan 2008, Jackson *et al.* 2008, van der Werf *et al.* 2009, Mildrexler *et al.* 2011, Pan *et al.* 2011) represent a source of error in current climate models (Fisher *et al.* 2010, McDowell *et al.* 2011).

Individual plants must maintain a hydraulic connection to the soil so that water lost from the leaves during gas exchange can be replaced. Evaporation from the sub-stomatal cavities in the leaves generates tension that propagates down the water column, exposing all conducting vascular tissue to varying tensions. Xylem conducting elements (vessels or tracheids) are susceptible to air embolism, a liquid- to vapor-phase change which disrupts conductance of liquids. Susceptibility to embolism depends on the physical characteristics of the vessels and intervessel pits and membranes; the relationship between declining tissue water potential and increasing loss of hydraulic conductance is described by a vulnerability curve (Sperry *et al.* 1988). When soil water potential declines due to drought, a freely-transpiring leaf will generate more-and-more negative water potentials along the hydraulic pathway. Declining water potentials will cause air embolisms in the xylem, leading to loss of hydraulic conductance, which then further increases the tension in the conductive elements of the xylem; this is termed "runaway cavitation" (Tyree & Sperry 1988). Plants must simultaneously regulate water loss to minimize xylem cavitation and the loss of hydraulic conductance, and maximize carbon gain so as to maintain a positive carbon balance. Stomatal regulation of leaf water potential (Ψ_l) is the primary mechanism for regulation of tissue water potential and cavitation along the hydraulic pathway (Jones & Sutherland 1991, Sperry *et al.* 1998).

One common measure of plant function is transpiration rate, since water loss is proportional to both hydraulic conductance and carbon gained from the atmosphere. Observations of transpiration over time, then, are informative of both the integrity of the vasculature and the probable carbon balance of a plant. Transpiration, E_l, can be expressed as the product of the water potential difference between the soil, Ψ_s, and the leaf (or canopy), Ψ_l, and the hydraulic conductance along that pathway, K_s:

$$E_l = K_s(\Psi_s - \Psi_l)$$

As described above, K_s is a function of Ψ and declines in a species- and tissue-specific manner along with xylem water potential. Drought has the potential to lower Ψ_s, Ψ_l, and K_s, all of which would lower E_l. Lower E_l reduces gas exchange and therefore carbon available for metabolism, respiration, defense, and growth. A slightly more complex version of the model (Whitehead 1984):

$$g_s = \frac{K_s \Delta\Psi A_s}{h\eta D A_l}$$

incorporates sapwood and leaf area (A_s and A_l, respectively) as well as h, height or path length; η, the temperature-dependent viscosity of water; and D, the vapor pressure deficit or evaporative demand from the atmosphere to predict g_s, stomatal conductance to water vapor. (Note that this equation does not account for axial gradients in K_s or A_s.) Thus, the short term effects of drought include reduced Ψ_l, K_s and E_s, while the effects of prolonged drought can also include changes in leaf:sapwood or leaf:root area ratios (Maseda & Fernández 2006, McDowell *et al.* 2006, Gyenge *et al.* 2012).

In order to achieve high rates of transpiration and gas exchange, even well-watered plants tolerate some degree of cavitation (recently estimated to be 33% for angiosperms and 26% for conifers; Manzoni *et al.* 2013). During drought, plants that

close their stomata at a relatively low percent loss of conductance (PLC) preserve hydraulic conductance. They may therefore achieve higher rates of gas exchange and carbon gain when drought is relieved and Ψ_s increases. Plants that tolerate some higher PLC may maintain a more favorable carbon balance during drought and be able to refill or replace cavitated xylem once drought is relieved. Low plant water potentials may also affect phloem circulation, plant physical defenses such as resin production, and the ability to grow (via cell expansion by turgor).

Piñon-juniper woodlands comprise a large fraction of western United States and occupy a region predicted to be a climate change hotspot (Seager & Vecchi 2010, Seager *et al.* 2012). Recent mortality related to regional drought during 2000-2003 (Breshears *et al.* 2005, Floyd *et al.* 2009) combined with contrasting characteristics of the dominant species make piñon-juniper woodlands a model system in which to study drought-related mortality. Data for Chapters 2 & 3 were collected from an ecosystem scale rainfall manipulation experiment located within the Sevilleta LTER in central New Mexico (Pangle *et al.* 2012). Plant physiological characteristics and environmental variables were measured within replicated drought (45% ambient precipitation removal), water addition (ambient precipitation + six 19 mm additions per year), ambient control, and infrastructure control plots. Mortality was greatest in the drought treatment for both species, and piñon mortality was mediated by bark and twig beetles and *Ophiostoma* fungi (Gaylord *et al.* 2013). In Chapter 2, I used plant water potentials and sapflow-estimated transpiration to parameterize the hydraulic model of Sperry *et al.* (1998). The model predicts the limits to transpiration for a given set of soil water potential and vulnerability curve (plant and soil) parameters. Comparing measured plant transpiration

and Ψ_l to modeled hydraulic limits is informative of both the cavitation level of the plant vasculature at a single point in time, and of the plant's tolerance to cavitation assessed over some longer drought duration. The goal was to see how close the co-occurring species were to their modeled hydraulic limits during the year preceding significant mortality in droughted piñon.

The longer-term effects of drought on tree function can be assessed using real-time datasets collected over multiple years or via dendrochronology or tree-ring isotope analysis. In Chapter 3 (Plaut *et al.* in review) I focused on the relationship between prolonged drought and the ability of piñon and juniper to respond to the pulsed precipitation characteristic of this semi-arid system. I used 5 years' of sapflow and environmental data from the site described above. Absolute levels of transpiration had been reduced in the drought treatment essentially since treatment initiation (Pangle *et al.* 2012, Plaut *et al.* 2012) but it was unknown how much of that effect was due to drier pre-pulse soil conditions and smaller realized pulses in the drought plots, and how much was due to changing plant physiological variables. Drought severity has consequences for plant function following re-wetting (e.g. Resco *et al.* 2009, Brodribb *et al.* 2010). Similar to other water-limited systems, soil moisture at this site occurs at plant-available levels only for distinct periods following precipitation events (Huxman *et al.* 2004, Loik *et al.* 2004). Thus, transpiration and gas exchange rates during these critical post-pulse periods provide an important perspective on the physiological function and relative carbon balance of these trees. In Chapter 4, mixed effects models control for pulse conditions to isolate the effects of prolonged drought on tree pulse response.

Two key differences between the species in the previous two chapters are their vulnerability to drought-induced xylem cavitation and their Ψ_l regulation strategy. Piñon is more vulnerable to cavitation than juniper and is typically described as "isohydric", i.e. it regulates Ψ_l above some minimum value (Tardieu & Simmoneau 1999). Juniper is more resistant to cavitation and is typically described as anisohydric, allowing its Ψ_l to decline with Ψ_s. McDowell *et al.* (2008) predicted that these two strategies could lead to different mechanisms of mortality during drought; isohydric species would be more likely to experience carbon starvation while anisohydric species might be more likely to experience complete hydraulic failure. In Chapter 4 (Plaut *et al.* in prep) I asked, for 153 species worldwide, whether Ψ_l regulation strategy was correlated with safety margins from either carbon starvation or hydraulic failure, and whether either of those relationships were predictive of drought-related mortality.

Plants must experience some period of drought stress prior to drought-related mortality. Studying the responses of plants to drought can therefore help elucidate the mechanisms of mortality, but ultimately we need direct measurements of trees dying from natural or experimentally-imposed drought. In this dissertation I aim to address the current knowledge gap of how drought effects, enhanced by climate change, will interact with plant physiology to change species distributions via drought-related mortality.

References

Allen CD, Macalady A, Chenchouni H, Bachelet D, McDowell N, Vennetier M, Gonzales P, Hogg T, Rigling A, Breshears D, *et al.* 2010. A global overview of drought and heat-induced tree mortality reveals emerging climate change risks for forests. *Forest Ecology and Management* **259**: 660–684.

Allison I, Bindoff NL, Bindschadler RA, Cox PM, de Noblet N, England MH, Francis JE, Gruber N, Haywood AM, Karoly DJ, *et al.* 2009. The Copenhagen Diagnosis, 2009: Updating the World on the Latest Climate Science. Sydney, Australia: The University of New South Wales Climate Change Research Centre

Bonan GB. 2008. Forests and climate change: forcings, feedbacks, and the climate benefits of forests. *Science* **320**: 1444-1449.

Breshears DD, Cobb NS, Rich PM, Price KP, Allen CD, Balice RG, Romme WH, Kastens JH, Floyd ML, Belnap J *et al.* 2005. Regional vegetation die-off in response to global-change type drought. *Proceedings of the National Academy of Sciences*, *USA* 102: 15144–15148.

Brodribb TJ, Bowman DJMS, Nichols S, Delzon S, Burlett R. 2010. Xylem function and growth rate interact to determine recovery rates after exposure to extreme water deficit. *New Phytologist* **188**: 533-542.

Brouwer NC, Mercer J, Lyons T, Poot P, Veneklaas E, Hardy G. 2013. Climate and landscape drivers of tree decline in a Mediterranean ecoregion. *Ecology and Evolution* **3**: 67–79

Dai A. 2013. Increasing drought under global warming in observations and models. *Nature Climate Change* **3**: 52-58.

Fisher R, McDowell NG, Purves D, Moorcroft P, Sitch S, Cox P, Huntingford C, Meir P, Woodward FI. 2010. Assessing uncertainties in a second-generation dynamic vegetation model caused by ecological scale limitations. *New Phytologist* **187**:666-681.

Floyd ML, Clifford M, Cobb NS, Hanna D, Delph R, Ford P, Turner D. 2009. Relationship of stand characteristics to drought-induced mortality in three southwestern piñon-juniper woodlands. *Ecological Applications* **19**: 1223–1230.

Gaylord ML, Kolb TE, Pockman WT, Plaut JA, Yepez EA, Macalady AK, Pangle RE, McDowell NG. 2013. Drought causes predisposition to insect attacks and mortality of piñon-juniper woodlands. *New Phytologist* doi: 10.1111/nph.12174

Gustafson EJ, Sturtevant BR. 2013 Modeling forest mortality caused by drought stress: implications for climate change. *Ecosystems* **16**:60-74.

Gyenge J, Fernández ME, Varela S. 2012. Short- and long-term responses to seasonal drought in ponderosa pines growing at different plantation densities in Patagonia, South America. *Trees – Structure and Function* **26**: 1905-1917.

Huxman TE, Snyder KA, Tissue D, Leffler AJ, Ogle K, Pockman WT, Snadquist DR, Potts DL, Schwinning S. 2004. Precipitation pulses and carbon fluxes in semiarid and arid ecosystems. *Oecologia* **141**: 254-268.

Jackson RB, Randerson JT, Canadell JG, Anderson RG, Avissar R, Baldocchi DD, Bonan GB, Caldeira K, Diffenbaugh NS, Field CB *et al.* 2008. Protecting climate with forests. *Environmental Research Letters* **3**: article number 044006, doi:10.1088/1748-9326/3/4/044006

Jones HG & Sutherland RA. 1991. Stomatal control of xylem embolism. *Plant, Cell and Environment* **14**: 607-612.

Loik M E, Breshears DD, Lauenroth WK, Belnap J. 2004. A multi-scale perspective of water pulses in dryland ecosystems: climatology and ecohydrology of the western USA. *Oecologia* **141**: 269-281.

Manzoni S, Vico G, Katul G, Palmroth S, Jackson R, Porporato A. 2013. Hydraulic limits on maximum plant transpiration and the emergence of the safety–efficiency trade-off. *New Phytologist* **198**: 169-178.

Maseda PH, Fernández RJ. 2006. Stay wet or else: three ways in which plants can adjust hydraulically to their environment. *Journal of Experimental Botany* **57**: 3963-3977.

McDowell NG. 2011. Mechanisms linking drought, hydraulics, carbon metabolism, and vegetation mortality. *Plant Physiology* **155**: 1051-1059.

McDowell NG, Adams HD, Bailey JD, Hess M, Kolb TE. 2006. Homeostatic maintenance of ponderosa pine gas exchange in response to stand density changes. Ecological Applications **16**: 1164-1182.

McDowell NG, Beerling D, Breshears D, Fisher R, Raffa K, Stitt M. 2011. Interdependence of mechanisms underlying climate-driven vegetation mortality. *Trends in Ecology and Evolution*, **26**: 523-532.

McDowell N, Pockman WT, Allen CD, Breshears DD, Cobb N, Kolb T, Plaut J, Sperry J, West A, Williams DG *et al.* 2008. Mechanisms of plant survival and mortality during drought: why do some plants survive while others succumb to drought? Tansley Review. New Phytologist 178: 719–739.

Mildrexler DJ, Zhao M, Running SW. 2011 A global comparison between station air temperatures and MODIS land surface temperatures reveals the cooling role of forests. *Journal of Geophysical Research*, **116**: G03025, doi:10.1029/2010JG001486

Pan Y, Birdsey RA, Fang J, Houghton R, Kauppi PE, Kurz WA, Phillips OL, Shvidenko A, Lewis SL, Canadell JG, *et al.* 2011. A large and persistent carbon sink in the World's forests. *Science* **333**: 988–993.

Notaro M, Mauss A, Williams J. 2012. Projected vegetation changes for the American Southwest: combined dynamic modeling and bioclimatic-envelope approach. *Ecological Applications* **22**: 1365-1388.

Noy-Meir I. 1973. Desert ecosystems: environment and producers. *Annual Review of Ecology and Systematics* **4**: 25–51.

Pangle RE, Hill JP, Plaut JA, Yepez EA, Elliot JR, Gehres N, McDowell NG, Pockman WT. 2012. Methodology and performance of a rainfall manipulation experiment in a piñon-juniper woodland. *Ecosphere* **3**: 28.

Plaut JA, Yepez EA, Hill J, Pangle R, Sperry JS, Pockman WT, McDowell NG. 2012. Hydraulic limits preceding mortality in a piñon-juniper woodland under experimental drought. *Plant, Cell & Environment* **35**: 1601-1617.

Resco V, Ewers BE, Sun W, Huxman TE, Weltzin JF, Williams DG. 2009. Drought-induced hydraulic limitations constrain leaf gas exchange recovery after precipitation pulses in the C_3 woody legume, *Prosopis velutina*. *New Phytologist* **181**: 672-682.

Rigling A, Bigler C, Eilmann B, Feldmeyer-Christe E, Gimmi U, Ginzler C, Graf U, Mayer P, Vacchiano G, Weber P, Wohlgemuth T, Zweifel R, Dobbertin M. 2013.

Driving factors of a vegetation shift from Scots pine to pubescent oak in dry Alpine forests. *Global Change Biology* **19**: 229-240.

Royer PD, Cobb NS, Clifford MJ, Huang C-Y, Breshears DD, Adams, HD, Villegas JC. 2011. Extreme climatic event-triggered overstorey vegetation loss increases understorey solar input regionally: primary and secondary ecological implications. *Journal of Ecology* **99**: 714-723.

Seager R, Ting M, Li C, Naik N, Cook B, Nakamura J, Liu H. 2012. Projections of declining surface-water availability for the southwestern United States. *Nature Climate Change* doi:10.1038/nclimate1787

Seager R, Vecchi G. 2010. Greenhouse warming and the 21st century hydroclimate of southwestern North America. *Proceedings of the National Academy of Science* **107**: 21277-21282.

Sperry JS, Adler FR, Campbell GS, Comstock JP. 1998. Limitation of plant water use by rhizosphere and xylem conductance: results from a model. *Plant, Cell and Environment* **21** 347– 359.

Sperry JS, Donnelly JR, Tyree MT. 1988. A method for measuring hydraulic conductivity and embolism in xylem. *Plant, Cell and Environment* **11**, 35–40.

Tardieu F, Simonneau T. 1998. Variability among species of stomatal control under fluctuating soil water status and evaporative demand: modelling isohydric and anisohydric behaviours. *Journal of Experimental Botany* **49**: 419-432.

Tyree MT, Sperry JS. 1988. Do woody plants operate near the point of catastrophic xylem dysfunction caused by dynamic water stress? *Plant Physiology* **88**:574-580.

van der Linde, JA, Roux J, Wingfield MJ, Six DL. 2013. Die-off of giant Euphorbia trees in South Africa: Symptoms and relationships to climate. *South African Journal of Botany* **83**: 172-185.

van der Werf GR, Morton DC, DeFries RS, Olivier JGJ, Kasibhatla PS, Jackson RB, Collatz GJ, Randerson JT. 2009. CO_2 emissions from forests. *Nature Geoscience* **2**: 737-738.

Whitehead D, Edwards WRN, Jarvis PG. 1984. Conducting sapwood area, foliage area, and permeability in mature trees of *Picea sitchensis* and *Pinus contorta*. *Canadian Journal of Forest Research* **14**: 940-947.

Williams AP, Allen CD, Macalady AK, Griffin D, Woodhouse CA, Meko DM, Swetnam TW, Rauscher SA, Seager R, Grissino-Mayer HD *et al.* 2012. Temperature as a potent driver of regional forest drought stress and tree mortality. *Nature Climate Change*. doi:10.1038/nclimate1693

Chapter 2

Hydraulic limits preceding mortality in a piñon-juniper woodland under experimental drought

Plant, Cell and Environment (2012) **35**: 1601-1617

Jennifer A. Plaut[1], Enrico A. Yepez[2], Judson Hill[1], Robert Pangle[1], John S. Sperry[3], William T. Pockman[1], Nate G. McDowell[4]

[1] Department of Biology, MSC03 2020, 1 University of New Mexico, Albuquerque, NM 87131-0001, USA

[2] Departamento de Ciencias del Agua y del Medio Ambiente, Instituto Tecnológico de Sonora, Ciudad Obregón Sonora, 85000, Mexico

[3]Department of Biology, University of Utah, 257 South 1400 East, Salt Lake City, UT 84112, USA

[4]Earth and Environmental Sciences Division, Los Alamos National Laboratory, Los Alamos, NM 87545, USA

Correspondence: J.Plaut, Department of Biology, MSC03 2020, 1 University of New Mexico, Albuquerque, NM 87131-0001, USA. Fax: 505 277 0304; e-mail: jplaut@unm.edu

Abstract

Drought-related tree mortality occurs globally and may increase in the future, but we lack sufficient mechanistic understanding to accurately predict it. Here we present the first field assessment of the physiological mechanisms leading to mortality in an ecosystem-scale rainfall manipulation of a piñon-juniper (*Pinus edulis-Juniperus monosperma*) woodland. We measured transpiration (E) and modeled the transpiration rate initiating hydraulic failure (E_{crit}). We predicted that isohydric piñon would experience mortality after prolonged periods of severely limited gas exchange as required to avoid hydraulic failure; anisohydric juniper would also avoid hydraulic failure, but sustain gas exchange due to its greater cavitation resistance. After one year of treatment, 67% of droughted mature piñon died with concomitant infestation by bark beetles (*Ips confusus*) and bluestain fungus (*Ophiostoma* spp.); no mortality occurred in juniper or in control piñon. As predicted, both species avoided hydraulic failure, but safety margins from E_{crit} were much smaller in piñon, especially droughted piñon, which also experienced chronically low hydraulic conductance. The defining characteristic of trees that died was a seven-month period of near-zero gas exchange, versus two months for surviving piñon. Hydraulic limits to gas exchange, not hydraulic failure *per se*, promoted drought-related mortality in piñon pine.

Key words: die-off, stomata, climate change, Sperry model, piñon, drought experiment

Introduction

Drought-related tree mortality is a global phenomenon with significant implications for ecosystem structure and function (Bonal *et al.* 2008; Fensham, Fairfax & Ward 2009; Horner *et al.* 2009, Allen *et al.* 2010). Hypotheses that, alone or in combination, explain drought-related mortality in the absence of physical disturbances include catastrophic hydraulic failure, carbon starvation, and biotic factors such as insect and fungal pathogens (Suarez, Ghermandi & Kitzberger 2004; McDowell *et al.* 2008; Worrall *et al.* 2008; Adams *et al.* 2009; Brodribb & Cochard 2009). The role of each of these factors, and interactions among them, in the mechanism of mortality is expected to vary depending on future patterns of drought duration and intensity (Bigler *et al.* 2007; McDowell *et al.* 2008). It is not yet clear how mortality and its underlying mechanisms will respond to the anticipated increase in the frequency of extreme drought events with continued fossil fuel emissions (IPCC 2007; Fensham *et al.* 2009). Although drought-related mortality is a complex phenomenon, its accurate prediction is critical to modeling ecosystem responses and feedbacks to global climate change (Friedlingstein *et al.* 2006; Sitch *et al.* 2008).

Hydraulic failure is the complete loss of water transport to the canopy resulting from xylem embolism, the blockage of xylem conducting elements by air pulled across a pit membrane from an air-filled to a water-filled conduit (Tyree & Sperry 1988). Hydraulic failure can also occur in the rhizosphere when soil water potential (Ψ_s; see Table 1 for a list of symbols) declines below the air entry pressure, breaking the root-soil hydraulic connection (Sperry *et al.* 1998). This occurs during drought because Ψ_s decreases dramatically with proximity to the surface of an absorbing root as transpiration

(E) continues. In both the xylem and the soil, hydraulic failure is linked to the decrease in water potential caused by flow at a given hydraulic conductance, and the associated decrease in hydraulic conductance that feeds back on water potential. The hydraulic limit to water transport is therefore defined as the critical transpiration rate (E_{crit}) which, under steady state conditions, generates a critical minimum xylem or soil water potential (Ψ_{crit}) that results in hydraulic failure (Sperry *et al.* 1998; Sperry *et al.* 2002). Drought-related loss of conductance along the soil-plant continuum is a well-documented phenomenon (Sparks & Black 1999; Brodribb & Holbrook 2003; Brodribb *et al.* 2009; Iovi, Kolovou & Kyparissis 2009), but the frequency of hydraulic failure in field settings (i.e. non-potted plants), and whether it leads directly to mortality, is not well understood (Galvez & Tyree 2009; Resco *et al.* 2009; McDowell 2011).

Plants reduce stomatal conductance in a manner consistent with regulating transpiration to avoid hydraulic failure (Sperry *et al.* 1998; Hacke *et al.* 2000; Cochard *et al.* 2002). Plant control of stomatal conductance and leaf water potential (Ψ_l) can be described by two broad strategies: isohydry and anisohydry (Tardieu & Simonneau 1998). Isohydric plants regulate Ψ_l above a minimum set-point; when drought pushes Ψ_s below this Ψ_l set-point, gas exchange ceases until precipitation increases Ψ_s. This stomatal response may minimize hydraulic failure, but it comes at the cost of limiting carbon assimilation and may predispose plants to carbon starvation, depending on the duration of the drought (McDowell *et al.* 2008; Breshears *et al.* 2009). Species with vulnerable xylem cannot experience a broad Ψ_l range without complete cavitation, and so would be expected to be relatively isohydric. Anisohydric plants allow Ψ_l to decrease with Ψ_s, allowing continued gas exchange during drought. Compared to isohydric

species, anisohydric species maintain carbon assimilation at higher rates and further into drought, but the anisohydric strategy requires more cavitation-resistant xylem or else risks hydraulic failure under severe drought (McDowell *et al.* 2008). We note that there is not always a clear distinction between these two strategies, and that even typically anisohydric plants must constrain stomatal conductance at some point to avoid hydraulic failure (McDowell *et al.* 2008; Plaut *et al.* unpublished manuscript).

Piñon-juniper woodland (here *Pinus edulis* Engelm. and *Juniperus monosperma* (Engelm.) Sarg.) is a model system in which to study the hydraulic contributions to mortality during drought. Compared to juniper, piñon is more vulnerable to drought-induced xylem cavitation (Linton, Sperry & Williams 1998), is generally isohydric in its regulation of Ψ_l while juniper is generally anisohydric (Linton *et al.* 1998; West *et al.* 2008), and has recently exhibited greater mortality during drought (McDowell *et al.* 2008; Breshears *et al.* 2009; Floyd *et al.* 2009). Piñon also experiences episodic attacks by bark beetle, *Ips confusus* (LeConte), a vector for *Ophiostoma* fungi; juniper does not seem to have a pest with similar symbionts or outbreak cycles (Floyd *et al.* 2009). Previous analysis of hydraulic strategies in piñon and juniper has demonstrated that piñon spends a greater amount of time with near-zero gas exchange than juniper, but juniper experiences greater cavitation than piñon (West *et al.* 2007a; West *et al.* 2008). The mechanisms distinguishing mortality and survival during drought have not been previously experimentally tested.

Our study was designed to explicitly investigate hydraulic mechanisms underlying mortality in the field, using an ecosystem scale precipitation reduction mimicking the deficit that resulted in widespread mortality in 2002-2003 (precipitation

~50% below ambient). After less than one year, 67% of mature piñon (basal diameter > 9 cm, excluding a 5 m buffer zone from the edge of the drought treatment; 25% of piñon if all size classes and trees up to the plot edge are included) were attacked by bark beetles, infected with bluestain fungus, and died, giving us the opportunity to examine for the first time the physiology of field-grown trees leading up to mortality in a manipulative experiment. Our primary objective was to test the hypothesis that piñon's avoidance of hydraulic failure is associated with drought-related mortality through severe constraints on gas exchange, while juniper can sustain gas exchange without hydraulic failure because of its greater resistance to cavitation.

Methods

Site description

The study was conducted in the Los Piños mountains within the Sevilleta National Wildlife Refuge, Socorro County, New Mexico (N 34º 23'13", W 106º31'29"), part of the US Long-Term Ecological Research network. The elevation at the site is approximately 1911 m, which is close to the lower-elevation limit of piñon. Piñon and juniper are the dominant woody species; shrub live oak (*Quercus turbinella* Greene) is the only other woody species of any stature at the site (Table 1). Soils were calcid aridisols characterized as Sedillo-Clovis association of fan alluvium derived from conglomerate (Soil Survey Staff, Natural Resources Conservation Service, United States Department of Agriculture. http://websoilsurvey.nrcs.usda.gov/ accessed February 28, 2011). Long-term mean monthly temperatures range from 2.6 ˚C in January to 23.1 ˚C in July; annual precipitation averages 362 mm at a meteorological station near the site (Cerro Montoso meteorological station, 2.2 km from and approximately 70 m higher than

the study site, 1989-2009, http://sev.lternet.edu/). Roughly half of the annual precipitation falls from convective storms during the North American Monsoon, typically during July through September.

The data for this study were acquired from a subset of plots in a larger precipitation manipulation experiment (Pangle *et al.* in press). The four treatments applied were 1) water addition, 2) water removal ("drought"), 3) cover control, and 4) ambient control. The larger experiment consisted of three blocks of the four treatments applied to 40 m x 40 m plots, established in the summer of 2007. We used study plots in a southeast-facing block of 8-18 degrees slope for the intensive physiology measurements to test our hypotheses. The water addition plots (#1 above) were not active during the period of this study and thus are not included in this paper.

The drought plot consists of UV-resistant clear acrylic sheets (Makrolon® SL, Sheffield Plastics, Massachusetts, USA) bent into troughs and screwed to rails approximately 1 m high. The sheets are 0.91 m wide and cover 0.81 m when bent. Troughs were inserted as far as possible into tree crowns without damaging the canopies, dammed, and connected to the trough on the far side of the canopy with flexible 7.6 cm diameter hoses. Troughs drain to gutters, which divert water to existing arroyos. The rows of troughs together cover 45% of the plot. The cover control plot consists of the same plastic bent in the same way, but installed in a concave orientation, which replicates the microenvironment under the water removal troughs without removing ambient precipitation (R. Pangle, in press). Installation of plastic covers on drought and cover control plots was completed on August 22, 2007. The ambient control plot had no treatment infrastructure installed.

Environmental data

A micrometeorological station at the research site included a Campbell Scientific HMP45C air temperature and relative humidity sensor, Campbell Scientific CS105 barometric pressure sensor, tipping bucket rain gauge equipped with a snowfall adapter (Texas Electronics), R.M. Young 05103 wind monitor (velocity and direction), Decagon EC-20 soil volumetric water sensor installed at 5 cm, net radiometer (model NR-LITE, Kipp & Zonen), and a LI190SB PPFD/quantum sensor (LI-COR, Lincoln, Nebraska). Sensors were operated via a Campbell Scientific CR10X datalogger, and continuous data were summed (rain gauge) or averaged over 30 minute intervals.

Within each plot, five trees of each species were chosen for physiological measurements. Target trees were centrally located within the plots and had stem(s) of at least 9 cm diameter. Additionally, five inter-canopy areas per plot were instrumented to measure soil water potential.

Soil moisture measurements

Plant-available soil moisture was measured with thermocouple psychrometers (Wescor Inc., Logan, Utah) controlled via Campbell Scientific CR-7 dataloggers (Campbell Scientific, Logan, Utah). Soil psychrometer profiles were placed under each target tree and at the 5 designated intercanopy areas for a total of 15 profiles per plot. Each profile consisted of sensors at: 1) 15 cm, 2) 20 cm, and 3) as deep as could be augered and installed horizontally into the side wall of the hole, generally between 50 and 100 cm. Sensors were calibrated with four NaCl solutions of known water potential prior to field deployment.

Thermocouple psychrometers are accurate in their calibrated range but have range limitations in dry soils. Our sensors returned out-of-range values below soil water potentials of -6.5 to -7.5 MPa, typically during the extended dry periods prior to the monsoons in 2007 and 2008, though some sensors continued to give valid output down to -8 MPa. Sensors that were observed to go out of range during those periods were assigned an end-point of -8 MPa at the first major monsoonal storm of each season and a linear interpolation was constructed between their last reasonable point and that end-point. This method avoids artificially raising the calculated mean as the driest sensors drop out of the array. This method is conservative because the general shape of a dry-down trajectory is exponential (van Genuchten, 1980), therefore approximating it with a linear function is more likely to overestimate than to underestimate water potential. The effect of this overestimation is likely to be minimal given that there is little plant-available water in the range of water potentials over which interpolation was conducted. Following soil re-wetting sensors regained function, so drought period failure did not affect sample size over the long term.

Plant water potentials

Predawn and midday leaf water potentials (Ψ_{pd} and Ψ_{md}, respectively) were measured throughout the study on each target tree using south-facing twigs with healthy foliage. Measurements were made monthly or with greater frequency when soil moisture was changing rapidly during each summer's dry-down and monsoon. Immediately following excision, samples were placed in a zip-top plastic bag with a small piece of damp paper towel (Kaufmann & Thor 1982; Kolb *et al.* 1998; Stone, Kolb & Covington 1999) and stored in a cooler until measurement with a Scholander-type pressure chamber

(PMS Instruments, Corvallis, OR). Midday samples were collected 10 at a time and measured sequentially to minimize the time since cutting, which was less than one hour.

Sap flow measurements

Transpiration, *E*, was estimated by measuring sap flux density with Granier heat dissipation probes (Granier 1987; Phillips & Oren 2001). Two probes were installed on each target tree at least 1 m from the ground (path length) at a point where tree diameter was ≥ 9 cm. Probes were constructed at the University of New Mexico and installed during fall 2006 and early spring 2007. Each probe consisted of four 10 mm needles inserted radially into the xylem, 10 cm apart vertically and 5 cm apart horizontally. Each needle had an internal thermocouple 5 mm from the tip. One downstream needle was wrapped with 1 ohm/cm Advance resistance wire (Pelican Wire, Naples, Florida) and an aluminum sleeve was placed in the xylem prior to needle insertion to homogenize the heat input. The heated needle was supplied with 0.067 W, while the reference thermocouple in the unheated needle above it completed the standard Granier configuration. This amount of power is within the range used in other studies (Goulden & Field 1994, Bush *et al.* 2010) though on the low end to reduce power consumption and the risk of sapwood damage. The pair of reference thermocouples horizontally adjacent corrected for ambient axial thermal gradients (Goulden & Field 1994), an addition we found necessary due to the open canopy structure of this ecosystem and the resulting exposure of shielded probe locations and adjacent stems to direct solar radiation. This reference thermocouple set was added to existing sap flow sensors during spring 2007, but the response to the correction was not universal (i.e. it could not be applied retroactively, data not shown); only corrected data are reported here.

Temperature differentials (ΔT) during the daytime are corrected for T differences at zero flow (ΔT_{max}; Granier 1987) to calculate sap flux density, J_s. ΔT_{max} is generally assumed to occur at times unlikely to generate sap flux, i.e. nights with low vapor pressure deficit (VPD), which are rare in this system. Applying each night's ΔT_{max} to the following day's temperature differentials removes the possibility of observing nighttime sap flow, which can be a significant portion of daily water loss (Snyder, Richards & Donovan 2003). Further, ΔT_{max} was observed to drift over time in some instances, though changes were not correlated with nighttime VPD. ΔT_{max} was also observed to shift periodically, sometimes randomly and at other instances when, for example, a probe was replaced. Therefore, we visually divided the time series of data into intervals of similar environmental characteristics and ΔT_{max} behavior (i.e. direction of change) for each probe. Linear regressions of ΔT_{max} against time were generated for each interval and ΔT_{max} was set for each probe/day based on the value from the previous night, calculated from the regression. ΔT_{max} values and J_s were calculated for each probe individually. This method may underestimate J_s because it does not guarantee that ΔT_{max} is calculated at zero flow conditions, but it does allow estimation of nighttime flow while accounting for long-term change in ΔT_{max}.

Trees were cored near each sap flow probe during summer 2009 to assess the validity of the assumption that the 10 mm probes were located entirely within sapwood. Corrections were applied to sensors found to be measuring <10 mm sapwood (Clearwater *et al.* 1999). This correction was necessary for four out of the ten juniper probes on each of the cover control and ambient control plots. No correction was necessary for any probes in piñon. For most of the juniper and all of the piñon, sapwood depth was greater

than the length of the probe measuring sap flux density, therefore we did not capture all of the variability in sap flux density. Sap flux density generally declines with distance from the cambium (Cohen *et al.* 2008) so we assume that we did capture the highest rates, but the scale of the project precluded installing probes at multiple depths. Based on site-specific equations (data not shown) we estimate that on average we sampled the outer 44% of sapwood area in piñon. In juniper, sapwood depth is so variable that while in most cases the probes were completely in sapwood, the average sapwood depth was less than the probe length. We used sap flux density as an indicator of plant functional status and did not scale to whole-tree water use (i.e. did not multiply measured sap flux densities by total sapwood area). For all results presented we converted J_s, g $m^{-2}s^{-1}$, to E_s, mol $m^{-2}s^{-1}$ and did not scale to leaf area due to potentially changing leaf area, particularly as a function of treatment, during the course of the experiment. We also used the empirically-derived coefficients in the Granier equation, which may have resulted in under-estimation of sap flux density, though errors due to a lack of a species-specific calibration are generally more egregious for ring-porous than diffuse-porous or tracheid-bearing species (Bush *et al.* 2010).

Cavitation vulnerability

Curves describing xylem vulnerability to drought-induced cavitation (Sperry, Donnelly & Tyree 1988) were generated using the centrifuge technique (Cochard 2002; Cochard *et al.* 2005), adopting the conductivity calculation and protocol proposed by Li *et al.* (2008). Branch and root segments were cut as long as possible in the field, wrapped in a damp paper towel in a large plastic bag, placed in a cooler, and transported 1 hr to the lab. Samples were stored in a refrigerator in the lab and measured on the centrifuge

within 24 hr. Upon measurement, samples were cut under water to produce a straight segment with no branching or bark scarring approximately 25.5 cm long. Segment ends were trimmed with a new razor blade. Xylem pressure was generated with a Sorvall Model RC5C centrifuge with custom rotors and conductance was measured using a 20 mM KCl solution filtered to 0.2 μm. Percent loss of conductance (PLC) was plotted against pressure and fit with a Weibull function to generate a vulnerability curve (Neufeld *et al.* 1992):

$$PLC = 100\left(1 - e^{-\left(-\frac{\Psi}{b}\right)^{c}}\right) \quad (1)$$

Xylem vulnerability was measured on five piñon branches (trimmed lengths 254-258 mm, diameter without bark 5.7 – 7.3 mm), harvested in April and October 2008, and four piñon roots (trimmed lengths 251-255 mm, diameter without bark 6.5 – 10.0 mm) harvested in October 2008. Additionally, two juniper branches and two roots were measured, but due to the small sample size, the hydraulic model was parameterized with published vulnerability curves for this species (Willson, Manos & Jackson 2008). The vulnerability curves developed for juniper at our site showed them to be more vulnerable to cavitation than the published values used for modeling (xylem pressure at which 50% of conductance is lost, P_{50}, was -8.25 MPa for on-site juniper branches compared to -11.6 MPa reported by Willson *et al.* (2008)). P_{50} for piñon branches was -2.75 MPa and P_{50} for piñon roots was -3.26 MPa, though the Weibull curve for the roots was steeper so that roots would achieve 100% cavitation earlier than branches. The Weibull function

parameters for piñon branches were: b = 3.43 and c = 1.65, and for roots, b = 3.57 and c = 4.07.

Hydraulic model

Plant hydraulic limits were assessed using Sperry *et al.*'s (1998) model of water transport. The model solves the steady state of

$$E = K(\psi_s - \psi_l) \quad (2)$$

where K, mol m^{-2} s^{-1} MPa^{-1}, is the Ψ-dependent conductance of the entire soil-canopy pathway. The K is expressed on the same area basis as E (sapwood area, in our study). The modeled K depends on the seasonal maximum conductance and the "b" and "c" parameters of the Weibull function vulnerability curves. The model increments E and solves for Ψ_l to arrive at the maximum possible E (E_{crit}) and lowest Ψ_l (Ψ_{crit}) for a set of Ψ_s and vulnerability curve inputs. E greater than E_{crit} or Ψ_l lower than Ψ_{crit} would, theoretically, result in hydraulic failure somewhere along the transport pathway. At the same time, the model predicts E (E_{pred}) from measurements or estimates of Ψ_l. Since we did not measure Ψ_{md} every day, linear interpolation between known points was used to generate a continuous Ψ_l record. Although it may be inaccurate when, for example, Ψ_{md} measurements bracket a large rain event, linear interpolation produced more reasonable estimates than linear models of Ψ_l based on physical parameters (data not shown).

Soil hydraulic conductivities were parameterized from soil texture data (Campbell 1985). Weibull parameters from the measured vulnerability curves were input separately for roots and canopy xylem to account for their differences in vulnerability to cavitation. The E_s value used for each day's model input was the average of the two-hour period

bracketing the daytime maximum E_s. Days with temperatures never above 0 ºC and/or when maximum photosynthetically active radiation, PAR, was below 70% of the nine day running maximum were excluded.

The model also requires the ratio of root:leaf area (A_r:A_l), which was not measured. Modeled E_{crit} saturates at high A_r:A_l as the xylem becomes more limiting than the rhizosphere. We chose A_r:A_l = 3 because it was sufficient to saturate E_{crit} in piñon, and to come within 5% of saturation averaged across the physiological range of Ψ_{pd} (approximately -1 to -8 MPa) in juniper.

Modeling scenario

In principle, the model can divide the rooting zone into three layers and use the measured soil water potentials as input. In practice, however, the data suggested that both species, though much more so for piñon, were drawing water from a missing soil layer that was wetter than any of the three measured layers. According to these data, on several days Ψ_{pd} and Ψ_{md} were less-negative than the wettest measured soil layer (a difference of several MPa in the case of piñon), and there was also significant soil water uptake as indicated by non-zero E_s. Furthermore, when Ψ_{md} is less-negative than the Ψ_s input for the model, the model cannot generate predictions of E_s, E_{crit}, or Ψ_l because there is no driving gradient for flow from the soil to the canopy. In the absence of the full soil moisture profile, the model was calibrated to predict Ψ_{pd} from the measured sap flow and Ψ_{md}:

$$\Psi_{pd-pred} = \frac{E_S}{K_{pred}} + \Psi_{md} \quad (3)$$

where K_{pred} is the soil-to-canopy hydraulic conductance at the Ψ_{md} calculated by the model for an arbitrarily small $\Psi_{pd} - \Psi_{md} = \Delta\Psi$ of 0.2 MPa. The calibration was run for the subset of days (between April 1 and October 31) on which Ψ_{pd} was measured (7-9 days each year). The mean square error (MSE) between the $\Psi_{pd\text{-}pred}$ and the measured Ψ_{pd} was minimized by varying the initial K (K_{sat}) at the beginning of the time series. In piñon during 2007, the monsoon season corresponded with an obvious systematic deviation where $\Psi_{pd\text{-}pred}$ became much more positive than the measured Ψ_{pd}, indicating that K_{pred} was under-predicted post-monsoon (data not shown). This suggested recovery of hydraulic conductance in piñon, consistent with previous findings (West *et al.* 2008). In these cases, the model was calibrated separately for pre-monsoon and post-monsoon data. The model was also calibrated separately for 2007 and 2008 (April-October data only) to account for any changes in tree K occurring in the November to March period that was not modeled.

Once the model was calibrated, it was used to generate the full time sequence of K_{pred} and $\Psi_{pd\text{-}pred}$. The $\Psi_{pd\text{-}pred}$ time sequence was then input as Ψ_s for the entire rooting zone (in lieu of accurate profiles for Ψ_s and rooting depth). From the sequence of Ψ_s and interpolated Ψ_{md}, the model calculated E_{pred} and E_{crit}. Modeled K_{pred} was converted to Percentage Loss of Conductance (PLC) relative to the maximum K_{sat} per species obtained from the model calibration across both years and treatments. Because the ambient and cover control plots proved broadly similar in terms of Ψ_s, piñon and juniper E_s, and Ψ_l (see below), we applied the model only to ambient control and drought treatments. This method of using $\Psi_{pd\text{-}pred}$ as an integrated measure of the spatially heterogenous Ψ_s profile has been successful previously (West *et al.* 2008) though most of the previous

applications of this model to isohydric *Pinus* species have been under relatively moist conditions (Ewers, Oren & Sperry 2000; Hacke *et al.* 2000, Domec *et al.* 2010).

Bark beetle activity

Ips confusus (bark beetle) was identified in the field from pitch tubes on the main bole and larger branches and excavated galleries under the bark of affected piñon. *I. confusus* was subsequently identified in the lab based on Chansler (1964) and Wood (1982) and verified against existing reference collections at Rocky Mountain Research Station (Flagstaff, Arizona) and the Northern Arizona University Entomology laboratory (Flagstaff, Arizona).

Statistical analyses

Treatment effects on Ψ_s, Ψ_l, and E_s were evaluated by comparing pre-treatment with post-treatment differences. All pre- and post-treatment differences are provided in Table S1. Welch's t-tests were used to compare treatment differences in post-treatment periods with pre-treatment differences. Wilcox signed-rank tests, which do not assume normal data distribution, were also used to compare daily E_s within species among plots. Because of the large number of tests performed, results were adjusted for a family-wise error rate of 5%. Effects of the rainfall manipulation treatments were considered significant if the post-treatment plot differences varied significantly from pre-treatment differences (Table S1). Matlab® (2007a, The Mathworks, Natick, MA) was used for all data management. R software (R Development Core Team 2009) was used for all statistical analysis.

Results

In 2007 and 2008, mean daily temperature ranged from -8 ºC to 30 ºC (Fig. 1a) with an absolute range of -14.4 to 36.4 ºC. Vapor pressure deficits ranged from 0.02 to 5.5 kPa (Fig. 1b). Annual precipitation in 2007 and 2008 was 666 mm and 331 mm, respectively, compared to the 20-year average of 362 mm. The spring moisture pulse in 2008 was significantly smaller than that in 2007, and there were no precipitation events larger than 10 mm before July of that year (Fig. 1c). Between treatment imposition in late August 2007 and indications of piñon mortality in early August 2008, the site received 365 mm of precipitation, with the drought plot receiving an estimated 201 mm (55% of ambient, Fig. 5c). Needle browning on droughted piñon was observed in early August 2008, after ~11 months of treatment (Fig. S1). Onset of needle browning coincided with evidence of attack by *I. confusus*, and dying trees were also infected with *Ophiostoma* fungi (A. Porras-Alfaro, *pers. comm*.). Total piñon mortality on the drought plot reached 25% by December 2008 (6 out of 24 piñon within the plot boundary), though 67% of candidate target trees (basal diameter ≥ 9 cm and inside the 5 m plot buffer) died by that point and 100% by the following spring, with zero mortality of either species on the ambient and cover control plots.

Soil and plant water potentials

Rainout structures produced significant differences in Ψ_s compared to plots receiving ambient rainfall (Table S1, Fig. 2). Treatment effects became apparent almost immediately after treatment installation (Fig. 1c). The drought plot, which was drier than the control plots at most depths pre-treatment, became significantly more so post-treatment (Table S1). Drought plot Ψ_s did not recover following the wet periods of the 2007 and 2008 monsoons and spring 2008 (Fig. 2).

During both years, Ψ_{pd} and Ψ_{md} of both species declined during the spring/summer dry-down, reached minima in July and recovered during the monsoon season (Fig. 3). Comparisons on individual dates show piñon Ψ_{pd} and Ψ_{md} were lower in the drought plot than the controls for the majority of 2008 (Fig. 3a, b). Juniper Ψ_{pd} and Ψ_{md} followed the same pattern, but were generally lower than piñon, and were more responsive to changes in Ψ_s than piñon (Figs 3 & 4).

We also observed, at the very end of the 2008 drought, piñon Ψ_{md} which on two days were less-negative than Ψ_{pd}. This occurred on all three plots, when Ψ_s was at the lowest values measured (Fig. 2) and E_s was also close to the minimum. The largest difference ($\Psi_{pd} - \Psi_{md} = \Delta\Psi$) was -0.73 MPa (Fig. 4 inset) and while the $\Delta\Psi$ standard error bars do not overlap with zero, that amount of a rise in Ψ_l during the day could still be within the measurement error. We discuss this pattern below.

Plant water use

Transpiration exhibited clear responses to the drought treatment. Drought plot piñon E_s was lower than either of the control plots' E_s, relative to pre-treatment differences (Table S1 and Fig. 5a, b). The largest differences between drought and control piñon E_s occurred during times of relatively high water availability (Fig. 5a-c), i.e. the end of the 2007 monsoon, early spring 2008, and the 2008 monsoon. Notably, the drought plot piñon had near-zero E_s (E_s< 0.3 mol m^{-2} s^{-2}) from February 2008 until they died in August 2008 (seven months). In contrast, control piñon E_s declined to near-zero in mid-April 2008 and started to rebound in July 2008, at the very beginning of the monsoon season and almost a month before drought plot piñon died (for a total time at minimum E_s of two and a half months). Diurnal patterns of E_s reveal a similar pattern

(Fig. S3a): drought plot piñon had a lower daily maximum E_s and longer period with relatively low E_s. Thus both the seasonal and diurnal time periods of relatively low gas exchange were extended in experimentally droughted piñon compared to controls. Drought plot juniper E_s was also significantly lower than either of the control plots post-treatment, relative to pre-treatment differences (Table S1 and Fig. 5d, e). Similar to piñon, significant differences between drought and control plot juniper E_s were common during the monsoon periods and the early spring of 2008 (April-June, Fig. 5c-e).

Model results

The model calibration succeeded in fitting measured Ψ_{pd} in piñon ($r^2 = 0.82$) and juniper ($r^2 = 0.97$; Fig. S2). The use of measured E_s to predict Ψ_{pd} naturally yielded an excellent inverse prediction of E_{pred} ($r^2 = 0.980$ in piñon, $r^2 = 0.998$ in juniper), providing confidence in the model prediction of E_{crit}. Neither species on either plot was predicted to reach hydraulic failure, i.e. $E_s \geq E_{crit}$. However, piñon approached E_{crit} much more closely than juniper, particularly in the drought plot (Fig. 6a, Fig. 7). The smallest safety margins were observed during the pre-monsoon drought of 2007, when plant water potentials were at the lowest observed values.

Modeled soil-to-canopy hydraulic conductance (K) was generally higher in piñon than juniper (Fig. 6b) within plot. Within species, K was markedly higher on the ambient plot than on the drought plot. Piñon on both plots experienced low K during the pre-monsoon period in 2007, prior to treatment installation. The monsoon coincided with infrastructure installation, and while K recovered in piñon on both plots, the increase was much greater in the ambient plot (Fig. 6b). The higher post-monsoon K in the ambient plot carried over to the following year while K in the drought plot stayed lower. Juniper

did not exhibit a post-monsoon recovery of K in 2007 or 2008, and overall the treatment difference was less pronounced.

Despite the lack of outright hydraulic failure (Fig. 6a), piñon experienced a much greater loss of conductance during the study than juniper, and a treatment effect was seen in both species. Droughted piñon spent over 75% of the measurement days above 70% PLC, and 10% of days above 90% PLC (Fig. 8a). In contrast, the ambient piñon spent 60% of days below 40% PLC and less than 2% of days above 80% PLC, with an average of 43% PLC. Juniper exhibited much lower PLC than piñon, with no days over 50% PLC; PLC averaged 15% for ambient juniper and 38% for droughted juniper (Fig. 8b).

Discussion

Piñon and juniper Ψ_l were consistent with isohydric and anisohydric stomatal regulation, respectively (Fig. 4), and the physiological responses of these species to ecosystem-scale manipulation of precipitation provided support for our hypotheses. Piñon mortality occurred after 11 months of drought treatment. During this time, soil water availability (Figs 2 & 3) and transpiration (Fig. 5) were substantially reduced. Consistent with our hypothesis, trees that died exhibited near-zero E_s for seven continuous months between treatment imposition and mortality, while piñon in other treatments, where no mortality occurred, exhibited similarly low E_s for *ca.* two months (Fig. 5). The hydraulic model did not implicate hydraulic failure as the cause of mortality on the drought plot, but droughted piñon did experience greater loss of soil-canopy hydraulic conductance than ambient piñon and all juniper (Fig. 8). Despite its tight regulation of Ψ_l, piñon's modeled safety margin from E_{crit} was smaller than juniper's (Fig. 6a) within-treatment.

Prolonged stomatal limitation of gas exchange and a more extensive loss of hydraulic conductance are both associated with mortality in this system, suggesting that both mechanisms interact to cause mortality (Sala, Piper & Hoch 2010, McDowell 2011). Droughted piñon exhibited chronically low soil-canopy hydraulic conductance relative to ambient trees, initially because of pre-treatment differences in Ψ_l during the 2007 drought. Ironically, this pre-treatment period was the closest the droughted trees came to hydraulic failure throughout the two years of measurement (Fig. 6a). The most critical effect of the rainout structures may have been to reduce the recovery response of the trees to the monsoon rains; low conductance in droughted piñon carried over into 2008. Over the period of measurement, droughted piñon spent more time with lower hydraulic conductance (Fig. 8), suggesting that hydraulic "impairment" could have contributed to the observed mortality even if hydraulic failure did not occur outright. This hydraulic impairment is reflected in the amount of time spent at near-zero E_s (242 d for drought versus 46 d for cover control and 51 d for ambient control trees). This is a similar period of minimal gas exchange, and probable negative carbon balance, observed during piñon mortality in the same region in 2002-2003 (Breshears *et al.* 2009). Further, even before arriving at near-zero E_s, drought piñon experienced depressed E_s and likely lower storage of carbon relative to control plots (Fig. 5a, 9/07-10/07), meaning that drought piñon had lower carbon reserves going into a longer period of stomatal limitation. One likely connection between carbon limitation and hydraulic failure is the energetic demands of the processes required to reestablish hydraulic function (McDowell 2011), including, but not limited to, xylem refilling and production of new fine roots (Bucci *et al.* 2003, Gaul *et al.* 2008, Salleo *et al.* 2009, Zwieniecki & Holbrook 2009, Kitajima *et al.* 2010,

Olesinski *et al.* 2011). We speculate that any efforts by droughted piñon to recover hydraulic conductance would have resulted in an additional carbon cost at a time when K, E_s, and Ψ_l were all depressed relative to the controls.

Comparison of results to carbon starvation and hydraulic failure hypotheses

Inasmuch as E_s is a proxy for carbon gain, our results are consistent with drought constraining piñon carbon balance in a way that predisposed those trees to successful colonization by bark beetles (Martinez-Vilalta *et al.* 2002, McDowell *et al.* 2008, Breshears *et al.* 2009). Piñon has been shown to experience zero net assimilation at water potentials of -2.3 MPa or lower (Lajtha & Barnes 1991). In our experiment, in the 347 d between treatment imposition and the onset of piñon mortality, drought plot piñon experienced 250 d (or 72%) when none of the measured soil layers were above -2.3 MPa. Cover control piñon experienced 95 d (27%) and ambient control piñon, 130 d (37%) during the same interval. Thus, while piñon under ambient field conditions experience a certain number of days each year when carbon assimilation is likely impossible, our drought treatment significantly extended that period of time with consequences for tree survival. Concurrent direct measurements of native xylem embolism with plant carbon balance, including phloem transport, are required to directly address hydraulic failure and carbon starvation hypotheses (Sala *et al.* 2010, McDowell 2011, Ryan 2011, Hudson *et al.* unpublished manuscript).

While prolonged periods of near-zero E_s are consistent with unfavorable carbon balance contributing to mortality, an alternate hypothesis is that the defense response against bark beetles was limited by low cellular water potentials in trees that died (Fig. 3). The low tissue water potentials observed in the drought piñon could constrain the

autonecrotic responses that exclude beetles from successful entry (Kolb *et al.* 2007, McDowell *et al.* 2011). While it seems clear that carbon and hydraulic constraints to survival were both involved in piñon mortality, further research is required to test the how these factors influence the defensive response during severe drought (Gaylord *et al.* unpublished data).

The added severity of the experimental drought treatment was physiologically significant for juniper because, unlike piñon, it was not already maximally stressed under ambient seasonal drought. The close association between measured Ψ_s and juniper Ψ_{pd} (Fig. 4) indicates that juniper is hydraulically connected to the soil layers we measured. While juniper's greater cavitation resistance may prevent it from completely losing hydraulic conductance under even extreme experimental drought conditions, the temporal and magnitude differences between drought and control treatment E_s on seasonal (Fig. 5) and diurnal (Fig. S3b) timescales suggest that experimentally droughted juniper may also be experiencing depressed carbon uptake. Leaf-level measurements confirm this prediction of lower net photosynthesis in both species under drought treatments (Limousin *et al.* unpublished data). Over extended periods, limits to carbon availability can lead to susceptibility to biotic attack by insects, fungi, or bacteria as a proximal mechanism of mortality (Guarin & Taylor 2005; Millar, Westfall & Delany 2007; Greenwood & Weisberg 2008). Since juniper lacks an insect pathogen with an effect equivalent to that of *I. confusus* in piñon, juniper mortality may only occur when hydraulic failure and/or carbon limitation progress to metabolic dysfunction.

Our results are counter to the prediction that anisohydric species like juniper would be at greater risk of hydraulic failure than isohydric species (McDowell *et al.*

2008). The safety margin between modeled E_{crit} and measured E_s was consistently positive for juniper (Fig. 6a) and, within-plot, greater than piñon's safety margin. However, despite its cavitation resistance (e.g. Pockman & Sperry 2000; West *et al.* 2007b; McDowell *et al.* 2008; Willson *et al.* 2008) and deep rooting (Foxx & Tierney 1987; West *et al.* 2007a), juniper appears unable to recover hydraulic conductance following drought (Fig. 6b). This result is consistent with the literature for *J. osteosperma* (West *et al.* 2007b). Soil drought sufficient for juniper to experience hydraulic failure may require multiple years of treatment to develop.

Anomalous plant water potential measurements

Predawn plant water potentials more-negative than midday water potentials ($\Psi_{pd} < \Psi_{md}$) are not commonly presented, though this pattern has been reported in the literature (e.g. Syvertsen, Cunningham & Feather 1975, Radosevich & Conrad 1980; Baker, Rundel & Parsons 1982; BassiriRad *et al.* 1999). We observed this pattern during the driest periods of measurement, consistent with the observations of Radosevich & Conrad (1980), when plant water potentials were very low and E_s was near zero (Fig. 4 inset). One explanation is the daytime condensation of water vapor in the rhizosphere driven by diurnal thermal gradients in the soil (Syvertsen, Cunningham & Feather 1975). It is also possible that roots refill at night and reestablish contact with dry soils, then cavitate during the day (resulting in hydraulic isolation) and therefore do not reflect the water potential of the soils to which they were previously connected (Sperry & Hacke 2002). Nighttime transpiration is another explanation, but one that we can exclude based on subsequent porometer measurements (data not shown). Finally, it is possible that hydraulic redistribution is occurring at night, and that the Ψ of the canopy (represented by

Ψ_{pd}) is equilibrated with the root crown Ψ, which is somewhere along the flow path between the very dry surface soils and wetter deep soils. This phenomenon warrants further investigation, but unfortunately during the acquisition of this dataset we did not have appropriate instrumentation in place (i.e. bi-directional sap flow sensors, sap flow sensors in roots, or stem psychrometers on roots). The hydraulic model we employed is not parameterized to predict this phenomenon over the time scale of interest (i.e. a single day).

Model performance

Performance of the hydraulic model was limited by three main factors: first, we did not have information about the cavitation vulnerability of leaf and fine root xylem, which has been shown to be more limiting than branch and coarse root xylem in many conifer species (Hacke *et al.* 2000; Brodribb & Cochard 2009). The inclusion of more-vulnerable xylem components in the model would narrow the safety margins for each species.

Second, the relationship between target tree rooting patterns and the location/depth of the soil psychrometers was unknown. Juniper appeared better-coupled to the soil we measured with psychrometers than piñon (Fig. 4), but preliminary efforts to parameterize the model with measured Ψ_s still failed when Ψ_{md} was less-negative than Ψ_s. Observations of $\Psi_{md} > \Psi_s$ may be evidence of hydraulic isolation, which might occur if fine roots in contact with very dry soil die or cavitate. During this period, the oxygen isotope ratio of xylem sap was substantially enriched relative to any source water, further supporting the plausibility of hydraulic isolation (Yepez *et al.* unpublished manuscript). Theoretically, the isohydric strategy combined with hydraulic isolation can result in plant

water potentials which are less negative than Ψ_s. If stomata close to prevent hydraulic failure, and fine root death/cavitation results in hydraulic isolation, then the plant is essentially a closed container, evaporating through its cuticle but otherwise conserving its water potential independent of the soil (Breshears *et al.* 2009, Sevanto *et al.* in prep). Positive sap flow measurements during this time contradict complete hydraulic isolation, however, and deep roots have been shown to be an important source of water in a variety of environments (e.g. Markewitz *et al.* 2010). Ultimately, the preponderance of evidence suggested that trees at this site had access to soil compartments deeper and wetter than those measured directly, so Ψ_{pd} was used as an integrated measure of the soils to which the trees were hydraulically connected.

Finally, there is a degree of uncertainty regarding measurements made with thermal dissipation probes which would confound efforts to fit modeled E_{pred} to measured E_s. Most relevant to our conclusions, the probes may overestimate low sap flow (Burgess, Adams & Bleby 2000; Burgess *et al.* 2001; R. Pangle unpublished data), and it is also possible that the minimum measured E_s may be a function of phloem-driven circulation rather than transpiration-driven water loss (Hölttä et al. 2006; McDowell & Sevanto 2010). We also did not measure radial variation in sap flux density, but we are not scaling to whole-tree or stand water use and sap flux density tends to be greater closer to the cambium (Cohen *et al.* 2008). Accounting for the lower sap flux density, either because of radial variation or poor sensitivity at low flows, would lower the average E_s; fitting E_{pred} to lower E_s would likely lower E_{crit} as well. It is difficult to tell whether this would result in predicted hydraulic failure because both parameters would shift in the same direction.

Ecosystem manipulation performance

The drought manipulation study described here was particularly effective for some aspects of the study of mortality mechanisms. Perhaps the most critical value of this study is that most of the piñon trees in the drought treatment died; very few studies of drought effects arrive at that end-point, which greatly limits our ability to infer mortality mechanisms (McDowell & Sevanto 2010). An additional value of the study is that our drought treatment accurately imitated the impact on piñon Ψ_{pd} of the 2000-2003 regional drought in southwestern USA that resulted in widespread piñon mortality. The 2002 piñon mortality event followed 10 months with Ψ_{pd} below -2 MPa and an associated negative carbon balance (Breshears *et al.* 2005, 2009). Our experimental drought produced Ψ_{pd} at or below the threshold for zero carbon gain for a total of eight months, in comparison to only six months for the control plots (Fig. 3).

The manipulation described here also has limitations for the study of mortality mechanisms. Though we accurately manipulated soil water during drought, we did not intentionally or systematically manipulate temperature (Pangle *et al.* in press). Drought typically results in both reduced precipitation and elevated temperatures (Breshears *et al.* 2005), and the latter may be a critical driver of mortality through its impacts on respiration and vapor pressure deficit (McDowell *et al.* 2008; Adams *et al.* 2009). To truly discriminate between mortality mechanisms one must understand not only hydraulic limits, but also the carbon balance of trees including non-structural carbohydrates, phloem transport, and defense compounds (Hölttä *et al.* 2009; McDowell & Sevanto 2010; Sala *et al.* 2010). Studies to address all of these aspects are ongoing and will provide valuable insight into mortality mechanisms.

Acknowledgments

We gratefully acknowledge the efforts of Jim Elliot, Monica Gaylord, Julie Glaser, Jennifer Johnson, Sam Markwell, Clif Meyer, Matt Spinelli, and numerous undergraduate assistants in the implementation of this experiment and collection of much of the data. Rosie Fisher, Sanna Sevanto, Jean-Marc Limousin and two anonymous reviewers provided valuable input. This project was supported by an award to NGM and WTP from the Department of Energy's Office of Science (BER) and to JP by the National Science Foundation's Graduate Research Fellowship Program. The project was also supported by the resources and staff of the Sevilleta LTER (funded by NSF DEB 0620482) and Sevilleta Field Station at the University of New Mexico.

References

Adams HD, Guardiola-Claramonte M, Barron-Gafford GA, Villegas JC, Breshears DD, Zou CB, Troch PA, Huxman TE. 2009. Temperature sensitivity of drought-induced tree mortality portends increased regional die-off under global-change-type drought. *Proceedings of the National Academy of Sciences USA* **106**: 7063–7066.

Allen CD, Macalady A, Chenchouni H, Bachelet D, McDowell N, Vennetier M, Gonzales P, Hogg T, Rigling A, Breshears D, *et al.* 2010. A global overview of drought and heat-induced tree mortality reveals emerging climate change risks for forests. *Forest Ecology and Management* **259**: 660–684.

Baker GA, Rundel PW, Parsons DJ. 1982. Comparative phenology and growth in three chaparral shrubs. *Botanical Gazette* **143:** 94-100.

BassiriRad H, Tremmel DC, Virginia RA, Reynolds JF, de Soyza AG, Brunell MH. 1999. Short-term patterns in water and nitrogen acquisition by two desert shrubs following a simulated summer rain. *Plant Ecology* **145:** 27-36.

Bigler C, Gavin DG, Gunning C, Veblen TT. 2007. Drought induces lagged tree mortality in a subalpine forest in the Rocky Mountains. *Oikos* **116:** 1983-1994.

Bonal D, Bosc A, Ponton S, Goret J-Y, Burban B, Gross P, Bonnefond J-M, Elbers J, Longdoz B, Epron D, *et al.* 2008. Impact of severe dry season on net ecosystem exchange in the Neotropical rainforest of French Guiana. *Global Change Biology* **14:** 1917-1933.

Breshears DD, Cobb NS, Rich PM, Price KP, Allen CD, Balice RG, Romm WH, Kastens JH, Floyd, ML, Belnap J, *et al.* 2005. Regional vegetation die-off in

response to global-change-type drought. *Proceedings of the National Academy of Sciences of the United States of America* **102:** 15144-15148.

Breshears DD, Myers OB, Meyer CW, Barnes FJ, Zou CB, Allen CD, Mcdowell NG, Pockman WT. 2009. Tree die-off in response to global change-type drought: mortality insights from a decade of plant water potential measurements. *Frontiers in Ecology and the Environment* **7:** 185-189.

Brodribb TJ, Cochard H. 2009. Hydraulic failure defines the recovery and point of death in water-stressed conifers. *Plant Physiology* **149**: 575-584.

B**rodribb TJ, Holbrook NM.** 2003. Changes in leaf hydraulic conductance during leaf shedding in seasonally dry tropical forest. *New Phytologist* **158:** 295-303.

Bucci SJ, Scholz FG, Goldstein G, Meinzer FC, Sternberg LDSL. 2003. Dynamic changes in hydraulic conductivity in petioles of two savanna tree species: factors and mechanisms contributing to the refilling of embolized vessels. *Plant, Cell & Environment* **26**: 1633–1645.

Burgess SSO, Adams MA, Bleby TM. 2000. Measurement of sap flow in roots of woody plants: a commentary. *Tree Physiology* **20:** 909-913.

Burgess SSO, Adams MA, Turner NC, Beverly CR, Ong CK, Khan AAH, Bleby TM. 2001. An improved heat pulse method to measure low and reverse rates of sap flow in woody plants. *Tree Physiology* **21:** 589-598.

Bush SE, Hultine KR, Sperry JS, Ehleringer JR. 2010. Calibration of thermal dissipation sap flow probes for ring- and diffuse-porous trees. *Tree Physiology* **30**: 1545–1554.

Campbell GS. 1985. *Soil Physics with Basic; Transport Models for Soil-Plant Systems.* Elsevier Science Publishers, Amsterdam.

Chansler JF. 1964. Overwintering habits of *Ips lecontei* Sw.and *Ips confusus* (Lec.) in Arizona and New Mexico. U.S. Department of Agriculture Forest Service, Rocky Mountain Forest and Range Experiment Station, Fort Collins, CO.

Clearwater MJ, Meinzer FC, Andrade JL, Goldstein G, Holbrook NM. 1999. Potential errors in measurement of nonuniform sap flow using heat dissipation probes. *Tree Physiology* **19:** 681-687.

Cochard H. 2002. A technique for measuring xylem hydraulic conductance under high negative pressures. *Plant Cell and Environment* **25**, 815-819.

Cochard H, Coll L, Le Roux X, Ameglio T. 2002. Unraveling the effects of plant hydraulics on stomatal closure during water stress in walnut. *Plant Physiology* **128:** 282-290.

Cochard H, Damour G, Bodet C, Tharwat I, Poirier M, Ameglio T. 2005. Evaluation of a new centrifuge technique for rapid generation of xylem vulnerability curves. *Physiologia Plantarum* **124**: 410-418.

Cohen Y, Cohen S, Cantuarias-Aviles T, Schiller G. 2008. Variations in the radial gradient of sap velocity in trunks of forest and fruit trees. *Plant and Soil* **305**: 49–59.

Domec J, King JS, Noormets A, Treasure E, Gavazzi MJ, Sun G, McNulty SG. 2010. Hydraulic redistribution of soil water by roots affects whole-stand evapotranspiration and net ecosystem carbon exchange. *New Phytologist* **187:**171-183.

Ewers BE, Oren R, Sperry JS. 2000. Influence of nutrient versus water supply on hydraulic architecture and water balance in Pinus taeda. *Plant Cell and Environment* **23:** 1055-1066.

Fensham RJ, Fairfax RJ, Ward DP. 2009. Drought-induced tree death in savanna. *Global Change Biology* **15:** 380-387.

Floyd ML, Clifford M, Cobb NS, Hanna D, Delph R, Ford P, Turner D. 2009. Relationship of stand characteristics to drought-induced mortality in three Southwestern pinon-juniper woodlands. *Ecological Applications* **19:** 1223-1230.

Foxx TS, Tierney GD. 1987. Rooting patterns in the pinyon-juniper woodlans. *Proceedings: pinyon–juniper conference*, pp. 69-79. U.S. Department of Agriculture, Forest Service, Intermountain Research Station, Reno, NV, USA, Reno, NV, USA.

Friedlingstein P, Cox P, Betts R, Bopp L, von Bloh W, Brovkin V, Cadule P, Doney S, Eby M, Fung I, *et al.* (2006) Climate-carbon cycle feedback analysis: Results from the C^4MIP model intercomparison. *Journal of Climate* **19:** 3337-3353.

Galvez DA, Tyree MT. 2009. Impact of simulated herbivory on water relations of aspen (*Populus tremuloides*) seedlings: the role of new tissue in the hydraulic conductivity recovery cycle. *Oecologia* **161:** 665-671.

Gaul, D, Hertel D, Borken W, Matzner E, Leuschner C. 2008. Effects of experimental drought on the fine root system of mature Norway spruce. *Forest Ecology and Management* **256:** 1151–1159.

Goulden ML, Field CB. 1994. Three methods for monitoring the gas exchange of individual tree canopies – ventilated- chamber, sap-flow and Penman-Monteith measurements on evergreen oaks. *Functional Ecology* **8**: 125–135.

Granier A. 1987. Evaluation of transpiration in a Douglas-fir stand by means of sap flow measurements. *Tree Physiology* **3:** 309–319.

Greenwood DL, Weisberg PJ. 2008. Density-dependent tree mortality in pinyon-juniper woodlands. *Forest Ecology and Management* **255:** 2129-2137.

Guarin A, Taylor AH. 2005. Drought triggered tree mortality in mixed conifer forests in Yosemite National Park, California, USA. *Forest Ecology and Management* **218:** 229-244.

Hacke UG, Sperry JS, Ewers BE, Ellsworth DS, Schafer KVR, Oren R. 2000. Influence of soil porosity on water use in Pinus taeda. *Oecologia* **124:** 495-505.

Horner GJ, Baker PJ, Mac Nally R, Cunningham SC, Thomson JR, Hamilton F. 2009. Mortality of developing floodplain forests subjected to a drying climate and water extraction. *Global Change Biology* **15:** 2176-2186.

Hölttä T, Vesala T, Sevanto S, Perämäki M, Nikenmaa E. 2006. Modeling xylem and phloem water flows in trees according to cohesion theory and Münch hypothesis. *Trees* **20:** 67-78.

Hölttä T, Cochard H, Nikinmaa E, Mencuccini M. 2009. Capacitive effect of cavitation in xylem conduits: results from a dynamic model. *Plant, Cell & Environment* **32:** 10-21.

Iovi K, Kolovou C, Kyparissis A. 2009. An ecophysiological approach of hydraulic performance for nine Mediterranean species. *Tree Physiology* **29:** 889-900.

IPCC. 2007. Climate Change 2007: The physical science basis. Contribution of Working Group I to the Fourth Assessment Report of the Intergovernmental Panel on Climate Change. pp. 1009. Cambridge University Press, Cambridge.

Kaufmann MR, Thor GL. 1982. Measurement of water stress in subalpine trees: effects of temporary tissue storage methods and needle age. *Canadian Journal of Forest Research* **12:** 969-972.

Kitajima K, Anderson KE, Allen MF. 2010. Effect of soil temperature and soil water content on fine root turnover rate in a California mixed conifer ecosystem. *Journal of Geophysical Research: Biogeosciences* 115: G04032, doi:10.1029/2009JG001210.

Kolb TE, Agee JK, Fulé PZ, McDowell NG, Pearson K, Sala A, Waring RH. 2007. Perpetuating old ponderosa pine. *Forest Ecology and Management* **249:** 141-157.

Kolb TE, Holmberg KM, Wagner MR, Stone JE. 1998. Regulation of ponderosa pine foliar physiology and insect resistance mechanisms by basal area treatments. *Tree Physiology* **18:** 375-381.

Lajtha K, Barnes FJ. 1991. Carbon gain and water-use in pinyon pine-juniper woodlans of northern New Mexico - field versus phytotron chamber measurements. *Tree Physiology* **9:** 59-67.

Li YY, Sperry JS, Taneda H, Bush SE, Hacke UG. 2008. Evaluation of centrifugal methods for measuring xylem cavitation in conifers, diffuse- and ring-porous angiosperms. *New Phytologist* **177:** 558-568.

Linton MJ, Sperry JS, Williams DG. 1998. Limits to water transport in *Juniperus osteosperma* and *Pinus edulis*: implications for drought tolerance and regulation of transpiration. *Functional Ecology* **12**: 906-911.

Markewitz D, Devine S, Davidson EA, Brando P, Nepstad DC. 2010. Soil moisture depletion under simulated drought in the Amazon: impacts on deeproot uptake. *New Phytologist* **187:** 592-607.

Martínez-Vilalta J, Pinol J, Beven K. 2002. A hydraulic model to predict drought-induced mortality in woody plants: an application to climate change in the Mediterranean. *Ecological Modeling* **155:** 127-147.

McDowell N, Pockman WT, Allen CD, Breshears DD, Cobb N, Kolb T, Plaut J, Sperry J, West A, Williams DG *et al.* 2008. Mechanisms of plant survival and mortality during drought: why do some plants survive while others succumb to drought? *New Phytologist* **178**, 719–739.

McDowell NG, Sevanto S. 2010. The mechanisms of carbon starvation: how, when, or does it even occur at all? *New Phytologist* **186**: 264-266.

McDowell NG. 2011. Mechanisms linking drought, hydraulics, carbon metabolism, and vegetation mortality. *Plant Physiology* **155**: 1051-1059.

McDowell NG, Beerling D, Breshears D, Fisher R, Raffa K, Stitt M. 2011. Interdependence of mechanisms underlying climate-driven vegetation mortality. *Trends in Ecology and Evolution*, **26**: 523-532.

Millar CI, Westfall RD, Delany DL. 2007. Response of high-elevation limber pine (Pinus flexilis) to multiyear droughts and 20th-century warming, Sierra Nevada, California, USA. *Canadian Journal of Forest Research* **37:** 2508-2520.

Neufeld HS, Grantz DA, Meinzer FC, Goldstein G, Crisosto GM, Crisosto C. 1992. Genotypic variability in vulnerability of leaf xylem to cavitation in water-stressed and well-irrigated sugarcane. *Plant Physiology* **100:** 1020-1028.

Olesinski J, Lavigne MB, Krasowski MJ. 2011. Effects of soil moisture manipulations on fine root dynamics in a mature balsam fir (*Abies balsamea* L. Mill.) forest. *Tree Physiology* **31:** 339-348.

Pangle RE, Hill JP, Plaut JA, Yepez EA, Elliot JR, Gehres N, McDowell NG, Pockman WT. 2012. Methodology and performance of a rainfall manipulation experiment in a piñon-juniper woodland. *Ecosphere* **3**: 28.

Phillips N, Oren R. 2001. Intra- and inter-annual variation in transpiration of a pine forest. *Ecological Applications* **11:** 385-396.

Pockman WT, Sperry JS. 2000. Vulnerability to xylem cavitation and the distribution of Sonoran desert vegetation. *American Journal of Botany* **87:** 1287-1299.

Radosevich SR, Conard SG. 1980. Physiological control of chamise shoot growth after fire. *American Journal of Botany* **67:** 1442-1447.

Resco V, Ewers BE, Sun W, Huxman TE, Weltzin JF, Williams DG. 2009. Drought-induced hydraulic limitations constrain leaf gas exchange recovery after precipitation pulses in the C_3 woody legume, *Prosopis velutina*. *New Phytologist* **181**: 672-682.

Ryan MG. 2011. Tree responses to drought. *Tree Physiology* **31:** 237-239.

Sala A, Piper F, Hoch G. 2010. Physiological mechanisms of drought-induced tree mortality are far from being resolved. *New Phytologist* **186**: 274–281

Salleo S, Trifilo P, Esposito S, Nardini A, LoGullo M. 2009. Starch-to-sugar conversion in wood parenchyma of field-growing Laurus nobilis plants: a component of the signal pathway for embolism repair? *Functional Plant Biology* **36**: 815–825.

Sitch S, Huntingford C, Gedney N, Levy PE, Lomas M, Piao SL, Betts R, Ciais P, Cox P, Friedlingstein P, *et al.* 2008. Evaluation of the terrestrial carbon cycle, future plant geography and climate-carbon cycle feedbacks using five Dynamic Global Vegetation Models (DGVMs). *Global Change Biology* **14:** 2015-2039.

Snyder KA, Richards JH, Donovan LA. 2003. Night-time conductance in C-3 and C-4 species: do plants lose water at night? *Journal of Experimental Botany* **54:** 861-865.

Sparks JP, Black RA. 1999. Regulation of water loss in populations of Populus trichocarpa: the role of stomatal control in preventing xylem cavitation. *Tree Physiology* **19:** 453-459.

Sperry JS, Adler FR, Campbell GS, Comstock JP. 1998. Limitation of plant water use by rhizosphere and xylem conductance: results from a model. *Plant, Cell and Environment* **21:** 347– 359.

Sperry JS, Donnelly JR, Tyree MT. 1988. A method for measuring hydraulic conductivity and embolism in xylem. *Plant Cell and Environment* **11:** 35-40.

Sperry JS, Hacke UG. 2002. Desert shrub water relations with respect to soil characteristics and plant function type. *Functional Ecology* **16:** 367-378.

Sperry JS, Hacke UG, Oren R, Comstock JP. 2002. Water deficits and hydraulic limits to leaf water supply. *Plant, Cell & Environment* **25:** 251–263.

Stone JE, Kolb TE, Covington WW. 1999. Effects of restoration thinning on presettlement *Pinus ponderosa* in northern Arizona. *Restoration Ecology* **7:** 172-182.

Suarez ML, Ghermandi L, Kitzberger T. 2004. Factors predisposing episodic drought-induced tree mortality in Nothofagus - site, climatic sensitivity and growth trends. *Journal of Ecology* **92:** 954-966.

Syvertsen JP, Cunningham GL, Feather TV. 1975. Anomalous diurnal patterns of stem xylem water potentials in *Larrea tridentata*. *Ecology* **56:** 1423-1428,

Tardieu F, Simonneau T. 1998. Variability among species of stomatal control under fluctuating soil water status and evaporative demand: modelling isohydric and anisohydric behaviours. *Journal of Experimental Botany* **49**: 419-432.

Tyree MT, Sperry JS. 1988. Do woody plants operate near the point of catastrophic xylem dysfunction caused by dynamic water stress? Answers from a model. *Plant Physiology* **88:** 574-580.

van Genuchten MT. 1980. A closed-form equation for predicting the hydraulic conductivity of unsaturated soils. *Soil Science Society of America Journal* **44**: 892-898.

West AG, Hultine KR, Burtch KG, Ehleringer JR. 2007a. Seasonal variations in moisture use in a pinon-juniper woodland. *Oecologia* **153:** 787-798.

West AG, Hultine KR, Jackson TL, Ehleringer JR. 2007b. Differential summer water use by *Pinus edulis* and *Juniperus osteosperma* reflects contrasting hydraulic characteristics. *Tree Physiology* **27:** 1711-1720.

West AG, Hultine KR, Sperry JS, Bush SE, Ehleringer JR. 2008. Transpiration and hydraulic strategies in a pinon-juniper woodland. *Ecological Applications* **18:** 911-927.

Willson CJ, Manos PS, Jackson RB. 2008. Hydraulic traits are influenced by phylogenetic history in the drought-resistant, invasive genus *Juniperus* (Cupressaceae). *American Journal of Botany* **95:** 299-314.

Wood SL. 1982. The bark and ambrosia beetles of North and Central America (Coleoptera: Scolytidae), a taxonomic monograph. Brigham Young University, Provo, UT.

Worrall JJ, Egeland L, Eager T, Mask RA, Johnson EW, Kemp PA, Shepperd WD. 2008. Rapid mortality of Populus tremuloides in southwestern Colorado, USA. *Forest Ecology and Management* **255:** 686-696.

Zwieniecki MA, Holbrook NM. 2009. Confronting Maxwell's demon: biophysics of xylem embolism repair. *Trends in Plant Science* **14**: 530–534.

Table 1. List of symbols

Symbol		*Units*
E	transpiration	
E_s	sapwood-specific transpiration	mol m^{-2} s^{-1} expressed on a sapwood area basis
E_{pred}	sapwood-specific transpiration predicted by the hydraulic model	mol m^{-2} s^{-1} expressed on a sapwood area basis
E_{crit}	critical transpiration rate which, if allowed to reach steady state, would result in hydraulic failure somewhere in the soil-plant-atmosphere continuum	mol m^{-2} s^{-1} expressed on a sapwood area basis
J_s	sap flux density	g m^{-2} s^{-1}
K	soil-to-canopy hydraulic conductance	mol m^{-2} s^{-1} MPa^{-1}
K_{pred}	soil-to-canopy conductance predicted by the hydraulic model at Ψ_{md} for a $\Delta\Psi$ of 0.2 MPa	mol m^{-2} s^{-1} MPa^{-1}
Ψ_l	leaf water potential	MPa
Ψ_{pd}	pre-dawn leaf water potential	MPa
$\Psi_{pd\text{-}pred}$	pre-dawn leaf water potential predicted by the hydraulic model using K_{pred} and interpolated Ψ_{md}	MPa
Ψ_{md}	midday leaf water potential	MPa
Ψ_{crit}	critical leaf water potential which would result in hydraulic failure somewhere in the soil-plant-atmosphere continuum	MPa
$\Delta\Psi$	difference between pre-dawn and midday water potential	MPa
Ψ_s	soil water potential	MPa
ΔT	difference between heated and unheated sap flow probes, corrected for the ambient axial temperature difference	°C
ΔT_{max}	maximum daily temperature difference between heated an unheated sap flow probes, representing conditions of zero flow	°C

Table 2. Stand structure data. Data presented are means and standard errors based on measurements in four 1600 m^2 plots.

Species	individuals ha^{-1}	basal area, m^2 ha^{-1}	crown area, m^2 ha^{-1}	height, m
Piñon	140.6 ± 38.7	4.3 ± 1.0	1170 ± 159	2.8 ± 0.2
Juniper	296.9 ± 43.0	28.2± 3.7	2635 ± 185.6	2.7 ± 0.1

Table 3. Model input parameters. Items preceded by an asterisk are calculated by the model but used as inputs. Ψ_e = -0.5(GMD)^-0.5 (Campbell 1985)

Parameter	Ambient piñon	Ambient juniper	Drought piñon	Drought juniper
Soil geometric mean particle size, mm	0.032	0.032	0.032	0.032
Geometric standard deviation of particle size	4.63	4.63	4.63	4.63
Soil bulk density	1.27	1.27	1.27	1.27
Silt fraction	0.4	0.4	0.4	0.4
Clay fraction	0.06	0.06	0.06	0.06
*Air entry potential, Ψ_e, MPa	-2.52	-2.52	-2.52	-2.52
*k_s, mol s^{-1} MPa^{-1} m^{-1} (saturated soil conductivity)	40.75	40.75	40.75	40.75
*b (soil texture parameter)	6.52	6.52	6.52	6.52
Branch Weibull b parameter	3.43	12.52	3.43	12.52
Branch Weibull c parameter	1.65	3.48	1.65	3.48
Root Weibull b	3.56	10.05	3.56	10.05
Root Weibull c	4.07	4.19	4.07	4.19
E_s at saturated k_l	0.69-2.65	0.9	0.8-1.2	0.6-0.8
*Saturated k_l, mol s^{-1} m^{-2} MPa^{-1}	0.6-2.3	1.04	0.92-1.38	0.69-0.92
LAI	1	1	1	1
A_r:A_l	3	3	3	3
r^2 of E_s:E_{pred}	0.99	0.998	0.87	0.995

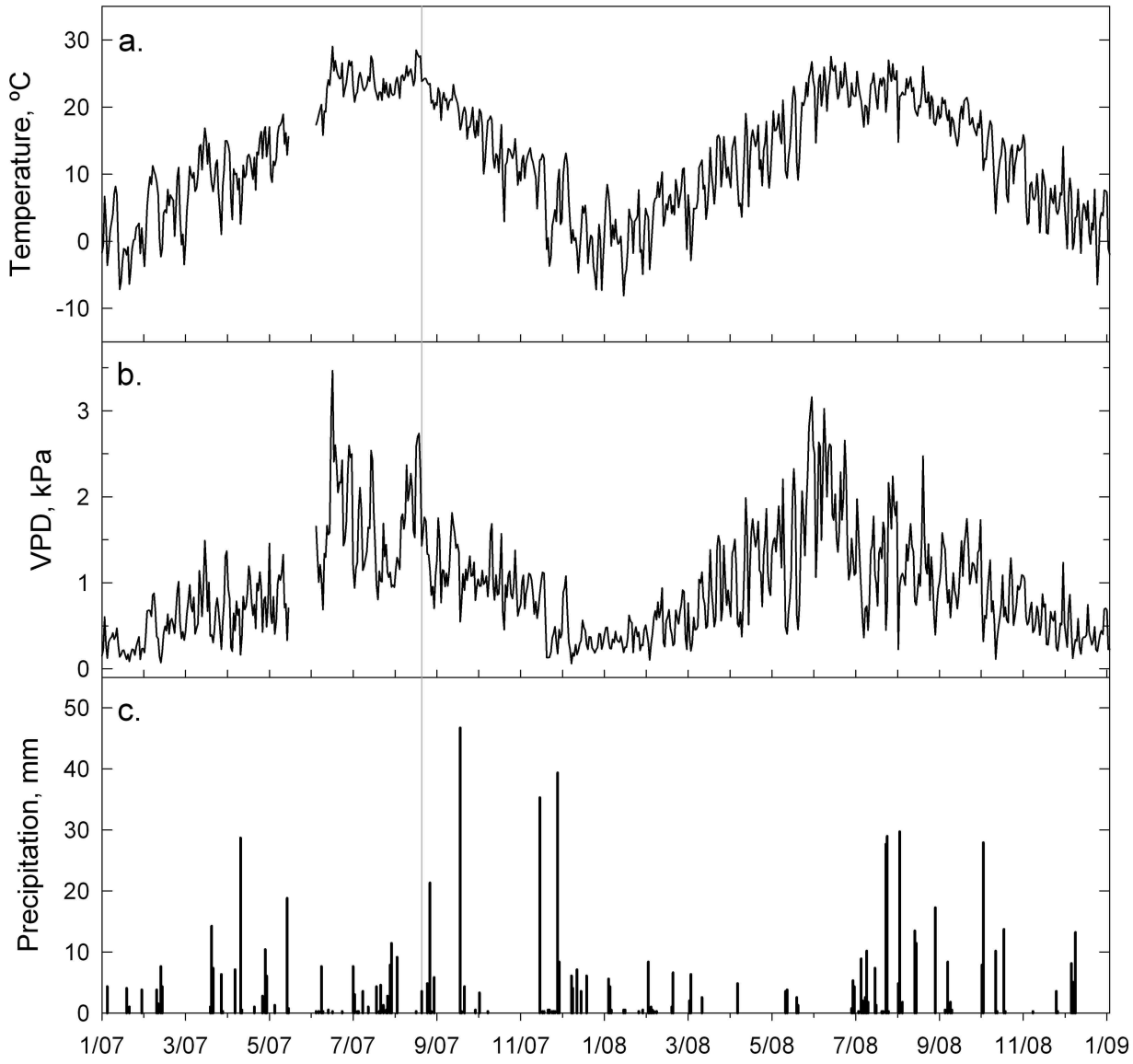

Figure 1. Climate data over the study period showing (a) mean daily temperature, (b) mean daily vapor pressure deficit (VPD), and (c) precipitation events. Vertical lines indicate initiation of treatments.

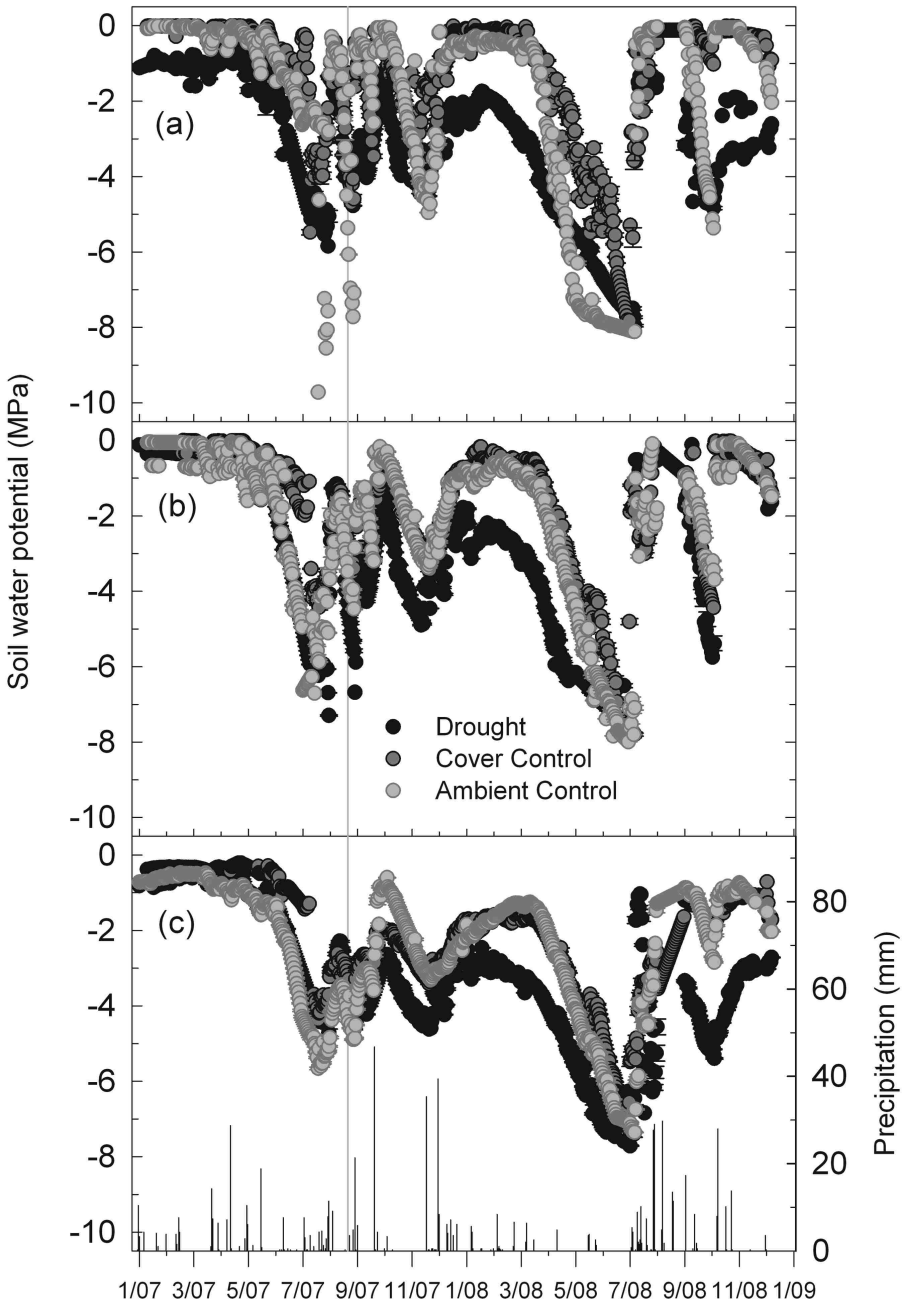

Figure 2. Soil water potential at (a) 15 cm, (b) 20 cm, and (c) 50-100 cm for the drought (black), cover control (dark gray) and ambient control (light gray) treatments. Symbols are the mean of 15 sensors ± standard error, weighted by cover type (piñon, juniper, intercanopy). Vertical lines indicate initiation of treatments.

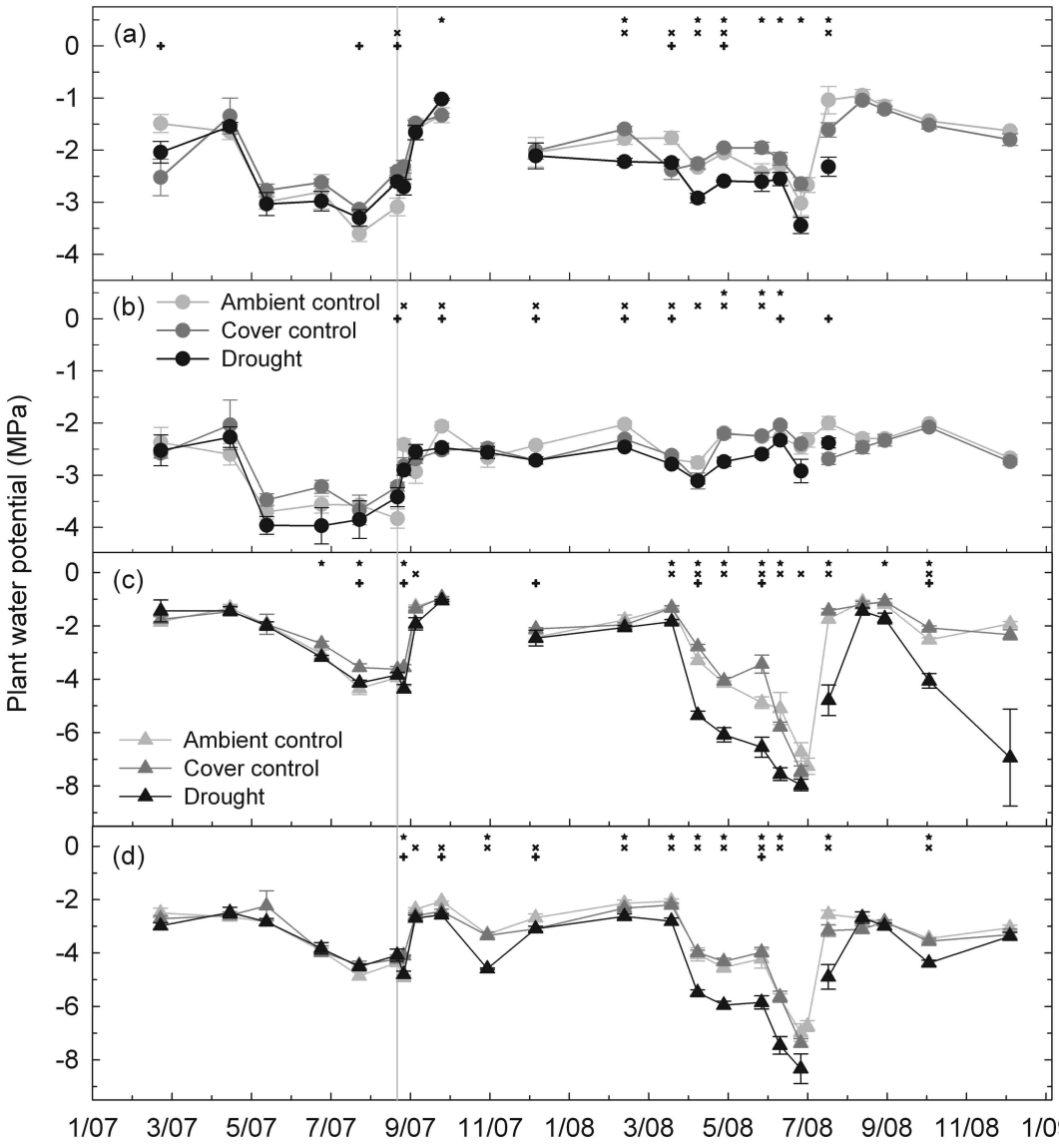

Figure 3. Plant water potentials: (a) piñon Ψ_{pd}, (b) piñon Ψ_{md}, (c) juniper Ψ_{pd}, and (d) juniper Ψ_{md} for trees in the drought (black symbols), cover control (dark gray) and ambient control (light gray) treatments. Symbols are the means of 5 trees ± standard error for piñon (circles) and juniper (triangles). Differences between treatments significant at the $P = 0.05$ level are indicated for the comparisons between drought and cover control

(★), drought and ambient control (×), and cover and ambient controls (+). Vertical lines indicate the initiation of treatments.

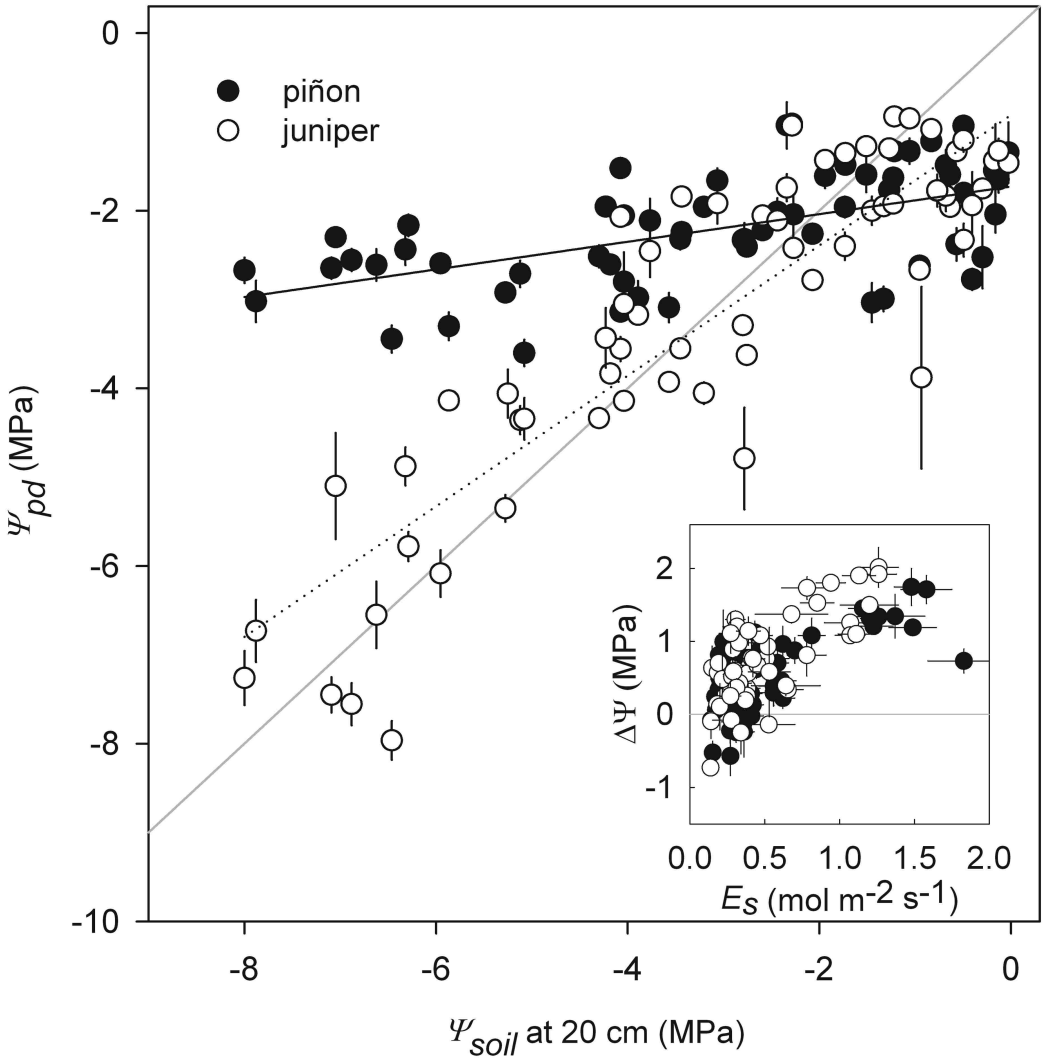

Figure 4. Ψ_{pd} response to Ψ_s (measured at 20 cm) for piñon (filled symbols, black line) and juniper (open symbols, dotted line). The 1:1 relationship is shown by the gray line. Inset shows $\Delta\Psi$ ($\Psi_{pd} - \Psi_{md}$) plotted against E_s with symbols as in the main figure. Error bars are standard error of the means. For piñon, $y = -1.73 + 0.156x$, $r^2 = 0.31$; for juniper $y = -0.92 + 0.73x$, $r^2 = 0.78$.

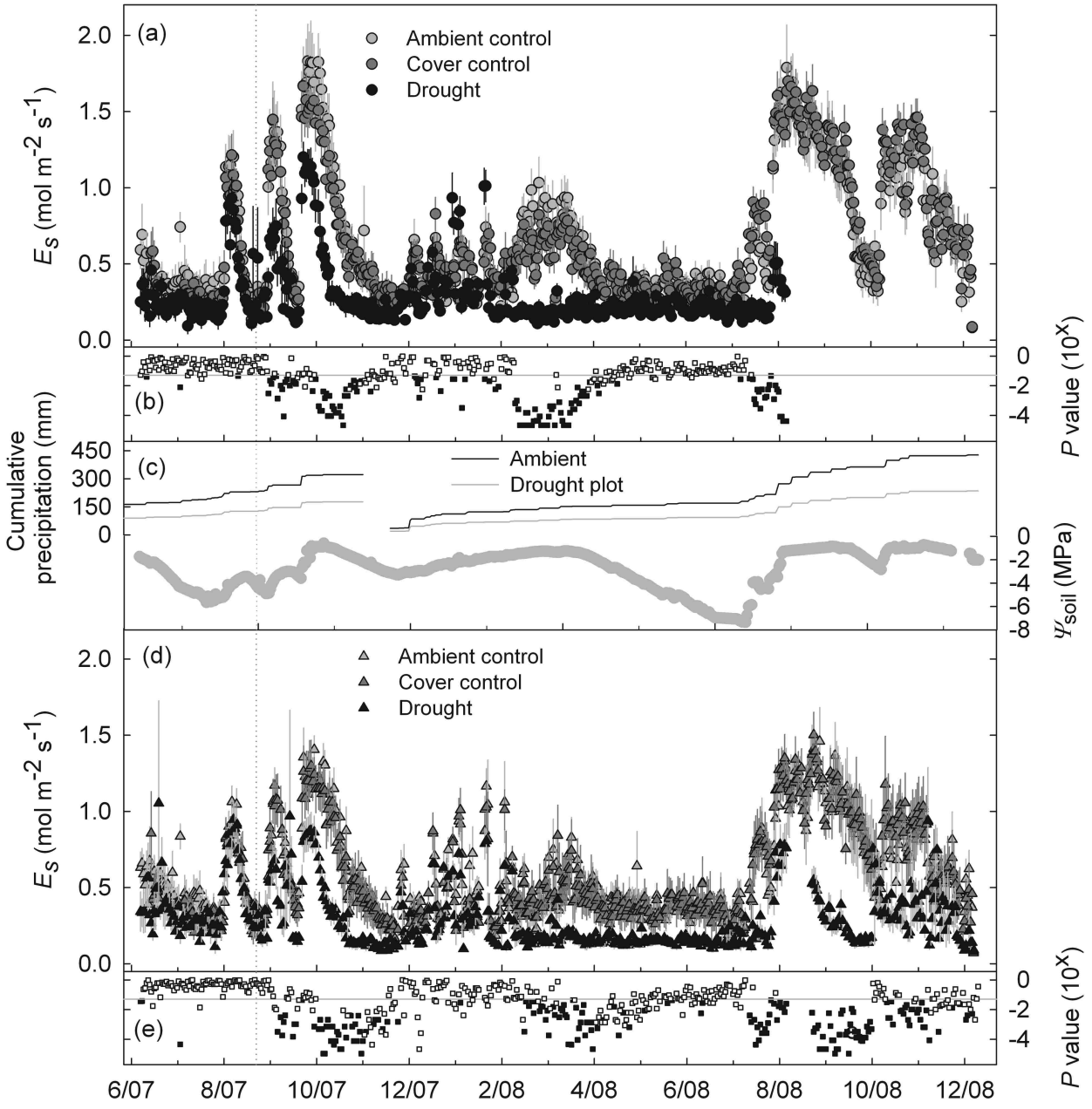

Figure 5. Time series of treatment effect on plant transpiration (E_s) in (a) piñon pine and (d) juniper. Symbols are the means of 5 trees ± standard error of the mean for drought (black), cover control (dark gray), and ambient control (light gray) treatments. T-test results for comparisons of daily maximum E_s shown in (b) and (e), showing where drought plot is significantly different from ambient control (below horizontal line, which

represents $P = 0.05$), ambient and cover controls (filled symbols) or neither of the controls (opens symbols above horizontal line). Panel (c) shows cumulative precipitation at the micrometeorological station (black line) and as calculated in the drought plot (gray line), and ambient control plot Ψ_s at 40-100 cm depth. Dotted vertical line indicates initiation of treatments.

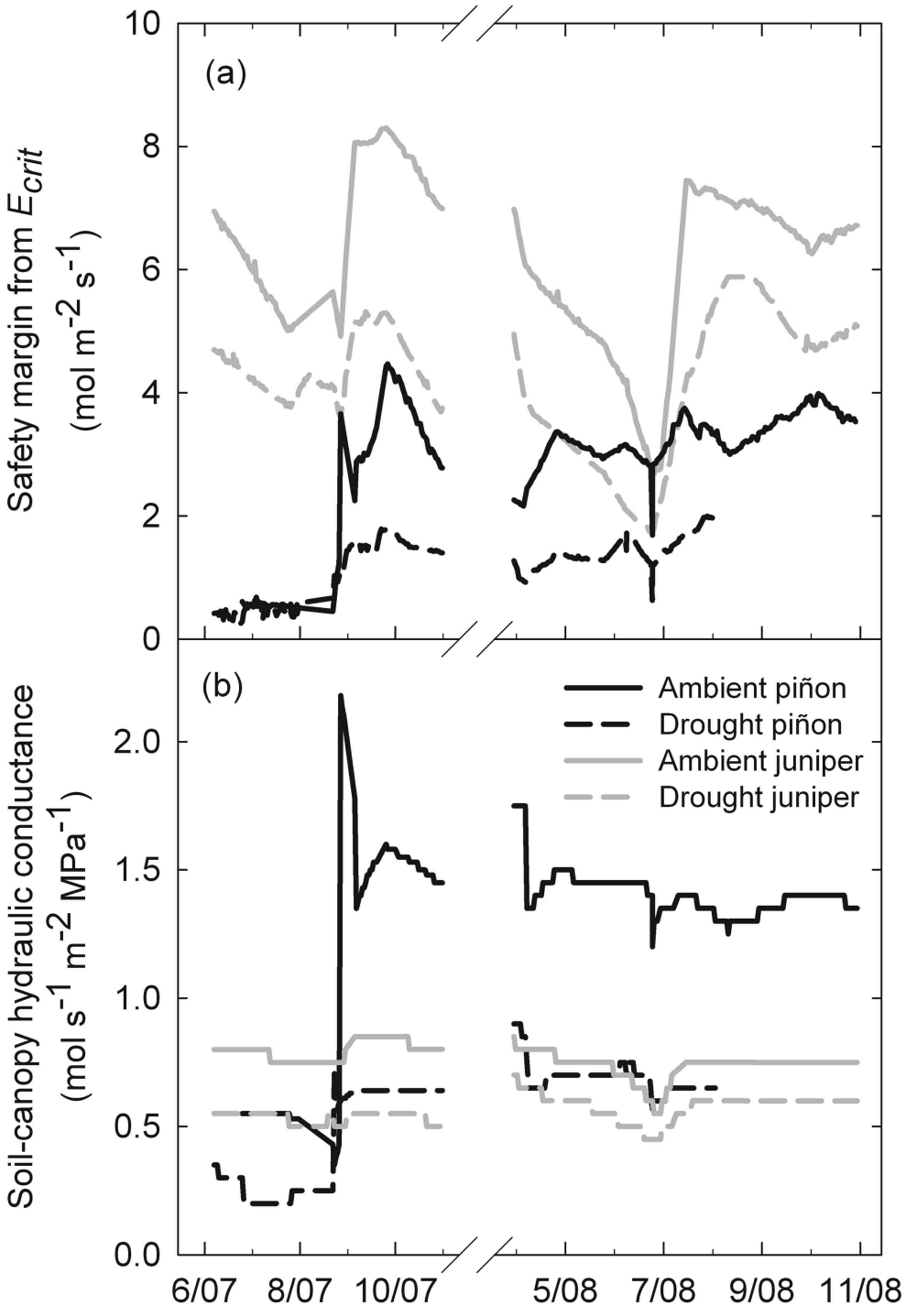

Figure 6. Time series of soil-canopy hydraulic conductance (a) and the safety margin between E_s and E_{crit} (b) for piñon (black lines) and juniper (gray lines) on the ambient (solid) and drought (dashed) plots.

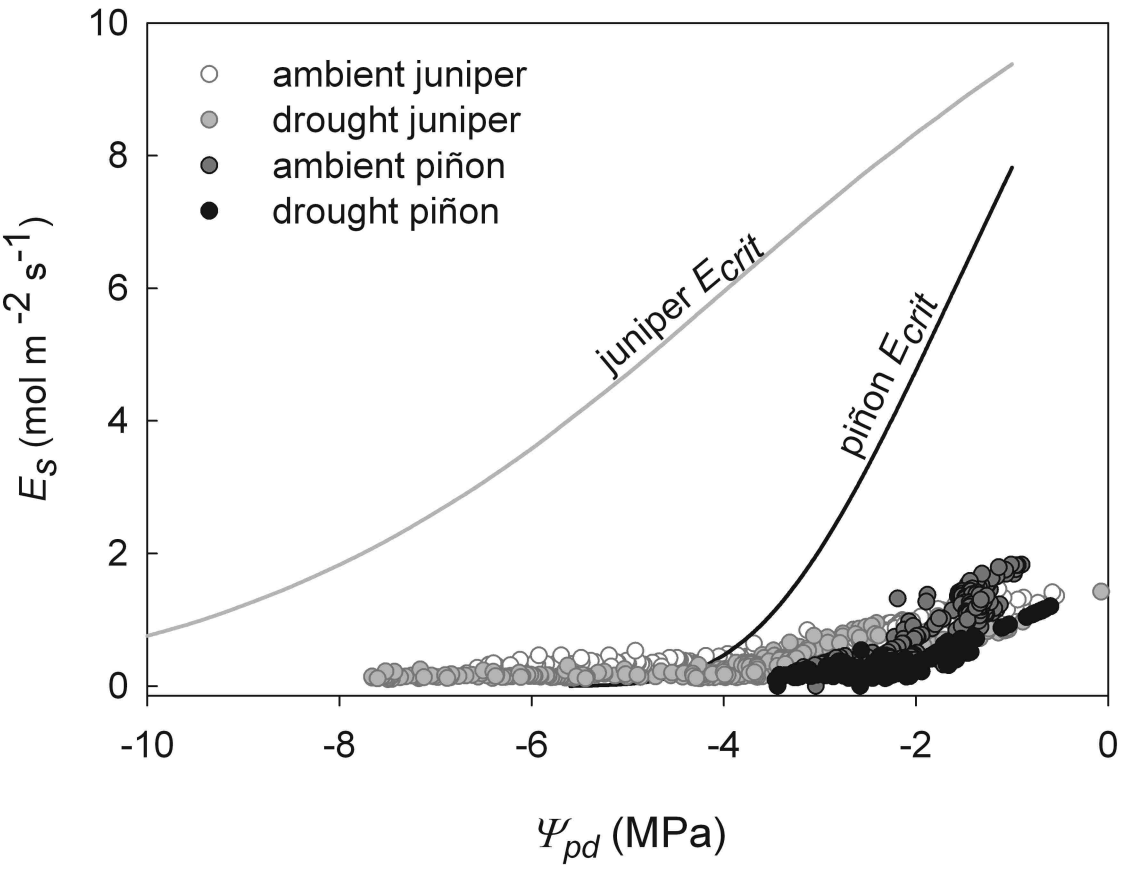

Figure 7. Maximum "envelopes" for steady-state sap flow per sapwood area (E_{crit}) as a function of predawn water potential. Curves indicate maximum values based on the maximum K_{sat} required for model calibration across years and treatments for each species (juniper, gray; piñon, black). Data points represent individual measurement days during the two years of monitoring for both ambient and droughted plots (juniper: open symbols, ambient control; light gray, drought; piñon: dark gray, ambient control; black, drought).

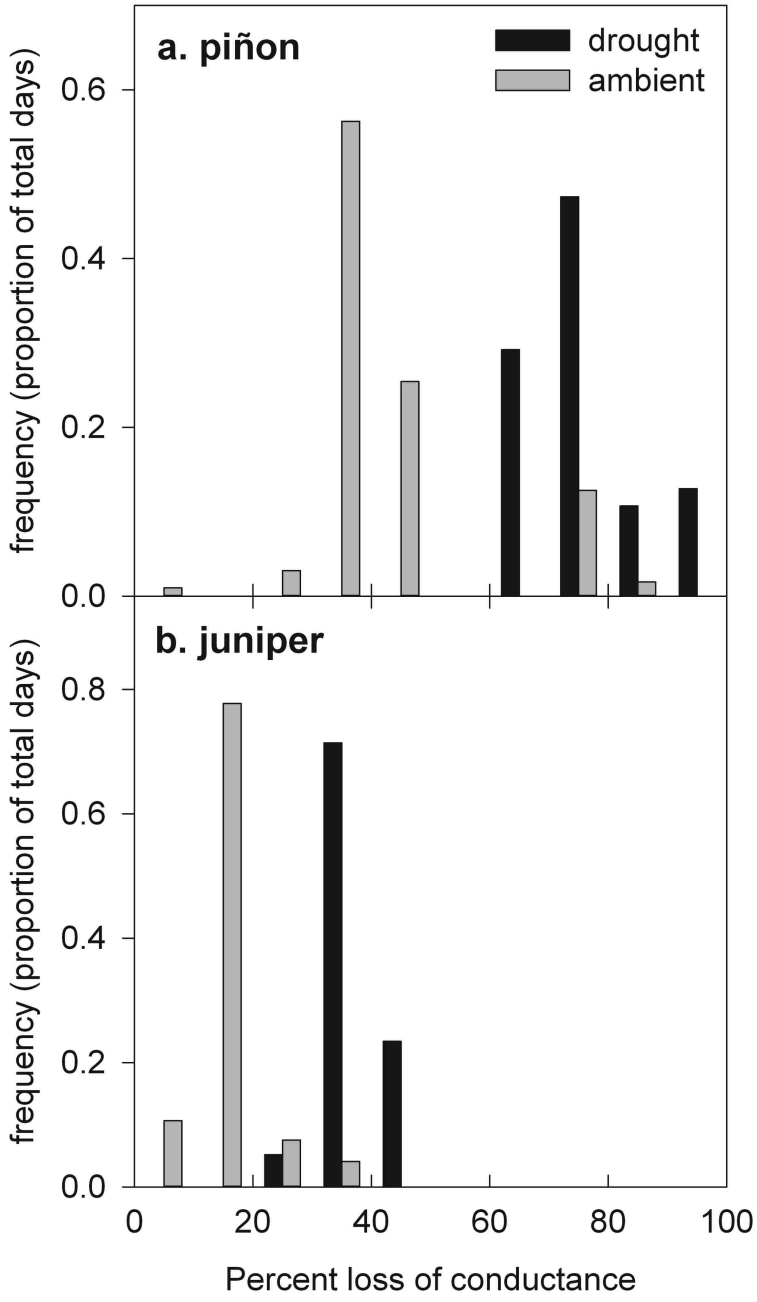

Figure 8. Frequency of measurement days spent at 10% classes of PLC (percentage loss of hydraulic conductance) for (a) piñon and (b) juniper in the ambient (gray) and drought (black) plots. Bars are paired within each 10% PLC class from 0 to 100%. The PLC for each species was calculated relative to the single maximum K_{sat} required for model calibration over both treatments and years.

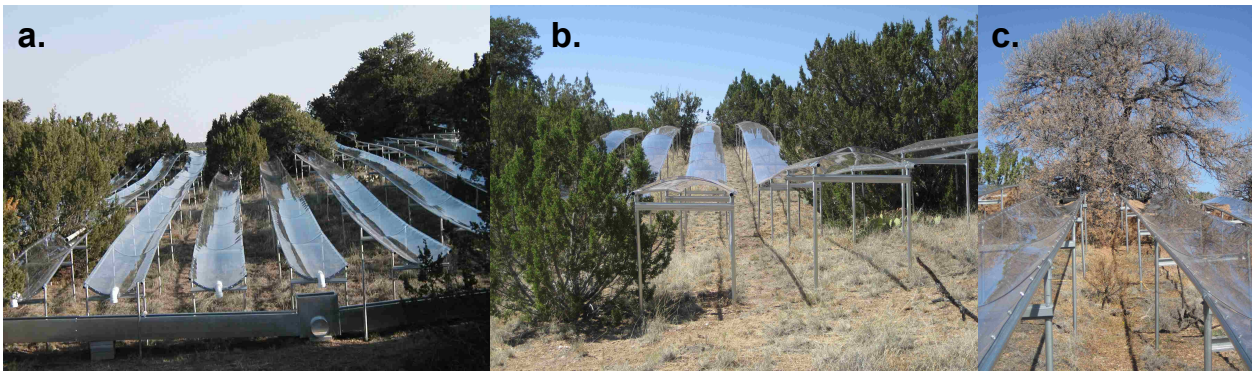

Figure S1. Photos depicting (a) drought plot on 8/21/2008 showing troughs draining to gutter, (b) cover control plot on 7/28/2007, and (c) piñon mortality in the drought plot on 10/22/2008. Photo credit: J. Hill (a,b) and J. Plaut (c).

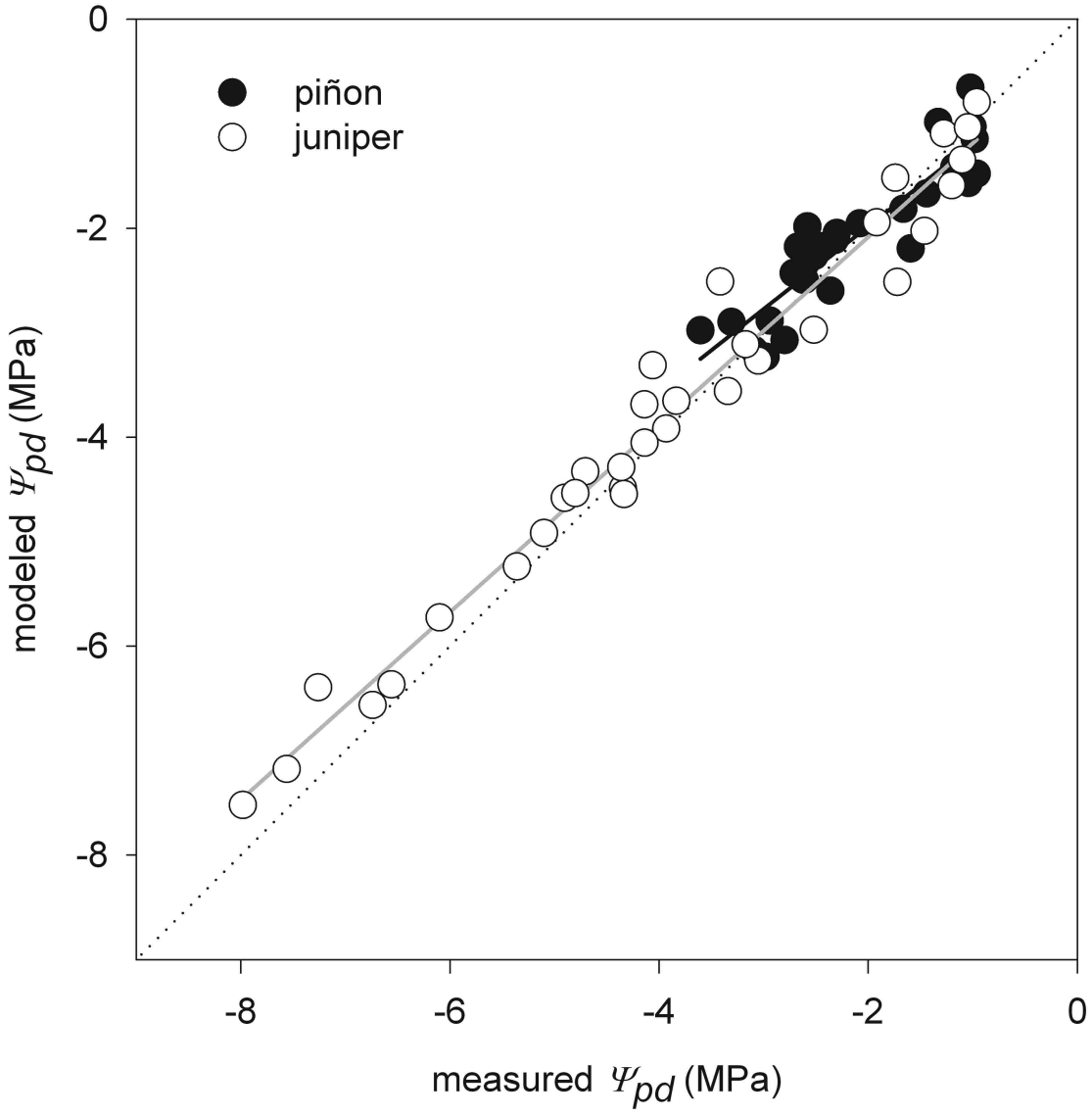

Figure S2. Modeled vs. measured predawn water potential compared across both plots and years (2007-2008) for piñon (solid symbols, black line) and juniper (open symbols, gray line). The 1:1 line (dotted) is shown for comparison. Data points represent plot means. Piñon $r^2 = 0.82$, juniper $r^2 = 0.97$.

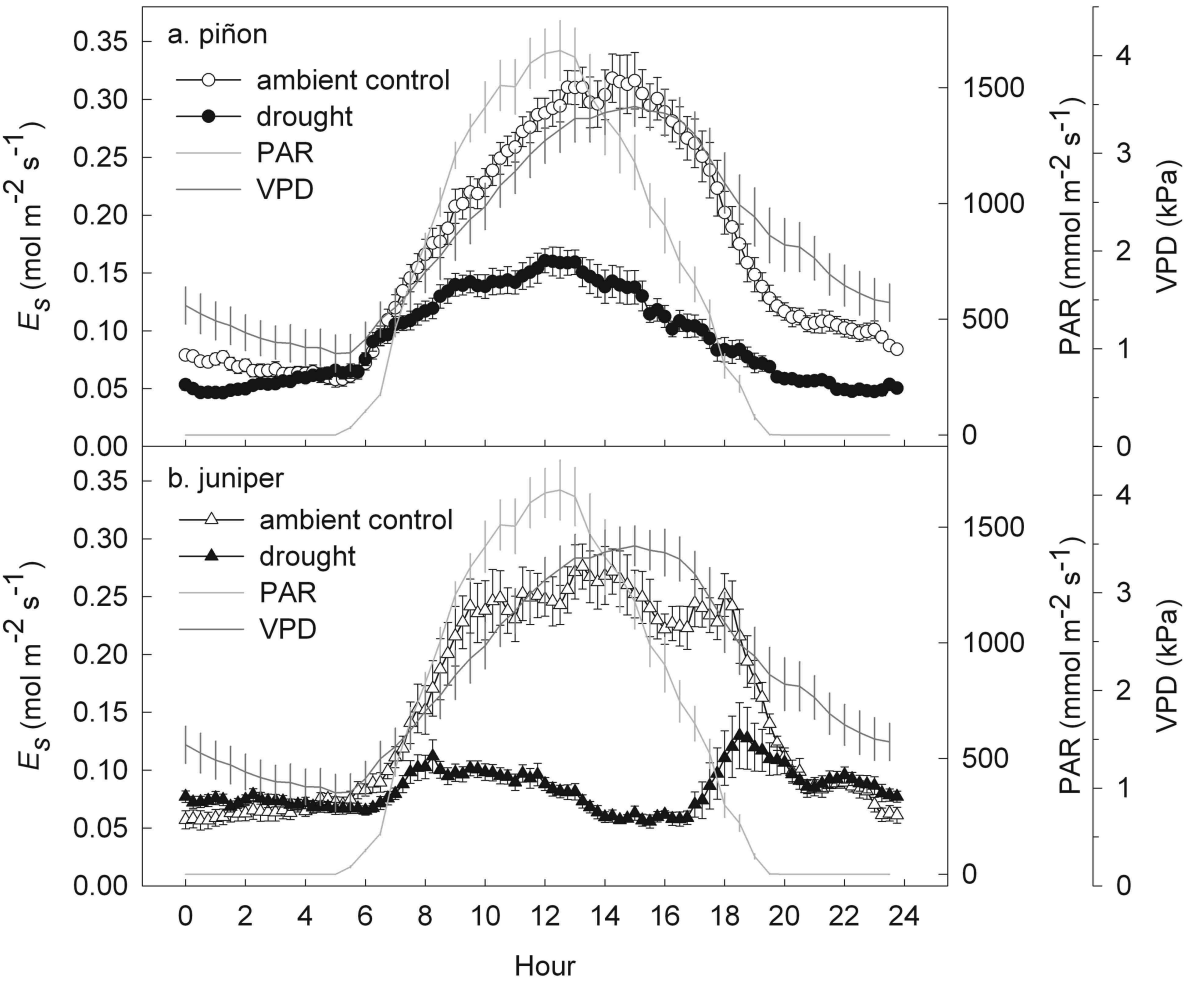

Figure S3. Piñon (a) and juniper (b) diurnal E_s averaged over the 10-day period June 21 – June 30, 2008 for drought (filled symbols) and ambient control (open symbols) treatments. Gray line indicates photosynthetically active radiation (PAR); black line indicates vapor pressure deficit (VPD). Data points represent plot means and all error bars represent the standard error of the mean.

Chapter 3

Reduced response to precipitation pulses precedes mortality in a piñon-juniper woodland subject to prolonged drought

Jennifer A. Plaut[1], W. Duncan Wadsworth[2], Robert Pangle[1], Enrico A. Yepez[3], Nate G. McDowell[4], William T. Pockman[1]

[1] Department of Biology, MSC03 2020, 1 University of New Mexico, Albuquerque, NM 87131-0001, USA

[2] Department of Statistics, MS 138, P.O. Box 1892, Rice University, Houston, TX 77251, USA

[3] Departamento de Ciencias del Agua y del Medio Ambiente, Instituto Tecnológico de Sonora, Ciudad Obregón Sonora, 85000, Mexico

[4] Earth and Environmental Sciences Division, Los Alamos National Laboratory, Los Alamos, NM 87545, USA

Correspondence: J.Plaut, Department of Biology, MSC03 2020, 1 University of New Mexico, Albuquerque, NM 87131-0001, USA. Fax: 505 277 0304; e-mail: jplaut@unm.edu

Abstract

Global climate change is predicted to alter the intensity and duration of droughts, but the effects of changing precipitation patterns on vegetation mortality are difficult to predict. Our objective was to determine whether prolonged drought or above-average precipitation altered the capacity to respond to the individual precipitation pulses that drive productivity and survival. We analyzed five years of data from a rainfall manipulation experiment in piñon-juniper (*Pinus edulis*-*Juniperus monosperma*) woodland using mixed effects models of maximum transpiration response to event size, pre-event soil moisture, and post-event vapor pressure deficit. Replicated treatments included irrigation, drought, ambient control and infrastructure control. Mortality was highest under drought. Treatment affected the transpiration response to precipitation indicating that the reduced post-pulse transpiration in the droughted trees was due not only to drier pre-pulse soil and reduced event size, but also to intrinsic changes (factors not included in the models). In particular, drought treatment reduced the transpiration response to increasing pre-event soil moisture while irrigated trees were more responsive to larger events. Prolonged drought initiates a downward spiral whereby trees are increasingly unable to utilize pulsed soil moisture. Thus, the additive effects of future, more frequent droughts may increase drought-related mortality.

Key words: mixed effects model, semiarid, hydraulic conductance, hydraulic failure, carbon starvation, die-off

Introduction

Anthropogenic climate change has the potential to cause rapid drought-related forest mortality, altering land cover, hydrologic and fire regimes, and ecosystem services (Allison *et al.* 2009, Adams *et al.* 2010, Allen *et al.* 2010, Royer *et al.* 2011) with feedbacks to regional and global climate (Bonan 2008, Jackson *et al.* 2008, van der Werf *et al.* 2009, Mildrexler *et al.* 2011, Pan *et al.* 2011). The physiological mechanisms of drought-related forest mortality are currently the subject of debate and ongoing research (Adams *et al.* 2009, Leuzinger *et al.* 2009, Sala 2009, McDowell & Sevanto 2010, McDowell 2011, Sala *et al.* 2010, Sala *et al.* 2012), delaying their explicit representation in global climate models and dynamic global vegetation models (Fisher *et al.* 2010, McDowell *et al.* 2011). Developing the needed mechanistic understanding requires knowledge of the underlying plant responses and their physiological manifestations during the progression to mortality. Long-term data describing tree physiology during drought (e.g. Breshears *et al.* 2009) are rare, but rainfall manipulation experiments with appropriate controls provide a valuable perspective on the physiological cause of drought responses. In this study, we use plant responses to individual precipitation events in a semi-arid woodland as an integrated measure of plant function across treatments in a long-term rainfall manipulation experiment.

In the Southwestern United States (SWUS), recent analyses suggest that by 2050, the frequency and extent of drought-induced forest mortality will increase above that of the worst mega-droughts in the last millennium (Williams *et al.* 2012). Increased regional aridity has already been suggested (Balling & Goodrich 2010, but see Sheffield *et al.* 2012), and is predicted to amplify in the 21st century (Dai 2012, Notaro *et al.* 2012, Ruff

et al. 2012, Seager *et al.* 2012), especially due to drier winters (Seager & Vecchi 2010). Low precipitation appears to be as important as rising temperature (and its effects on vapor pressure deficit) in driving vegetation impacts in SWUS (Notaro *et al.* 2012, Williams *et al.* 2012). Moreover, Williams et al. (2012) suggest that future vegetation mortality in the SWUS is likely to be sensitive to possible changes in the amount and/or timing of precipitation associated with the North American monsoon (Notaro & Gutzler 2012, Taylor *et al.* 2012).

Much of the SWUS is semi-arid, with plant transpiration driven by relatively short periods of soil moisture availability following precipitation (Noy-Meir 1973, Loik *et al.* 2004). Drought intensity and duration determine plant function not only by limiting gas exchange during rainless periods but also via structural and physiological changes that alter the ability of plants to utilize soil water following precipitation (Blackman *et al.* 2009, Resco *et al.* 2009, Brodribb *et al.* 2010). Some physiological changes such as leaf drop or hydraulic isolation via mortality of fine roots may promote immediate survival but decrease a tree's ability to respond to soil moisture when it becomes available. Similarly, xylem cavitation, a consequence of low plant water potential, may provide water for transpiration via capacitance (Meinzer *et al.* 2009). During prolonged (versus diel) drought, however, cavitation has negative effects since both woody tissue growth and xylem refilling (Bucci *et al.* 2003, Salleo *et al.* 2009, Zwieniecki & Holbrook 2009) are apparently carbon-costly processes, and the consequence of not replacing lost conducting tissue is lower potential for gas exchange due to reduced xylem hydraulic conductance. Thus, drought can initiate positive feedback whereby plants suffer

increasing drought stress but are also increasingly unable to take advantage of precipitation pulses.

To determine how precipitation regime affects the ability of plants to utilize water from individual rainfall events, we compared transpiration following precipitation in piñon pine (*Pinus edulis* Engelm.) and oneseed juniper (*Juniperus monosperma* (Engelm.) Sarg.) across differing precipitation treatments of an ecosystem-scale rainfall manipulation experiment from 2007-2011. The drought treatment experienced 45% year-round precipitation removal, and led to significant piñon mortality (Plaut *et al.* 2012, Gaylord *et al.* 2013), while the irrigation plots received 57-112 mm in supplemental growing-season irrigation (total precipitation was 117-142% of ambient) starting in 2008. The duration and multiple treatments in our study allowed us to test whether pulse responses in the drought treatment were simply proportional responses to smaller events or whether they were smaller than the control response to an event of similar size. Our ultimate goal was to determine how the transpiration pulse response of these species changes under prolonged precipitation manipulation. This analysis does not differentiate between the physiological mechanisms underlying pulse response differences, but rather, focuses on the integrated, whole-plant response of the trees to long-term precipitation changes.

Methods

Approach

We sought to differentiate the instantaneous effects of pulse characteristics (event size and antecedent soil moisture) from the accumulated effects of four years of drought

or irrigation. To this end, we used mixed effects models to predict the transpiration response of piñon and juniper trees to ambient, experimentally-enhanced, and experimentally-reduced precipitation events. Our null hypothesis was that there was a species-specific response function that was unchanged across treatments (i.e. no treatment effect); the observed differences in absolute transpiration (Pangle *et al.* 2012, Plaut *et al.* 2012) would be explained by differences in event size and soil moisture under rainfall manipulation. For example, piñon in all the treatments would have the same response to a rainfall event of a given size. Alternatively, a model with treatment effects might be required because within species trees in different treatments respond differently to similar-sized events. For instance, piñon in the drought treatment might have a reduced response to a 10 mm event because of emergent effects of prolonged drought on tree physiology such as hydraulic conductance or allometry.

Study site

Our study site was in an open-canopy woodland at an elevation of 1911 m on the eastern slope of the Los Pinos mountains in central New Mexico, USA (34°23'11'' N, 106°31'46'' W, Pangle *et al.* 2012, Plaut *et al.* 2012). Mean annual precipitation is 358 mm (Sevilleta LTER Cerro Montoso station #42, elevation 1976 m, 2.2 km from site, 21 y record; http://sev.lternet.edu/) and mean annual temperature is 12.7°C.

Experimental design

The experiment consists of three replicated blocks of four treatments; 1) irrigation, 2) drought, 3) cover control, and 4) ambient control (see Pangle *et al.* 2012 for

details). The irrigation plots were designed to receive ambient rainfall plus six ~19 mm equivalent events, with reverse-osmosis water applied via overhead sprinklers but full irrigation did not occur in 2008-2009 due to supply problems (Table 1). Drought plots were equipped with clear plastic troughs mounted on waist-high rails to remove ~45% of ambient precipitation year-round. Cover control plots received the same plastic coverage, but troughs faced downward allowing precipitation to reach the plot surface (Pangle *et al.* 2012). The ambient control treatment received no infrastructure. These treatments were replicated in: 1) a flat block, 2) a north-aspect block, and 3) a southeast-aspect block, selected to represent landscape heterogeneity. Within each plot, five piñon and five juniper trees that were centrally located were selected as target trees for physiological measurements. Initially, Block 3 was selected for intensive physiological measurements, assuming that drought effects would be most intense on the slopes with the shallowest soils and most direct solar radiation exposure (Pangle *et al.* 2012). Instrumentation of Blocks 1 & 2 occurred in 2009 (see below).

Observed mortality and branch dieback

In August 2008, one year after drought and cover control plots were completed, Block 2 & 3 drought-plot piñon were attacked by bark beetle (*Ips confusus* [LeConte]), infected with *Ophiostoma* fungi, and subsequently died (54% in 2008 and the remaining mature trees by July 2009), in some cases having also been attacked by twig beetle (*Pityophthorus opaculus* [LeConte]). Extensive stem and branch dieback occurred in drought-plot juniper in Block 2 & 3 over the course of the experiment without observed insect or fungal pathogens (Gaylord *et al.* in press). By the end of 2011, 25% of drought-

plot juniper site-wide had <15% green canopy remaining, including the 12.5% which were completely dead. On nine non-drought plots, five piñon have died during the experiment. When possible, dead target trees (initially n = 5 per plot) were replaced with trees of sufficient size and distance from the plot edge. After July 2009, however, no appropriate living mature piñon remained within the Block 2 & 3 drought plots.

Data collection and timeline

Sensor installation increased over the life of the experiment. Prior to the August 2007 start date, volumetric soil water content was measured at 5 cm depth under each species and in open spaces on all 12 plots (Decagon Devices model EC-20, Pullman, WA, USA) using CR-1000 dataloggers (Campbell Scientific, Logan, UT, USA). Following the rapid piñon mortality described above, additional soil moisture sensors (Decagon Devices model EC-5, Pullman, WA, USA) were installed at -15 cm, -20 cm, and as deep as possible (generally ~-60 cm) in Blocks 1 & 2 in 2009. EC-5 profiles were installed under three target trees of each species and at three intercanopy locations, for a total of n = 9 profiles per plot in Blocks 1 & 2.

Heat dissipation sapflow probes were installed on Block 3 by April, 2007. Each of the five target trees per species had two sensors installed, ≥1 m (pathlength) from the ground, on stems ≥9 cm in diameter. The sapflow sensors were built at the University of New Mexico, and modified according to Goulden & Field (1994) to correct for ambient axial thermal gradients associated with the open canopy structure at the site. Heated 10 mm needles were supplied with a constant 0.067 W, and sap flux density calculated according to the standard Granier equation (Granier 1987) using a daily maximum

temperature difference (ΔT_{max}). This amount of power consumption per probe is within the range used in other studies (Goulden & Field 1994), and any effect on sapflow estimates would be consistent site-wide. The empirically derived coefficients in the Granier equation may underestimate sap flux density, though errors due to non-species-specific calibration are generally greater for ring-porous than diffuse-porous or tracheid-bearing species (Bush *et al.* 2010). Limited testing showed that radial decline in sapflow (Cohen *et al.* 2008) was minimal in piñon and juniper at this site (R. Pangle, pers. comm.), thus the 0-10 mm sapflow rates were deemed accurate for quantification of sapflow response patterns. Furthermore, the scale of the project precluded installing probes at multiple depths site-wide. Piñon sapwood depth was consistently deeper than the 10 mm probe length, so the risk of heartwood installation was minimal. Juniper sapwood depth was circumferentially asymmetrical therefore great care was taken to install sensors in radial portions of the stem with the highest percent of sapwood, avoiding dead zones. A very small subset of juniper probes with muted J_s were subsequently identified and removed from this analysis, thus avoiding the need to correct for partial probe insertion into heartwood (see Clearwater *et al.* 1999). Sapflow sensors were measured with CR-1000 dataloggers equipped with AM 16/32 multiplexers (Campbell Scientific, Logan, UT, USA).

Following the 2008 piñon mortality, one remaining piñon tree within the Block 3 drought plot had sapflow sensors installed in November 2008; Block 2 drought plot piñon were also instrumented in 2008. Due to declining tree condition in Block 2 & 3 droughted juniper, additional target trees were identified and instrumented in 2009 (five in the Block 2 drought plot, four in the Block 3 drought plot). The remaining target trees in Blocks 1

& 2 were instrumented with two sapflow sensors each during 2009, though as stated earlier, all Block 2 & 3 drought plot piñon were dead by the end of 2009. Sapflow sensors on Block 3 were replaced in 2010.

Micrometeorological data

A micrometeorological station at the research site measured air temperature and relative humidity (Campbell Scientific HMP45C) and precipitation (TE525 tipping bucket rain gauge with Series 525 snowfall adapter, Texas Electronics, Dallas, TX, USA). Sensors were measured using a Campbell Scientific CR10X datalogger, and continuous data were summed (rain gauge) or averaged over 15 minute intervals. To model responses to precipitation events of different sizes, precipitation on the drought plots was assumed to be 55% of the measured ambient precipitation after August 2007 (Pangle *et al.* 2012). On the irrigation plots, the application of a known volume of water over a known area allowed calculation of "event size". The standard application of ~31.23 m^3 of water over an area of 1600 m^2 produced ~19 mm after accounting for 3.3% water loss in the irrigation system (see Table 1 for actual amounts).

Description of data used in the models

Our mixed effects models analyzed the response of midday sapflow to individual precipitation events in the context of environmental conditions before and after each event. Events were defined as days with precipitation sums >1 mm over the 24 hr period (14:00-13:59) preceding the calculation of our response variable, midday sapflow, (J_s; g m^{-2} s^{-1}), which was calculated as the tree-average (mean of two probes) maximum

midday (10:00-14:00) J_s within 7 days of each event. To allow the effects of individual events to be separated, only events followed by two dry days were included in the analysis. Thus, in the case of two precipitation events on consecutive days, only the second event was considered for the purposes of the mixed effects model, though soil VWC would reflect the first event.

Data input to the model included environmental conditions before and after each precipitation event (natural or experimental irrigation, Table 1). We represented pre-event conditions with the soil volumetric water content (VWC) at -5 cm on the day before the event. Tree-specific data were used when possible. For trees without VWC sensors, the cover type mean VWC (piñon or juniper) for the plot was used. Although we measured deep soil moisture, the data were inappropriate for mixed model analysis because of different sensor types in different blocks and non-random data gaps during very dry periods (Plaut *et al.* 2012). Post-event meteorological conditions were recorded as the average midday photosynthetically active radiation (PAR) and vapor pressure deficit (VPD) within 7 days following an event. PAR is rarely limiting at this site, therefore it was used as a filter, and events with post-event PAR < 600 μmol m^{-2} s^{-1} were excluded from the analysis. Temperature is highly correlated with VPD, and therefore inappropriate to include in the models, but we restricted the analysis to the period March 1 – October 31 in order to exclude freezing conditions, which down-regulate tree function and also complicate the interpretation of sap flow measurements. Post-event soil VWC was calculated as the maximum VWC in the ≤7 days after each event. We did not use post-event soil VWC as an input parameter for the J_s mixed effects models because it was highly correlated with pre-event VWC, but it was checked as a response variable to see

how soil moisture varied by treatment. VPD, VWC, and event size were mean-centered to aid interpretation and Markov chain Monte Carlo (MCMC) convergence (see Supporting Information Methods S1). Sufficient data were available for Block 3 during the period 2007-2011 and for Blocks 1 & 2 during the period 2009-2011.

Mixed effects models

To test the above hypotheses, we built a mixed effects model for each species (piñon and juniper) to predict maximum midday J_s for each tree (named J_s in the model; see Table 2 for variable names and definitions) in the seven days following each event, based on event size and soil and atmospheric conditions. Shallow (-5 cm) soil VWC on the day before the event (named VWC_{pre}), event size, and mean midday VPD in the 7 days following the event (named VPD) were included as fixed effects in the model (Table 2), with the rainfall manipulation treatment as an interaction term. Year, aspect (block), and individual tree ID were included as random effects (Table 2). As a preliminary step, we built general linear models using the same fixed effects but excluding the random effects. The general linear models were judged significant, but the residuals were highly non-normal and heteroskedastic. The mixed-effects model approach was implemented to avoid this departure from statistical assumptions. This approach allows testing for treatment effects with respect to certain variables of interest while controlling for heterogeneity across groups (i.e. plot) and heterogeneity across individuals (i.e. trees). By including interaction terms in the model the fitted coefficients can be interpreted as slopes and intercepts. That is, conditional on the effects of other variables, the response to each variable has its own intercept and slope. For further details, see Supporting

Information Methods S1 and also Pinheiro & Bates (2000) and Gelman & Hill (2007). The main mixed effect models (for piñon and juniper transpiration response) were developed using both Frequentist and Bayesian frameworks.

To learn more about the differences between the piñon that died and those that survived, we repeated the piñon mixed effects model, splitting the data into two time periods: August 2007 (when drought treatment was imposed) – 2009 (when the Block 2 & 3 drought treatment piñon were dead or nearly so) and 2010 – 2011, when only the Block 1 drought treatment piñon were surviving and thus measured. For this analysis, "Year" was removed as a random effect because there were few years in each period, and added as a fixed effect instead. Thus, for the period 2007-2009, the drought treatment piñon all suffered mortality, while for the period 2010-2011, the measured drought treatment piñon all survived through 2011.

We built a similar mixed effects model of shallow maximum VWC (VWC_{post}) after each event to determine whether the treatments resulted in differential soil moisture. This model used event size and shallow VWC_{pre} as fixed effects; random effects were the same as in the J_s models (Table 2). For the VWC_{post} mixed effects model, the dataset was restricted to individual sensors; tree ID was used as a random effect to account for sensor ID, but plot means were not added to the dataset. We did not use the intercanopy sensors in this model because they are not included in the J_s mixed model described above and we wanted the results to be consistent and comparable. Similarly, we excluded data from sensors under dead trees after those trees died, on the premise that infiltration would be greater and fine root absorption would be lower compared to when the trees were alive.

Initial tests showed that species was not an important predictor of VWC_{post}, therefore sensors were pooled by plot.

Dataset preprocessing was performed in Matlab (R2011a), and mixed effects modeling performed in R (R Core Team 2012) using the package lme4 (Bates *et al.* 2012) and in OpenBUGS (Lunn *et al.* 2009).

Results

The ambient and experimental precipitation variation during the five years of this study provided a large variety of event conditions. Total annual precipitation ranged from a low of 152 mm in the drought treatment in 2011 to a high of over 400 mm in the irrigation treatment in 2010 (Fig. 1). Ambient precipitation ranged from 250 mm in 2011 to 340 mm in 2007. Drought treatment was continuous starting in August 2007, and in terms of absolute precipitation delivered, the drought simulated by the experimental infrastructure was likely more intense than what the trees had experienced in the past century. In Socorro, NM, 50 km SW of the field site, 1942-1956 precipitation was 76.2% of, or 0.86 standard deviations below, the 1914-1941 mean (Western Regional Climate Center, Soccorro station, accessed November 7, 2012; http://www.wrcc.dri.edu/cgi-bin/sod_xtrmts1x.pl?298387). In Mountainair, NM, 31 km ENE of the field site, 1953-1956 precipitation was 54.8% of, or 1.58 standard deviations below, the 1914-1952 mean (Western Regional Climate Center, Mountainair station, accessed November 7, 2012; http://www.wrcc.dri.edu/cgi-bin/cliMAIN.pl?nm5965). Applying the experimental precipitation reduction (55% of ambient) to the 2008-2011 annual precipitation at the nearby Sevilleta LTER Cerro Montoso micrometeorological station, the effective rainfall

in the drought treatment was 44.9% of, or 2.3 standard deviations below, the 1991-2007 mean, which represents the available record. The irrigation treatment was tested in 2007, moderate in 2008 and 2009, and maximal in 2010 and 2011 (Table 1). The mean event size was 2.1, 3.8, and 4.5 mm in the drought, control, and irrigation treatments, respectively.

Soil volumetric water content (VWC) was lower in the drought treatment relative to the controls and higher in the irrigation treatment following the irrigations (Fig. 2a). A comparison of shallow and deeper pre-pulse VWC (VWC_{pre}) in the two blocks with similar sensors (Blocks 1 & 2) showed that drought treatment VWC_{pre} was lower at both depths (Supporting Information Fig. S1; see Table 2 for variable definitions), likely an effect of prolonged drought limiting the conductance of water to deeper soil layers. Sapflow was lower in the drought treatment and higher in the irrigation treatment following irrigations (Fig. 2b,c). The irrigation treatment appears to have had a stronger effect on J_s in 2010 and 2011 (Fig. 2b,c), when more additions were applied compared to 2007-2009 (Table 1). Mortality over the period 2007-2011 was highest in the drought treatment and higher in piñon than juniper (Fig. 3).

The intercept terms given in the model output (Table 3) describe overall treatment differences in post-pulse J_s, while the slope terms indicate the strength of the response to each environmental parameter (VWC, VPD, and event size). The significance of each term indicates whether it is different from zero (in the case of the ambient control treatment) or whether it is different from the ambient control (in the case of the other treatments). The parameter estimates generated by the Frequentist and Bayesian frameworks agreed quite well with one another. Estimates of significance also largely

agreed, though the Bayesian framework tended to find the irrigation and cover control treatments to be significantly different from ambient control in some cases where the Frequentist estimates did not (Table 3). The intercept terms show that in piñon, cover control and irrigation had similar J_s responses to similar precipitation events compared to ambient control (Table 3), whereas drought treatment piñon had a lower J_s pulse response than ambient control (Table 3, Fig. 4a-c).

All of the environmental (i.e., fixed) effects were found to significantly affect J_s. Drought and ambient control piñon responded similarly to increasing VPD with slightly lower maximum J_s, while irrigation and cover control had a more negative response. Relative to VWC_{pre} and event size, VPD was not a strong driver of variation in post-pulse J_s (Fig. 4a), likely because during the time period examined (March – October) VPD was almost always high enough to drive evaporation from the leaves.

Increasing shallow VWC_{pre} , or wetter pre-pulse conditions, had a strong positive effect on piñon post-pulse transpiration (Table 3, Fig. 4b). The Bayesian framework estimated the irrigation and cover control slope differences from ambient control to be more significant than the Frequentist estimates indicated (Table 3). However, both frameworks indicated that the discrepancy between drought and ambient response was greater for wetter pre-pulse conditions. Increasing event size also resulted in greater post-pulse transpiration, a response which was similar among the ambient control, cover control, and drought treatments but greater in the irrigation treatment (Table 3, Fig. 4c).

Splitting the piñon dataset into two time periods allowed us to isolate the pulse response characteristics of the piñon that died in 2008/9 from those that survived through 2011. While the reduction in sample size makes those results less conclusive, the analysis

suggests that while the trees that survived through 2011 had pulse responses similar to the ambient piñon (Fig. 5d-f), trees that died in 2008/9 had lower pulse response (Fig. 5a-c). In particular, the trees that died in 2008/9 were much less responsive to shallow VWC_{pre} (Fig. 5b). The drought-ambient comparisons from the isolated dataset including only trees that died agree broadly with the larger model's results (compare Fig. 4a-c with Fig. 5a-c), allowing us to draw inferences about mortality from the more robust model, which includes all the data.

Juniper ambient control, cover control, and irrigation treatments all had similar intercepts, while drought juniper had a significantly lower intercept, indicating overall lower J_s despite controlling for the environmental (fixed) effects in the model (Table 3, Fig. 4d-f). Juniper responses to environmental conditions were largely consistent with piñon in magnitude and direction. While juniper was overall less-responsive to VPD compared to piñon, the drought treatment had a significantly different response, which was actually positive (Fig. 4d). Juniper J_s also responded positively to increasing shallow VWC_{pre}, with similar responses in ambient and cover control and a shallower response slope in the drought treatment (Fig. 4e). The irrigation treatment had a greater response to shallow VWC_{pre}, a difference which the Bayesian framework identified as significant although the Frequentist framework did not (Table 3). Increasing event size had a positive effect on J_s, and the irrigation treatment had a significantly greater response to increasing event size compared to the other treatments, the slopes of which were all similar (Fig. 4f).

The final mixed effects model examined treatment differences in post-pulse shallow soil VWC (shallow VWC_{post}). Not surprisingly, VWC_{post} increased with both

increasing shallow VWC_{pre} and increasing event size (Table 4, Fig. 6). Irrigation and cover control VWC_{post} had lower slopes in response to event size compared to ambient control, while drought treatment was not different. In response to increasing VWC_{pre}, all of the treatments differed in slope from ambient control, but the differences were small (Fig. 6b).

Discussion

Our analysis of the sapflow response to precipitation pulses across treatments revealed emergent effects of prolonged drought and irrigation after four full years of treatment in this piñon-juniper woodland. That is, the reduced transpiration in the drought treatment (Fig. 2b,c) was not only due to drier soils (Fig. 2a) and smaller events, but also to intrinsic changes in the trees themselves. Likewise, the higher transpiration in the irrigation treatment (Fig. 2b,c) was not only due to additional soil moisture (Fig. 2a) but also to some increased response to event size (Fig. 4c). Pulse response in the ambient treatment (both species) was reduced by increasing vapor pressure deficit (VPD) and enhanced by wetter pre-pulse conditions (VWC_{pre}) and larger precipitation pulses (Fig. 4). For both species, the significantly lower drought treatment intercept term (Table 3, Fig. 4) indicates that relative to the other treatments, trees in the drought treatment had lower transpiration response to precipitation after accounting for the effects of VPD, shallow VWC_{pre}, and event size. Thus, both realized and potential J_s was lower in droughted piñon and juniper than in the other treatments.

Loss of hydraulic conductance may constrain pulse response in droughted pinon

Our analysis suggests that at some point either the severity or length of the drought constrains piñon's ability to respond to moisture pulses. Previous work has emphasized the importance of stomatal closure in minimizing cavitation in piñon during drought (Linton *et al.* 1998, West *et al.* 2008). Due to its relatively narrow hydraulic safety margin, however, piñon still experiences reduced hydraulic conductance during seasonal drought, with subsequent recovery after rain events (West *et al.* 2007). Piñon at our site experienced low xylem water potentials in 2007, prior to drought treatment installation (as low as -4 MPa in some individuals, Plaut *et al.* 2012). In Block 3, the ambient trees were able to recover whole-plant hydraulic conductance (K_h) while the drought treatment trees had lower modeled K_h going into 2008 (Plaut *et al.* 2012), and started dying in August of that year. Measured root and shoot hydraulic conductivity was lower in the drought plot in Block 1 in 2012 compared to the other treatments (P. Hudson, unpublished data), though we lack comparable measurements for the trees that actually died in 2008/9. Other physiological changes which may account for the reduced pulse response in droughted piñon include reductions of leaf area (Limousin *et al.* 2009) or stomatal conductance (Limousin *et al.* unpublished). It is unlikely that the immediate reduction in J_s in the Block 3 drought plot piñon (Plaut *et al.* 2012) is attributable to canopy leaf area reduction, since needle fall did not begin until late August 2008 and reduced new growth would not have had such a dramatic effect. Maximum stomatal conductance (g_s) was not significantly different in drought and ambient control piñon within Block 1 (Limousin *et al.* unpublished), but given that the pulse response was also similar in the Block 1 drought and ambient plots (Fig. 5d-f) while differing in the Block 3 drought and ambient plots (Fig. 5a-c), evidence would not seem to support similar g_s

among Block 2 & 3 treatments. Therefore we hypothesize that for piñon, a possible reduction in canopy leaf area, combined with lower root and shoot hydraulic conductance due to lower water potentials and greater cavitation, lead to the observed lower J_s pulse response.

Loss of both leaf area and hydraulic conductance may cause similar pattern in juniper

Some of the same physiological changes can be invoked to explain the drought treatment effect of lowered pulse response in juniper (Fig. 4d-f), but juniper differs from piñon in key attributes. In the drought treatment, decreasing canopy area (Gaylord *et al.* in press), has demonstrated that junipers die via a slow loss of branches in contrast to piñon, which maintains all of its foliated branches until death. Additionally, juniper has lower maximum stomatal conductance (g_s) in the drought treatment compared to the ambient control (Limousin *et al.* unpublished) and lower modeled K_h in the drought treatment (Plaut *et al.* 2012). Juniper roots and shoots, measured in 2012, were less vulnerable to drought-induced cavitation in the drought treatment relative to the others, though still exhibiting lower sapwood-specific hydraulic conductivity (P. Hudson, unpublished data). Together, these conductance and gas exchange measurements suggest that juniper responds to prolonged drought by reducing leaf area and adjusting its xylem to be more resistant to cavitation. In light of the reduced pulse response identified by the mixed effects model (Fig. 4d-f), we speculate that: 1) the increase in xylem cavitation resistance is occurring via loss of conductance of the most-vulnerable xylem rather than new growth of more resistant xylem, resulting in less conducting tissue overall, 2) there is some cost in terms of maximum hydraulic conductance (a safety-efficiency trade-off), or

3) despite that adjustment, the lower water potentials experienced by the droughted trees (Pangle *et al.* 2012, Plaut *et al.* 2012) are still causing greater loss of conductance relative to other treatments.

Thus, while the physiology of the two species varies considerably, piñon and juniper both exhibit reduced pulse response due to prolonged drought (Fig. 4). Other data collection and modeling efforts at this site have detailed some of the physiological changes induced by such prolonged drought (see above); this analysis documents the negative effects of those changes on both species' ability to utilize transient soil moisture. Both species are less responsive to wetter pre-pulse shallow soil in the drought treatment compared to ambient (Fig. 4b,e). Interestingly, the absolute difference in pulse response between ambient and drought treatments is greater for juniper than piñon (Fig. 4), but juniper has nonetheless maintained a higher survival rate than piñon (Fig. 3).

Both species had higher overall J_s in the irrigation treatment (Fig. 2b,c), but the mixed effects models showed that there was no systemic increase in J_s pulse response beyond that attributable to the event size effect (Fig. 4c,f). It is possible that an increase in whole-plant hydraulic conductance or stomatal conductance or in the leaf area to sapwood area ratio underlies this increased responsiveness to larger rain events. Alternatively, ambient rainfall was below average during the period of study (Fig. 1) and it could be that the supplemental irrigations have simply prevented the irrigated trees from losing the degree of function that the ambient trees have.

The consequences of shifts between dry and wet periods may become increasingly important under climate change scenarios

An outstanding question is the effect of physiological adjustments to drier or wetter periods on survival of subsequent drought. In particular, the effects of adjustment to above-average precipitation on survival or mortality during subsequent drought remain unexamined. Drought intensity affects the ability of some species to recover function following rewetting via effects on photosynthesis and stomatal conductance (Yan *et al.* 2000), and hydraulic conductance of roots (Trifilò *et al.* 2004, Domec *et al.* 2010), stems (Gallé *et al.* 2007, Schuldt *et al.* 2011), and leaves (Lo Gullo *et al.* 2003, Blackman *et al.* 2009, Brodribb & Cochard 2009). Some studies have documented lagged mortality from drought due to cavitation fatigue (Anderegg *et al.* 2013) or depletion of carbon stores (Galiano *et al.* 2012). Our results show that prolonged drought reduces the transpiration response to pulses of precipitation. This decreased pulse response limits the ability of trees to assimilate new carbon required to grow new tissue (absorbing roots, xylem, or leaf area) and replace carbon reserves. In semiarid regions subject to pulsed precipitation (versus the permanent relief of water deficit as in many glasshouse experiments), more intense or frequent drought may preclude complete recovery, leading to greater susceptibility to mortality during subsequent droughts.

This additive effect of drought on tree species subject to pulsed precipitation suggests increased forest mortality under climate change projections. Precipitation projections span a range of uncertainty (e.g. Seager *et al.* 2012, Notaro *et al.* 2012, Ruff *et al.* 2012, vs. Taylor *et al.* 2012), but the effects of temperature on VPD are better-constrained and indicate that in the SWUS trees in the future will essentially be spending more water on assimilating carbon. This increase in evaporative demand will enhance drought experienced by the trees, with predicted widespread mortality impacts (Williams

et al. 2012). Our analysis supports that projection in that prolonged drought is associated with reduced pulse response and increased mortality in piñon and juniper. Any change in the hydrologic regime which results in greater frequency of dry periods would therefore contribute to this pulse response reduction.

Soil moisture dynamics are key to understanding both pulse responses and the effects of future hydrologic regimes

The lower drought treatment J_s in both species is not an artifact of reduced shallow soil saturation because maximum shallow VWC has not been changed by the prolonged drought, as indicated by the similar response of shallow VWC_{post} in the drought and ambient control treatments (Table 4, Fig. 6). Interestingly, shallow VWC_{post} was lower in the irrigation treatment and responded less to increasing event size in the cover control compared to ambient control (Fig. 6a,b). For the irrigation treatment, two non-exclusive explanations are that: 1) water is being transferred to deeper soil faster because of greater soil hydraulic conductance, and 2) water is being extracted from shallow soil faster because of greater root absorbing area, root hydraulic conductance, and/or transpiring leaf area. That both species exhibit a greater J_s response to event size in the irrigation treatment (Fig. 4c,f) suggests that the latter is occurring (water being removed from shallow soil by trees), though it does not preclude the former. The lower cover control slope may be due to some sensors being under the plastic domes: the domes do not remove water from the plot, but they may redistribute it at a fine scale such that mean shallow VWC_{post} is lower.

The positive J_s response to VWC_{pre} observed in both species (Fig. 4b,e) highlights prior conditions as drivers of plant response following a rain event (Huxman *et al.* 2004, Emmerich & Verdugo 2008, Resco *et al.* 2008, Zeppel *et al.* 2008). Lower responses in the drought treatment for both species (Fig. 4b,e) may illustrate the legacy effect of prolonged drought on deep soil moisture. Shallow soil may saturate similarly in different treatments, but be accompanied by much drier deep soil in the drought treatment compared to the others. Indeed, the range of shallow VWC_{pre} values by which the drought treatment overlaps with the other treatments represents drier deep VWC_{pre} in the drought plot compared to the others (Supporting Information Fig. S1). Thus, J_s response is more similar among treatments at lower shallow VWC_{pre} and diverges (for the drought treatment, Fig. 4b,e) at higher shallow VWC_{pre} because the corresponding deep VWC_{pre} values are lower in the drought treatment.

Data from several semi-arid systems indicate that recharge of deep soil moisture is a rare but important event, which requires large storms (Reynolds *et al.* 2004, Yaseef *et al.* 2010). A key unanswered question, then, is whether a future, more intense hydrologic regime could actually reduce the soil drought experienced by semi-arid systems (Knapp *et al.* 2008). This appears to be the case for semi-arid grasslands (Heisler-White *et al.* 2009, Thomey *et al.* 2011), but in shrublands and forests, the greater inter-pulse drought could offset the effects of any larger precipitation events (Ross *et al.* 2012). We were not able to test multiple scenarios with the fixed-trough rainout shelter design, but the effect of precipitation intensity on shrubs and trees remains an important knowledge gap.

Acknowledgments

We gratefully acknowledge the efforts of Jim Elliot, Judson Hill, Nathan Gehres, Don Natvig, Renee Brown, Jennifer Johnson, Julie Glaser, Clif Meyer, Sam Markwell, Matt Spinelli, Greg Brittain, Jake Ring, and numerous undergraduate students in implementing this experiment and collecting much of the data. This project was supported by an award to N.G.M. and W.T.P. from the Department of Energy's Office of Science (BER) and to J.A.P. by the National Science Foundation's Graduate Research Fellowship Program. W.D.W. was supported by NIH Grant NCI T32 CA096520 at Rice University. The project was also supported by the resources and staff of the Sevilleta LTER (funded by NSF DEB 0620482), the Sevilleta Field Station at the University of New Mexico, and the US Fish and Wildlife Service, who provided access to the Sevilleta National Wildlife Refuge.

References

Adams HD, Guardiola-Claramonte M, Barron-Gafford GA, Villegas JC, Breshears DD, Zou CB, Troch PA, Huxman TE. 2009. Temperature sensitivity of drought-induced tree mortality portends increased regional die-off under global-change-type drought. *Proceedings of the National Academy of Sciences USA* **106**: 7063–7066.

Adams HD, Macalady AK, Breshears DD, Allen CD, Stephenson NL, Saleska SR, Huxman TE, McDowell NG. 2010. Climate induced tree mortality: earth system consequences. *Eos* **91**: 153–154.

Allen CD, Macalady A, Chenchouni H, Bachelet D, McDowell N, Vennetier M, Gonzales P, Hogg T, Rigling A, Breshears D, *et al.* 2010. A global overview of drought and heat-induced tree mortality reveals emerging climate change risks for forests. *Forest Ecology and Management* **259**: 660–684.

Allison I, Bindoff NL, Bindschadler RA, Cox PM, de Noblet N, England MH, Francis JE, Gruber N, Haywood AM, Karoly DJ, *et al.* 2009. The Copenhagen Diagnosis, 2009: Updating the World on the Latest Climate Science. Sydney, Australia: The University of New South Wales Climate Change Research Centre

Anderegg WRL, Plavcová L, Anderegg LDL, Hacke UG, Berry JA, Field CB. 2013. Drought's Legacy: Multi-year hydraulic deterioration underlies widespread aspen die-off and portends increased future risk. *Global Change Biology* 10.1111/gcb.12100

Balling, Jr. RC, Goodrich GB. 2010. Increasing drought in the American Southwest? A continental perspective using a spatial analytical evaluation of recent trends. *Physical Geography* **31:** 293–306.

Bates D, Maechler M, Bolker B. 2012. lme4: Linear mixed-effects models using S4 classes. R package version 0.999999-0. http://CRAN.R-project.org/package=lme4

Blackman CJ, Brodribb TJ, Jordan GJ. 2009. Leaf hydraulics and drought stress: response, recovery and survivorship in four woody temperate plant species. *Plant, Cell and Environment* **32**: 1584-1595.

Bonan GB. 2008. Forests and climate change: forcings, feedbacks, and the climate benefits of forests. *Science* **320**: 1444-1449.

Bréda N, Granier A, Aussenac G. 1995. Effects of thinning on soil and tree water relations, transpiration and growth in an oak forest (Quercus petraea (Matt.) Liebl.). *Tree Physiology* **15**: 295-306.

Breshears DD, Myers OB, Meyer CW, Barnes FJ, Zou CB, Allen CD, McDowell NG, Pockman WT. 2009. Tree die-off in response to global change-type drought: mortality insights from a decade of plant water potential measurements. *Frontiers in Ecology and the Environment* **7**: 185–189.

Brodribb TJ, Cochard H. 2009. Hydraulic failure defines the recovery and point of death in water-stressed conifers. *Plant Physiology* **149**: 575-584.

Brodribb TJ, Bowman DJMS, Nichols S, Delzon S, Burlett R. 2010. Xylem function and growth rate interact to determine recovery rates after exposure to extreme water deficit. *New Phytologist* **188**: 533-542.

Bucci SJ, Scholz FG, Goldstein G, Meinzer FC, Sternberg LDSL. 2003. Dynamic changes in hydraulic conductivity in petioles of two savanna tree species: factors and mechanisms contributing to the refilling of embolized vessels. *Plant, Cell & Environment* **26**: 1633–1645.

Bush SE, Hultine KR, Sperry JS, Ehleringer JR. 2010. Calibration of thermal dissipation sap flow probes for ring- and diffuse-porous trees. *Tree Physiology* **30**: 1545–1554.

Cohen Y, Cohen S, Cantuarias-Aviles T, Schiller G. 2008. Variations in the radial gradient of sap velocity in trunks of forest and fruit trees. *Plant and Soil* **305**: 49–59.

Dai A. 2013. Increasing drought under global warming in observations and models. *Nature Climate Change* **3**: 52-58.

Domec J-C, Schäfer K, Oren R, Kim HS, McCarthy HR. 2010. Variable conductivity and embolism in roots and branches of four contrasting tree species and their impacts on whole-plant hydraulic performance under future atmospheric CO_2 concentration. *Tree Physiology* **30**: 1001-1015.

Emmerich WE, Verdugo CL. 2008. Precipitation thresholds for CO2 uptake in grass and shrub plant communities on Walnut Gulch Experimental Watershed. *Water Resources Research*, **44**:W05S16, doi:10.1029/2006WR005690

Fisher R, McDowell NG, Purves D, Moorcroft P, Sitch S, Cox P, Huntingford C, Meir P, Woodward FI. 2010. Assessing uncertainties in a second-generation dynamic vegetation model caused by ecological scale limitations. *New Phytologist* **187**:666-681.

Galiano L, Martínez-Vilalta J, Sabaté S, Lloret F. 2012. Determinants of drought effects on crown condition and their relationship with depletion of carbon reserves in a Mediterranean holm oak forest. *Tree Physiology* **32**, 478–489.

Gallé, A., P. Haldimann and U. Feller. 2007. Photosynthetic performance and water relations in young pubescent oak (*Quercus pubescens*) trees during drought stress and recovery. *New Phytologist* **174**: 799–810.

Gaylord ML, Kolb TE, Pockman WT, Plaut JA, Yepez EA, Macalady AK, Pangle RE, McDowell NG. *in press*. Drought causes predisposition to insect attacks and mortality of piñon-juniper woodlands. *New Phytologist*

Gelman A, Hill J. 2007. Data Analysis Using Regression and Multilevel/Hierarchical Models. New York, NY, USA: Cambridge University Press.

Goulden ML, Field CB. 1994. Three methods for monitoring the gas exchange of individual tree canopies – ventilated- chamber, sap-flow and Penman-Monteith measurements on evergreen oaks. *Functional Ecology* **8**: 125–135.

Granier A. 1987. Evaluation of transpiration in a Douglas-fir stand by means of sap flow measurements. *Tree Physiology* **3**: 309–319.

Heisler-White JL, Blair JM, Kelly EF, Harmoney K, Knapp AK. 2009. Contingent productivity responses to more extreme rainfall regimes across a grassland biome. *Global Change Biology* **15**: 2894–2904.

Huxman TE, Snyder KA, Tissue D, Leffler AJ, Ogle K, Pockman WT, Snadquist DR, Potts DL, Schwinning S. 2004. Precipitation pulses and carbon fluxes in semiarid and arid ecosystems. *Oecologia* **141**: 254-268.

Jackson RB, Randerson JT, Canadell JG, Anderson RG, Avissar R, Baldocchi DD, Bonan GB, Caldeira K, Diffenbaugh NS, Field CB *et al.* 2008. Protecting climate with forests. *Environmental Research Letters* **3**: article number 044006, doi:10.1088/1748-9326/3/4/044006

Knapp AK, Beier C, Briske DD, Classen AT, Luo Y, Reichstein M, Smith MD, Smith SD, Bell JE, Fay PA *et al.* 2008. Consequences of more extreme precipitation regimes for terrestrial ecosystems. *BioScience* **58**: 811–821.

Leuzinger S, Bigler C, Wolf A, Körner C. 2009. Poor methodology for predicting large-scale tree die-off. *Proceedings of the National Academy of Sciences USA* **106**: E106; author reply E107.

Limousin J-M, Rambal S, Ourcival JM, Rocheteau A, Joffre R, Rodriguez-Cortina R. 2009. Long-term transpiration change with rainfall decline in a Mediterranean *Quercus ilex* forest. *Global Change Biology* **15**: 2163-2175.

Linton MJ, Sperry JS, Williams DG. 1998. Limits to water transport in *Juniperus osteosperma* and *Pinus edulis*: implications for drought tolerance and regulation of transpiration. *Functional Ecology* **12**: 906-911.

Lo Gullo MA, Nardini A, Trifilò P, Salleo S. 2003. Changes in leaf hydraulics and stomatal conductance following drought stress and irrigation in *Ceratonia siliqua* (Carob tree). *Physiologia Plantarum* **117**: 186-194.

Loik M E, Breshears DD, Lauenroth WK, Belnap J. 2004. A multi-scale perspective of water pulses in dryland ecosystems: climatology and ecohydrology of the western USA. *Oecologia* **141**: 269-281.

Lunn D, Spiegelhalter D, Thomas A, Best N. 2009. The BUGS project: Evolution, critique, and future directions. *Statistics in Medicine* **28**: 3049-3067.

McDowell NG. 2011. Mechanisms linking drought, hydraulics, carbon metabolism, and vegetation mortality. *Plant Physiology* **155**: 1051-1059.

McDowell NG, Beerling D, Breshears D, Fisher R, Raffa K, Stitt M. 2011. Interdependence of mechanisms underlying climate-driven vegetation mortality. *Trends in Ecology and Evolution*, **26**: 523-532.

McDowell NG, Sevanto S. 2010. The mechanisms of carbon starvation: how, when, or does it even occur at all? *New Phytologist* **186**: 264-266.

Meinzer FC, Johnson DM, Lachenbruch B, McCulloh KA, Woodruff DR. 2009. Xylem hydraulic safety margins in woody plants: coordination of stomatal control of xylem tension with hydraulic capacitance. *Functional Ecology* **23**: 922–930.

Mildrexler DJ, Zhao M, Running SW. 2011 A global comparison between station air temperatures and MODIS land surface temperatures reveals the cooling role of forests. *Journal of Geophysical Research*, **116**: G03025, doi:10.1029/2010JG001486

Notaro M, Gutzler D. 2012. Simulated impact of vegetation on climate across the North American monsoon region in CCSM3.5. *Climate Dynamics* **38**: 795-814.

Notaro M, Mauss A, Williams J. 2012. Projected vegetation changes for the American Southwest: combined dynamic modeling and bioclimatic-envelope approach. *Ecological Applications* **22**: 1365-1388.

Noy-Meir I. 1973. Desert ecosystems: environment and producers. *Annual Review of Ecology and Systematics* **4**: 25–51.

Pan Y, Birdsey RA, Fang J, Houghton R, Kauppi PE, Kurz WA, Phillips OL, Shvidenko A, Lewis SL, Canadell JG, *et al.* 2011. A large and persistent carbon sink in the World's forests. *Science* **333**: 988–993.

Pangle RE, Hill JP, Plaut JA, Yepez EA, Elliot JR, Gehres N, McDowell NG, Pockman WT. 2012. Methodology and performance of a rainfall manipulation experiment in a piñon-juniper woodland. *Ecosphere* **3**: 28.

Pinheiro JC, Bates DM. 2000. Mixed-effects models in S and S-PLUS. New York, NY, USA: Springer.

Plaut JA, Yepez EA, Hill J, Pangle R, Sperry JS, Pockman WT, McDowell NG. 2012. Hydraulic limits preceding mortality in a piñon-juniper woodland under experimental drought. *Plant, Cell & Environment* **35**: 1601-1617.

R Core Team. 2012. R: A language and environment for statistical computing. Vienna, Austria. R Foundation for Statistical Computing.

Resco V, Ewers BE, Sun W, Huxman TE, Weltzin JF, Williams DG. 2009. Drought-induced hydraulic limitations constrain leaf gas exchange recovery after precipitation pulses in the C_3 woody legume, *Prosopis velutina*. *New Phytologist* **181**: 672-682.

Reynolds JF, Kemp PR, Ogle K, Fernández RJ. 2004. Modifying the 'pulse-reserve' paradigm for deserts of North America: precipitation pulses, soil water, and plant responses. *Oecologia* **141**: 194-210.

Ross I, Misson L, Rambal S, Arneth A, Scott RL, Carrara A, Cescatti A, Genesio L. 2012. How do variations in the temporal distribution of rainfall events affect

ecosystem fluxes in seasonall water-limited Northern Hemisphere shrublands and forests? *Biogeosciences* **9**: 1007-1024.

Royer PD, Cobb NS, Clifford MJ, Huang C-Y, Breshears DD, Adams, HD, Villegas JC. 2011. Extreme climatic event-triggered overstorey vegetation loss increases understorey solar input regionally: primary and secondary ecological implications. *Journal of Ecology* **99**: 714-723.

Ruff TW, Kushnir Y, Seager R. 2012. Comparing twentieth- and twenty-first-century patterns of interannual precipitation variability over the western United States and northern Mexico. *Journal of Hydrometeorology* **13**: 366-378.

Sala A. 2009. Lack of direct evidence for the carbon-starvation hypothesis to explain drought-induced mortality in trees. *Proceedings of the National Academy of Sciences USA* **106**: E68; author reply E69.

Sala A, Piper F, Hoch G. 2010. Physiological mechanisms of drought-induced tree mortality are far from being resolved. *New Phytologist* **186**: 274–281

Sala A, Woodruff DR, Meinzer FC. 2012. Carbon dynamics in trees: feast or famine? *Tree Physiology* **32**: 764-775.

Salleo S, Trifilo P, Esposito S, Nardini A, LoGullo M. 2009. Starch-to-sugar conversion in wood parenchyma of field-growing Laurus nobilis plants: a component of the signal pathway for embolism repair? *Functional Plant Biology* **36**: 815–825.

Schuldt B, Leuschner C, Horna V, Moser G, Köhler M, van Straaten O, Barus H. 2011. Change in hydraulic properties and leaf traits in a tall rainforest tree species

subjected to long-term throughfall exclusion in the perhumid tropics. *Biogeosciences* **8**: 2179-2194.

Seager R, Ting M, Li C, Naik N, Cook B, Nakamura J, Liu H. 2012. Projections of declining surface-water availability for the southwestern United States. *Nature Climate Change* doi:10.1038/nclimate1787

Seager R, Vecchi G. 2010. Greenhouse warming and the 21st century hydroclimate of southwestern North America. *Proceedings of the National Academy of Science* **107**: 21277-21282.

Sheffield J, Wood E, Roderick M. 2012. Little change in global drought over the past 60 years. *Nature* **491**: 435-438.

Taylor CM, de Jeu RAM, Guichard F, Harris P, Dorigo W. 2012. Afternoon rain more likely over drier soils. *Nature* **489**: 423-426.

Thomey ML, Collins SL, Vargas R, Johnson JE, Brown, RF, Natvig DO, Friggens MT. 2011. Effect of precipitation variability on net primary production and soil respiration in a Chihuahuan Desert grassland. *Global Change Biology* **17**: 1505-1515.

Trifilò P, Raimondo F, Nardini A, Lo Gullo MA, Salleo S. 2004. Drought resistance of Ailanthus altissima: root hydraulics and water relations. *Tree Physiology* **24**: 107-114.

van der Werf GR, Morton DC, DeFries RS, Olivier JGJ, Kasibhatla PS, Jackson RB, Collatz GJ, Randerson JT. 2009. CO_2 emissions from forests. *Nature Geoscience* **2**: 737-738.

West AG, Hultine KR, Jackson TL, Ehleringer JR. 2007. Differential summer water use by *Pinus edulis* and Juniperus osteosperma reflects contrasting hydraulic characteristics. *Tree Physiology* **27**: 1711-1720.

West AG, Hultine KR, Sperry JS, Bush SE, Ehleringer JR. 2008. Transpiration and hydraulic strategies in a piñon-juniper woodland. *Ecological Applications* **18**: 911–927.

Williams AP, Allen CD, Macalady AK, Griffin D, Woodhouse CA, Meko DM, Swetnam TW, Rauscher SA, Seager R, Grissino-Mayer HD *et al.* 2012. Temperature as a potent driver of regional forest drought stress and tree mortality. *Nature Climate Change*. doi:10.1038/nclimate1693

Yan S, Wan C, Sosebee RE, Wester DB, Fish EB, Zartman RE. 2000. Responses of photosynthesis and water relations to rainfall in the desert shrub creosote bush (*Larrea tridentata*) as influenced by municipal biosolids. *Journal of Arid Environments* **46**: 397–412.

Yaseef NR, Yakir D, Rotenberg E, Schiller G, Cohen S. 2010. Ecohydrology of a semi-arid forest: partitioning among water balance components and its implications for predicted precipitation changes. *Ecohydrology* 3: 143-154.

Zeppel M, Macinnis-Ng CMO, Ford C, Eamus D. 2008. The response of sap flow to pulses of rain in a temperate Australian woodland. *Plant Soil* **305**: 121-130.

Zwieniecki MA, Holbrook NM. 2009. Confronting Maxwell's demon: biophysics of xylem embolism repair. *Trends in Plant Science* **14**: 530–534.

Tables

Table 1. Irrigation dates, amounts, and annual total supplemental irrigation applied to each plot in the irrigation treatment.

Year	Date	Amount (mm)	Annual total (mm)
2007	3 Oct (system test)	2	2
2008	24 June	19	
	15 July	19	
	26 August	19	57
2009	24 April	12.5	
	19 May	19	
	30 June	19	
	28 Oct	19	69.5
2010	5 May	19	
	2 June	19	
	29 June	19	
	3 August	19	
	5 October	17	112
2011	19 April	14	
	17 May	19	
	21 June	19	
	19 July	17	
	23 August	19	
	4 October	19	107

Table 2. Response and predictor variables for the mixed effects models; predictor variables preceded by ([1]) were used only in the J_s mixed models and all continuous variables were centered.

	Variable	Description	Effect	Type	Levels
Responses	J_s	maximum midday sapflow in the 7 days post-event (g m^{-2} s^{-2})	-	continuous	-
	VWC_{post}	maximum soil VWC at -5 cm in the 7 days post-event (m^3 m^{-3})	-	continuous	-
Predictors	[1]VPD	post-event mean midday VPD (kPa)	fixed	continuous	-
	VWC_{pre}	pre-event soil VWC at -5 cm (m^3 m^{-3})	fixed	continuous	-
	event size	amount of rainfall (mm)	fixed	continuous	-
	treatment	rainfall manipulation treatment	fixed	nominal	Irrigation Drought Cover Control Ambient Control
	year	year of measurements	random	nominal	2007-2011
	aspect	aspect of the measurement block	random	nominal	Block 1 = flat Block 2 = N-facing Block 3 = SE-facing
	tree ID	individual tree ID	random	nominal	1-129

Table 3. Summary of the mixed models with post-pulse maximum midday J_s as the response variable. Bold values indicate significance at the $P < 0.05$ level (frequentist) or < 10% of MCMC samples overlapping zero (Bayesian framework).

piñon	Frequentist point estimate	Frequentist Std. Error	Frequentist t value	Bayesian posterior mean	Posterior 95% Left Credible Interval	Posterior 95% Right Credible Interval	Proportion MCMC samples > 0
(Intercept)	**13.56**	**2.16**	**6.27**	**14.07**	**6.20**	**26.26**	**1.00**
VPD	**-0.89**	**0.37**	**-2.44**	**-0.90**	**-1.62**	**-0.20**	**0.01**
VWC_{pre}	**99.37**	**5.65**	**17.60**	**98.86**	**0.26**	**0.41**	**1.00**
event size	**0.34**	**0.04**	**9.01**	**0.34**	**87.46**	**109.50**	**1.00**
treatment Irrigation	2.82	1.52	1.85	**2.79**	**-0.47**	**6.14**	**0.96**
treatment Drought	**-3.46**	**1.71**	**-2.03**	**-3.48**	**-6.99**	**0.03**	**0.03**
treatment Cover Control	2.25	1.58	1.426	**2.21**	**-1.19**	**5.39**	**0.91**
VPD x Irrigation	**-1.09**	**0.45**	**-2.43**	**-1.05**	**-1.93**	**-0.19**	**0.01**
VPD x Drought	0.68	0.64	1.06	0.71	-0.56	1.99	0.86
VPD x Cover Control	**-1.12**	**0.49**	**-2.28**	**-1.08**	**-2.02**	**-0.16**	**0.01**
VWC_{pre} x Irrigation	-12.13	7.63	-1.59	**-11.50**	**-25.44**	**3.80**	**0.08**
VWC_{pre} x Drought	**-30.94**	**14.24**	**-2.17**	**-29.48**	**-57.94**	**-2.86**	**0.02**
VWC_{pre} x Cover Control	10.67	8.46	1.26	**11.79**	**-4.43**	**28.11**	**0.93**
event size x Irrigation	**0.11**	**0.05**	**2.12**	**0.11**	**0.01**	**0.21**	**0.99**
event size x Drought	0.09	0.10	0.86	0.09	-0.10	0.27	0.80
event size x Cover Control	-0.01	0.05	-0.10	-0.00	-0.11	0.09	0.48
juniper							
(Intercept)	**15.36**	**2.59**	**5.92**	**14.76**	**6.91**	**24.36**	**1.00**
VPD	-0.42	0.31	-1.35	**-0.42**	**-1.02**	**0.24**	**0.10**
VWC_{pre}	**69.11**	**4.96**	**13.94**	**69.03**	**59.28**	**78.95**	**1.00**
event size	**0.23**	**0.03**	**6.82**	**0.23**	**0.17**	**0.30**	**1.00**
treatment Irrigation	1.59	1.97	0.81	1.65	-2.53	5.62	0.79
treatment Drought	**-5.48**	**1.80**	**-3.04**	**-5.41**	**-9.27**	**-1.66**	**0.00**
treatment Cover Control	-1.71	1.98	-0.86	-1.69	-5.63	1.97	0.21

Table 3. (*continued*)

VPD x Irrigation	0.16	0.39	0.40	0.16	-0.63	0.89	0.64
VPD x Drought	**1.09**	**0.39**	**2.76**	**1.09**	**0.26**	**1.94**	**0.99**
VPD x Cover Control	0.51	0.43	1.18	0.50	-0.31	1.39	0.87
VWC_{pre} x Irrigation	12.33	7.37	1.67	**12.53**	**-2.65**	**26.11**	**0.95**
VWC_{pre} x Drought	**-19.74**	**7.58**	**-2.60**	**-19.31**	**-34.05**	**-4.27**	**0.01**
VWC_{pre} x Cover Control	0.96	7.32	0.13	1.05	-12.96	15.45	0.57
event size x Irrigation	**0.12**	**0.04**	**2.85**	**0.12**	**0.04**	**0.20**	**1.00**
event size x Drought	0.04	0.07	0.59	0.04	-0.09	0.16	0.68
event size x Cover Control	0.04	0.05	0.78	0.04	-0.06	0.13	0.77

Table 4. Summary of the mixed effects model with post-pulse shallow VWC as the response variable. Bold values indicate significance at the $P < 0.05$ level.

		Estimate	Std. Error	t value
$VWC_{S\text{-}post}$	(Intercept)	0.002	0.005	0.52
	event_size	**0.003**	**0.000**	**37.79**
	vwcs_pre	**0.931**	**0.014**	**66.98**
	treatmentIrrigation	**-0.008**	**0.004**	**-2.20**
	treatmentDrought	0.002	0.004	0.50
	treatmentCover Control	0.003	0.004	0.91
	event_size:treatmentIrrigation	**-0.001**	**0.0001**	**-8.90**
	event_size:treatmentDrought	0.0002	0.0002	1.12
	event_size:treatmentCover Control	**-0.001**	**0.0001**	**-7.49**
	vwcs_pre:treatmentIrrigation	**-0.066**	**0.021**	**-3.19**
	vwcs_pre:treatmentDrought	**-0.148**	**0.026**	**-5.61**
	vwcs_pre:treatmentCover Control	**-0.053**	**0.021**	**-2.50**

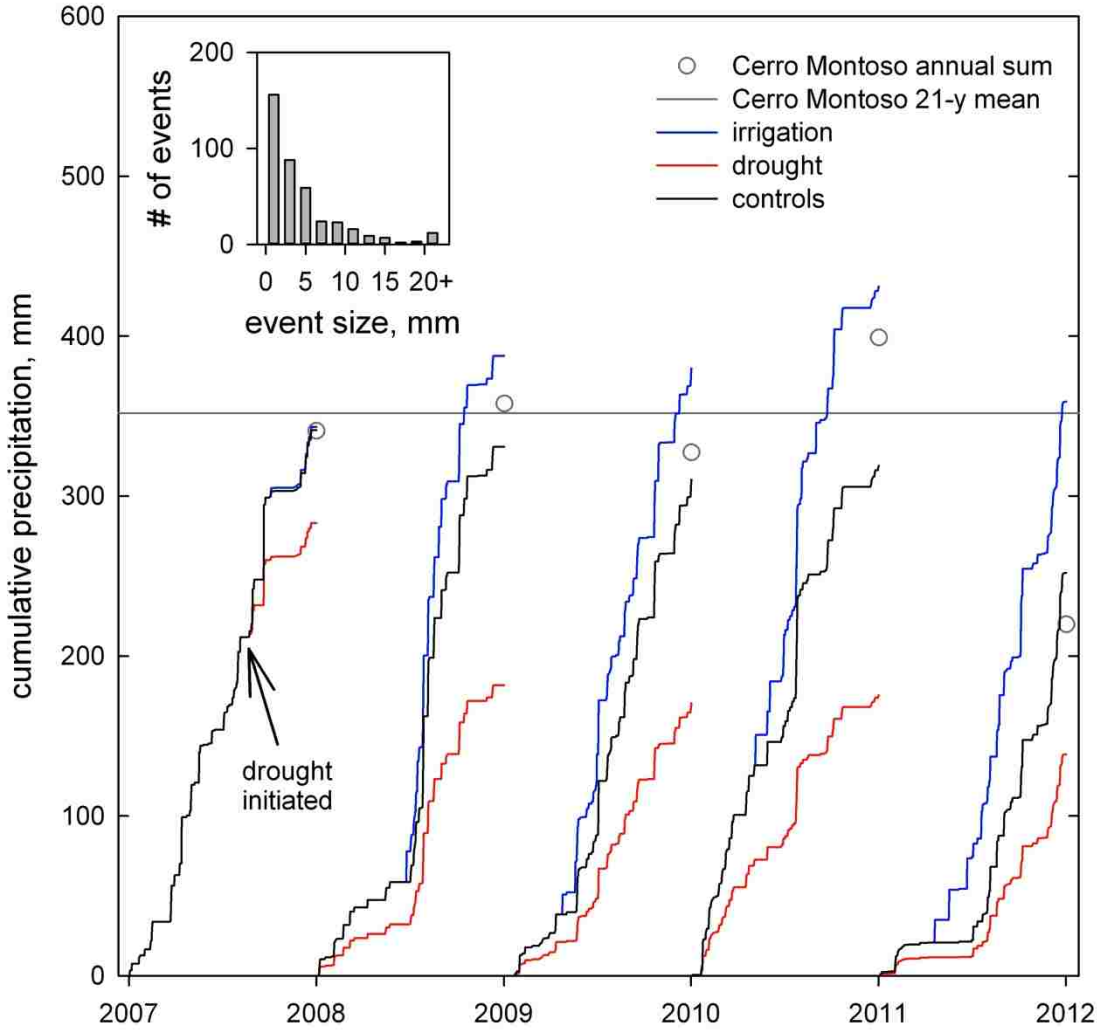

Figure 1. Precipitation over the course of the experiment showing the cumulative precipitation for each treatment in each year of the study. Drought (red line) and cover control (black line, equal to ambient) treatments initiated August 2007; irrigation (blue line) implemented at ~50% in 2008. The horizontal gray line indicates the 21-year mean annual precipitation at a Sevilleta LTER meteorological station near the site; open circles indicate total annual precipitation at the Cerro Montoso station. The inset shows the distribution of ambient event size since treatment inception in August 2007.

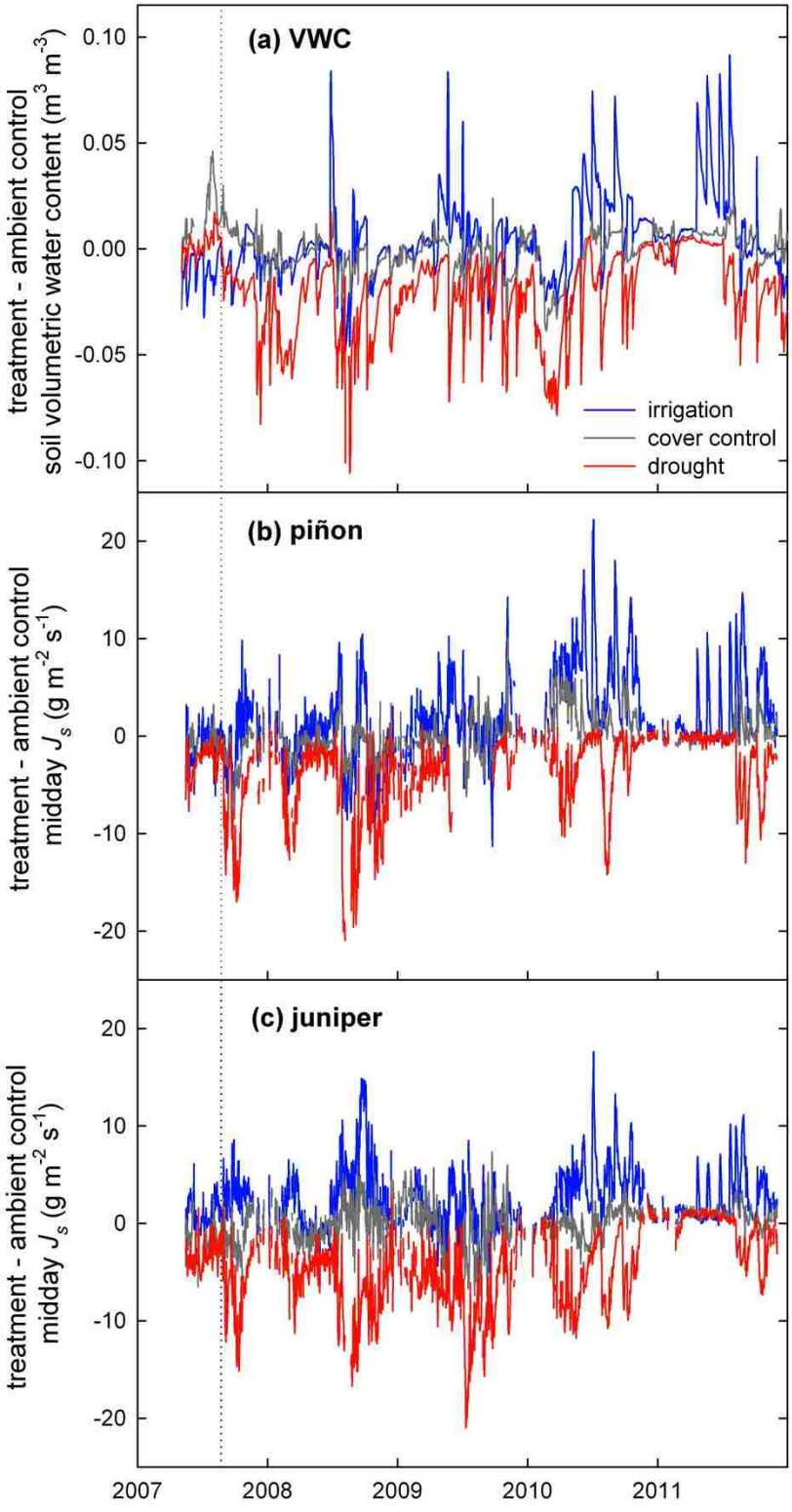
(a) VWC
treatment - ambient control
soil volumetric water content (m3 m-3)
0.10
0.05
0.00
-0.05
-0.10
irrigation
cover control
drought
(b) piñon
treatment - ambient control
midday Js (g m-2 s-1)
20
10
0
-10
-20
(c) juniper
treatment - ambient control
midday Js (g m-2 s-1)
20
10
0
-10
-20
2007
2008
2009
2010
2011

Figure 2. Time series of the treatment effect on soil volumetric water content at -5 cm (a), and midday mean J_s for piñon (b) and juniper (c). Lines represent the mean of (treatment – ambient control) for each block for the irrigation (blue), cover control (gray) and drought (red) treatments. The vertical dotted line indicates initiation of the drought treatment. See Table 1 for irrigation amounts.

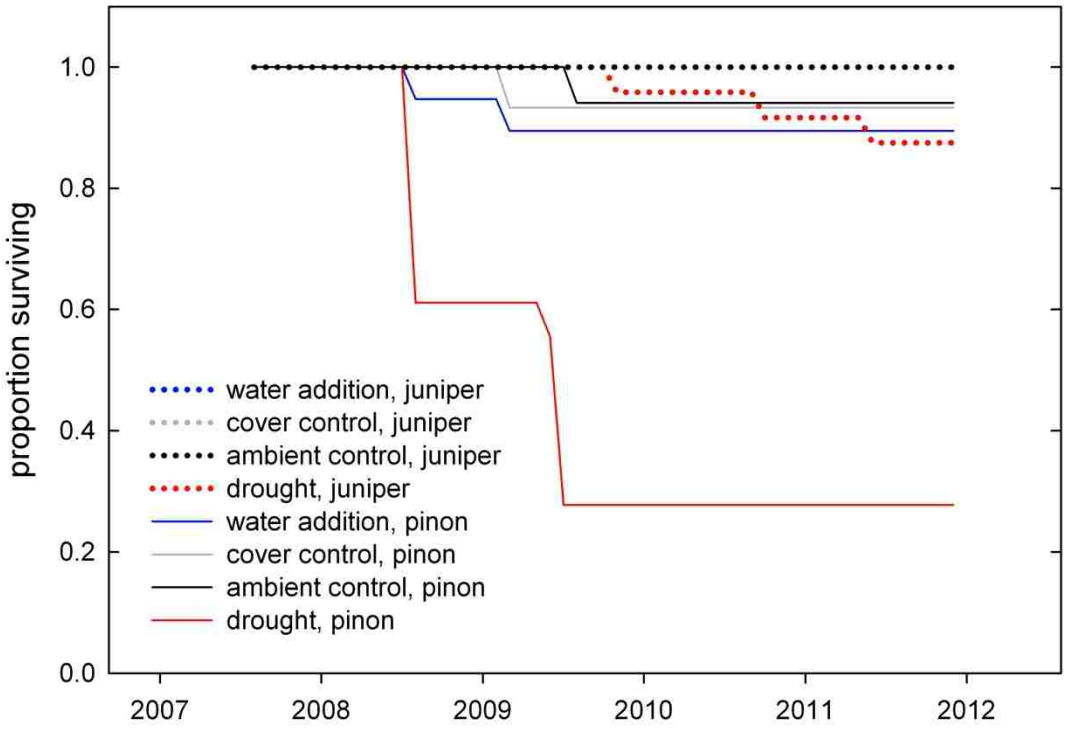

Figure 3. Proportion of piñon (solid lines) and juniper (dotted lines) target trees surviving after treatments were implemented in August 2007, in the irrigation (blue), cover control (gray), ambient control (black) and drought (red) treatments. Juniper mortality is defined as 0% green canopy.

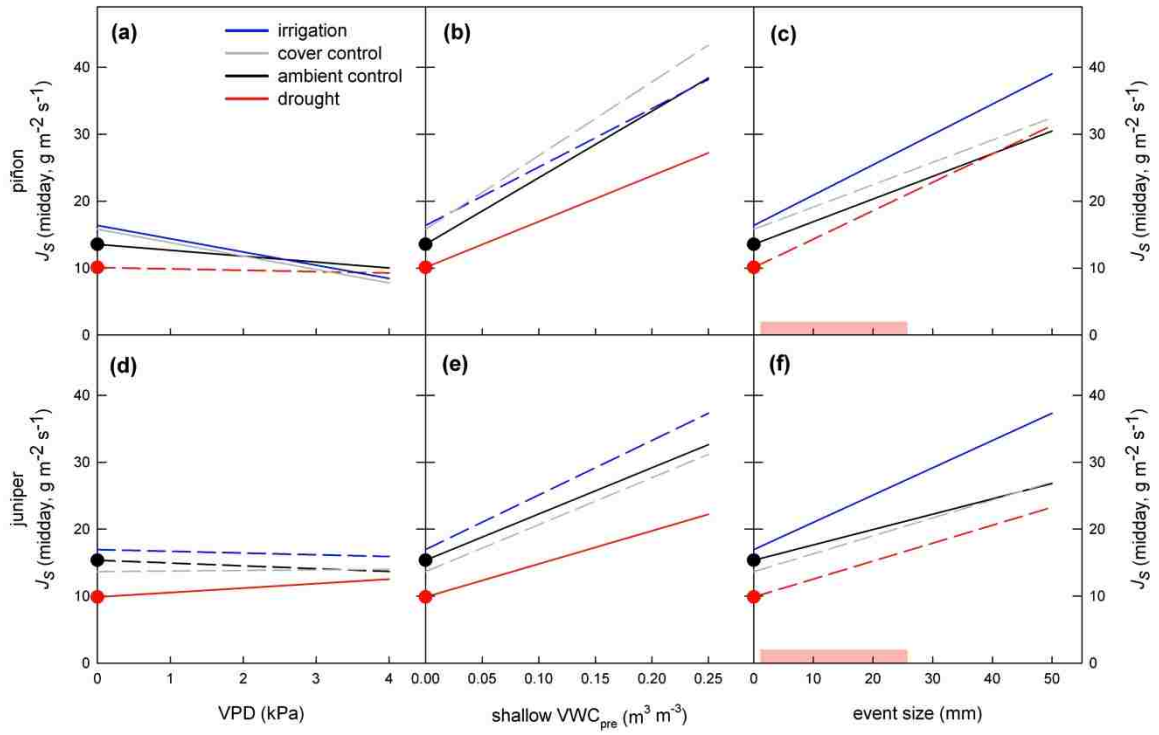

Figure 4. Mixed effects model predictions for post-pulse maximum transpiration (J_s) in piñon (a-c) and juniper (d-f) in response to VPD (a,d), shallow VWC_{pre} (b,e), and event size (c,f) for the irrigation (blue), cover control (gray), ambient control (black) and drought (red) treatments. Filled symbols on the y-axis represent intercepts which are significantly different from zero (for ambient control) or significantly different from the ambient control (for other treatments). Solid lines represent slopes which are significantly different from zero (ambient control) or significantly different from ambient control (other treatments). Dashed lines have slopes which either are not different from zero (ambient control) or are not different from the ambient control (other treatments). The shaded red bar in (c,f) indicates the range of observed event size in the drought treatment; the rest of the model predictions are constrained by data over the range presented here.

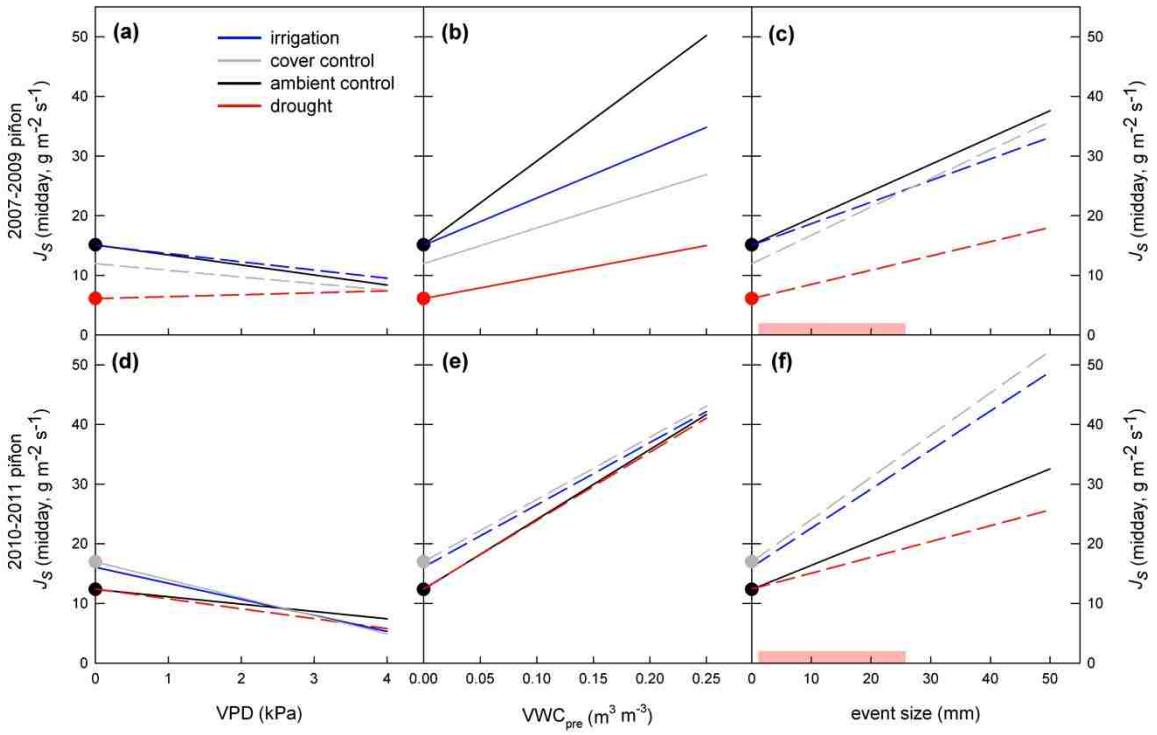

Figure 5. Mixed effects model predictions for post-pulse maximum transpiration (J_s) in piñon in 2007-2009 (a-c) and 2010-2011 (d-f) in response to VPD (a,d), shallow VWC_{pre} (b,e), and event size (c,f) for the irrigation (blue), cover control (gray), ambient control (black) and drought (red) treatments. Filled symbols on the y-axis represent intercepts which are significantly different from zero (for ambient control) or significantly different from the ambient control (for other treatments). Solid lines represent slopes which are significantly different from zero (ambient control) or significantly different from ambient control (other treatments). Dashed lines have slopes which either are not different from zero (ambient control) or are not different from the ambient control (other treatments). The shaded red bar in (c,f) indicates the range of observed event size in the drought treatment; the rest of the model predictions are constrained by data over the range presented here.

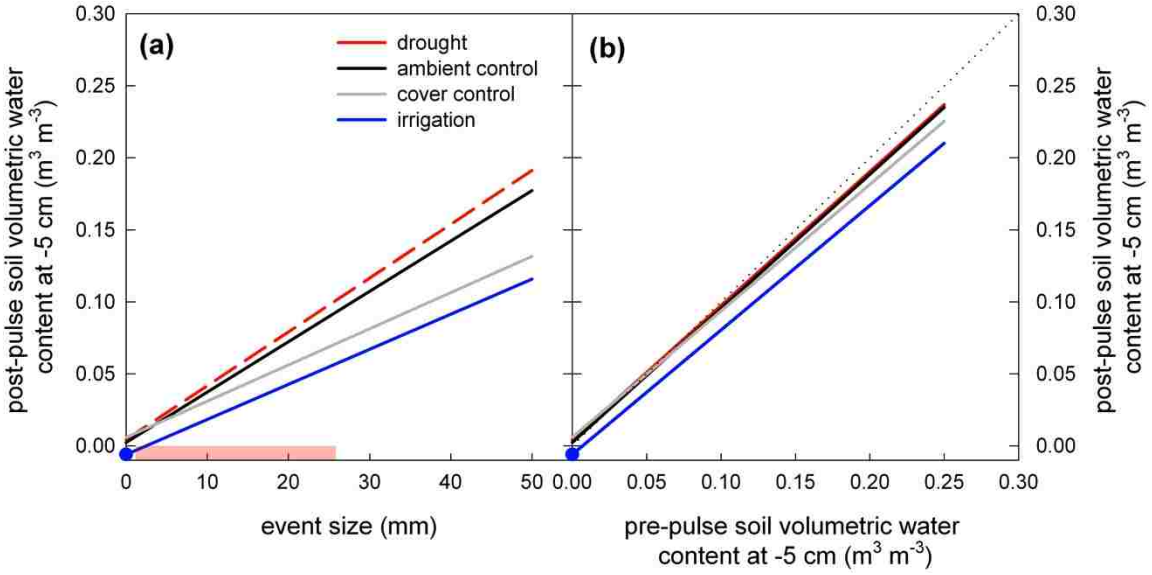

Figure 6. Mixed effects model predictions for post-pulse shallow soil volumetric water content in response to event size (a) and pre-pulse VWC (b) for the ambient control (black), cover control (gray), irrigation (blue) and drought (red) treatments. Filled symbols on the y-axis represent intercepts which are significantly different from zero (for ambient control) or random intercepts which are significantly different from the ambient control (for other treatments). Solid lines represent slopes which are significantly different from zero (ambient control) or significantly different from ambient control (other treatments). The shaded red bar in (a) indicates the range of observed event size in the drought treatment; the rest of the model predictions are constrained by data over the range presented here.

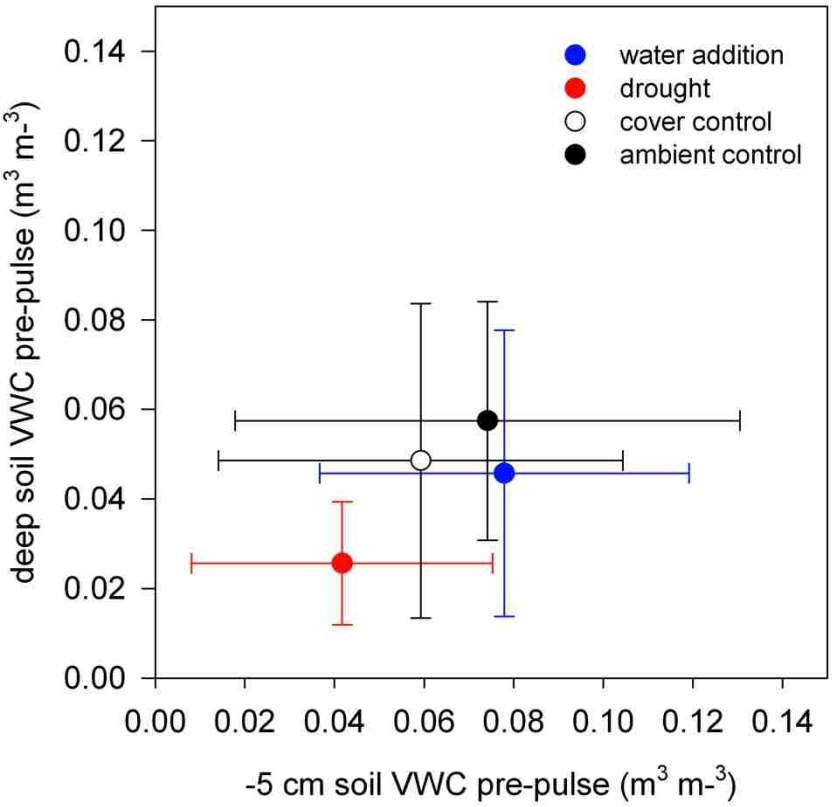

Figure S1. Relationship between measured soil volumetric water content (VWC) measured at -5 cm (x-axis) and -40 to -100 cm (y-axis) from sensors placed under piñon and juniper trees (i.e. used in the J_s mixed model). Data are shown only from flat and N-facing blocks where shallow and deep sensors are of the same type. Symbols represent irrigation (blue), drought (red), cover control (open), and ambient control (black). Error bars indicate one standard deviation from the mean.

Supporting Information

Introduction

Linear mixed-effects models (LMMs) are a flexible modeling framework which extend the standard linear model (i.e. regression and ANOVA) to settings with correlated observations, repeat measurements on individuals, and groupings which are not experimentally imposed. Standard MMs (as compared to Generalized LMMs) have a continuous response variable and two types of covariates, or predictors: fixed and random. One may think of the fixed effects as representing the mean structure in a dataset, while the random effects represent the variance structure in a dataset. Unfortunately, there is no clear consensus on the definition of either fixed or random effects so they their selection and assignment should be seen as part of the model choice process (Gelman and Hill, 2007). In this application, covariates of interest are included as fixed effects, especially treatment effects, while random effects covariates are included to satisfy the model assumptions and account for heterogeneity amongst experimental (pseudo)replicates.

Fitting

The process of fitting LMMs to data falls under two categories: Frequentist and Bayesian. The Frequentist method is more classical while the Bayesian method is more flexible; we present results from both. In the Frequentist setting, a likelihood is specified which is then solved numerically, thereby obtaining parameter estimates for the fixed effects and "conditional point estimates" for the random effects (Pinheiro and Bates, 2000). This is the method that most readers familiar with standard linear models will be

have knowledge of. Bayesian estimation of the parameters in a LMM involves obtaining a posterior distribution for each parameter in the model by combining an expression for the likelihood with an expression for prior understanding about that parameter. Here we used flat, or non-informative priors, which allows the data to "speak for itself". The posterior distributions of all but the simplest of models are too complicated to calculate directly and so must be obtained through Markov chain Monte Carlo (MCMC) simulation.

Model specification

The general form of a LMM is $Y = X\beta + Zu + \varepsilon$, where Y is the response variable, X is the fixed effects design matrix, β is the fixed effects parameter vector, Z is the random effects design matrix, u is the random effects parameter vector, and ε is the error term with mean zero and a general covariance matrix. Because we are interested in the interaction between the experimental treatments and the three fixed effects covariates, we use an Analysis of Covariance (ANCOVA) type model for the fixed effects. In other words, the fixed effects portion can be written:

$$\begin{aligned} X\boldsymbol{\beta} = \beta_0 &+ x_1\beta_1 + x_2\beta_2 + x_3\beta_3 + x_4\beta_4 \ldots \\ &+ x_5\beta_5 + x_6\beta_6 + x_1x_4\beta_7 + x_1x_5\beta_8 \ldots \\ &+ x_1x_6\beta_9 + x_2x_4\beta_{10} + x_2x_5\beta_{11} \ldots \\ &+ x_2x_6\beta_{12} + x_3x_4\beta_{13} + x_3x_5\beta_{14} + x_3x_6\beta_{15} \end{aligned}$$

The $n \times 1$ vectors which make up the design matrix are: x_1 - Irrigation treatment, x_2 – Drought treatment, x_3 - Cover Control treatment, x_4 – Vapor Pressure Deficit, x_5 – Volumetric Water Content, and x_6 - Rain Event size. Note that the Ambient treatment is considered the intercept and that the notation $x_i x_j$ indicates element-wise vector multiplication. The random effects portion can be written:

$$ZU = z_1 u_1 + z_2 u_2 + z_3 u_3$$

where the submatrices which make up the random effects design matrix are: z_1 – Tree ID, z_2 - Year, z_3 – Block Aspect.

Prior specification

The elements of the parameter vector β were assumed to follow a Normal(0, $\sigma_F^2 I$) distribution and the elements of the parameter vector u, were assumed to follow a Normal(0, $\sigma_R^2 I$) distribution. The priors for σ_F^2 and σ_R^2 were given Uniform(0, 100) distributions.

References

Gelman A, Hill J. 2007. Data Analysis Using Regression and Multilevel/Hierarchical Models. New York, NY, USA: Cambridge University Press.

Pinheiro JC, Bates DM. 2000. Mixed-effects models in S and S-PLUS. New York, NY, USA: Springer.

Chapter 4

The iso-anisohydry continuum and susceptibility of mature woody plant species to drought-related mortality

Jennifer A. Plaut[1], Nate G. McDowell[2], William T. Pockman[1]

[1] Department of Biology, MSC03 2020, 1 University of New Mexico, Albuquerque, NM 87131-0001, USA

[2] Earth and Environmental Sciences Division, Los Alamos National Laboratory, Los Alamos, NM 87545, USA

Correspondence: J.Plaut, Department of Biology, MSC03 2020, 1 University of New Mexico, Albuquerque, NM 87131-0001, USA. Fax: 505 277 0304; e-mail: jplaut@unm.edu

Abstract

Drought-related plant mortality is a globally important phenomenon but we currently lack the ability to predict the conditions under which plants in a given ecosystem will succumb to drought. Our objective was to determine whether broad categories of leaf water potential (Ψ_l) regulation strategies were predictive of drought-related mortality. We examined Ψ_l regulation in relation to xylem cavitation vulnerability and the Ψ_l of predicted stomatal closure for 157 species. It was not possible to categorize the entire dataset into isohydric and anisohydric species due to the continuum of Ψ_l regulation. Conifers maintained larger safety margins between Ψ_{min} and Ψ_{50}, and Ψ_{50} was more conservative relative to the Ψ_l of stomatal closure, relative to angiosperms. The majority of conifers in our dataset have been documented to experience drought-related mortality, suggesting that this conservative hydraulic strategy confers considerable risk of mortality, through mechanisms not directly linked to hydraulic failure (e.g., carbon starvation). Hydraulic failure may have a stronger impact on mortality of angiosperms due to the small and often negative safety margins between Ψ_{min} and various measures of xylem cavitation.

Introduction

Drought-related vegetation mortality is a global phenomenon whose importance will likely grow, based on predicted shifts in precipitation and temperature regimes due to anthropogenic climate change (Allen *et al.* 2010, Allison *et al.* 2009, Williams *et al.* 2013). Vegetation mortality has important effects on ecosystem processes and feedbacks on climate change (Bonan 2008, Jackson *et al.* 2008, van der Werf *et al.* 2009, Mildrexler *et al.* 2011, Pan *et al.* 2011) but is difficult to incorporate in dynamic global vegetation models because of limited knowledge of the the underlying mechanisms (Fisher *et al.* 2010, McDowell *et al.* 2011). Although there has been extensive research and debate regarding mortality mechanisms (Adams *et al.* 2009, Leuzinger *et al.* 2009, McDowell & Sevanto 2010, McDowell 2011, Sala *et al.* 2010, Sala *et al.* 2012), the importance of differences in Ψ_l regulation have received less attention. Here we use a global database to link Ψ_l regulation to factors associated with mortality mechanisms across a range of conifer and angiosperm species from many environments.

Leaf water potential (Ψ_l) integrates fluctuations in soil water potential (Ψ_s) over days to weeks and daily decreases below Ψ_s in proportion to the transpiration rate allowed by stomata. Pre-dawn Ψ_l (Ψ_{pd}) is often taken as an index of soil water availability, although hydraulic redistribution (Dawson 1993, Hultine *et al.* 2003, Domec *et al.* 2012), hydraulic isolation (North *et al.* 1992, North & Nobel 1997, Carminati *et al.* 2009), and nocturnal conductance (Donovan *et al.* 2003, Barbour & Buckley 2007, Kavanagh *et al.* 2007) can somewhat complicate this relationship. Mid-day Ψ_l (Ψ_{md}) reflects the decrease in Ψ_l determined by flow and hydraulic conductance (k_l). Variation in Ψ_{md} over a range of Ψ_{pd} therefore integrates species-specific solutions to the competing

autotrophic needs for carbon gain via photosynthesis and maintenance of hydraulic function required for sustained plant survival, growth and reproduction. Empirical and modeling studies show that regulation of stomatal conductance is complex, integrating environmental variables such as irradiance, vapor pressure deficit (D) and temperature, physical signals such as hydrostatic tension and transpiration rate, and biological signals such as net assimilation and hormones (Cowan & Farquhar 1977, Farquhar & Sharkey 1982, Mott & Parkhurst 1991, Tardieu & Davies 1992, Saliendra *et al.* 1995, Whitehead 1998, Salleo *et al.* 2000, Oren *et al.* 2001). The result of this integration, reflected in Ψ_l regulation, is that the balance of transpiration and photosynthesis can approach theoretical optima (Cowan & Farquhar 1977, Katul *et al.* 2009).

Stomatal regulation of Ψ_{md} is commonly categorized as isohydric or anisohydric (Tardieu & Simmoneau 1999); isohydric plants regulate Ψ_{md} at or above some observed minimum value as Ψ_s fluctuates while anisohydric plants allow Ψ_{md} to decrease with declining Ψ_s (Fig. 1a). Importantly, isohydric species are generally more vulnerable to cavitation than anisohydric species that allow Ψ_{md} to decrease to maintain gas exchange over a broader range of Ψ_{pd} (Fig. 1). This link between Ψ_l regulation and xylem cavitation vulnerability is key, though not generally highlighted in reference to isohydry and anisohydry. The observation that isohydric species cease gas exchange at higher Ψ_l than anisohydric species suggests that during drought they should be more vulnerable to carbon starvation (see below) while anisohydric species would be more vulnerable to hydraulic failure (see below) due to maintenance of transpiration and progressively lower tissue water potentials as Ψ_s decreases (McDowell *et al.* 2008). Hydraulic models (e.g.

Sperry *et al.* 1998, 2002) clearly predict that all plants must prevent decreases in Ψ_l to avoid catastrophic hydraulic failure at some Ψ_s.

We use the term carbon starvation here to describe both the state of insufficient carbohydrate reserves for metabolism and respiration, and also the state of insufficient defensive compounds (e.g. McDowell 2011). Hydraulic failure is defined as the point of 100% loss of hydraulic conductance between the soil and the leaf, occurring at some leaf water potential Ψ_{crit}, though the leaf need not be point of failure (Sperry *et al.* 1998, 2002). Ψ_{crit} defines the point of hydraulic failure but requires fairly intensive modeling to estimate, therefore it is more common to estimate safety margins from the Ψ_l causing 50% loss of hydraulic conductance (Ψ_{50}) or another relevant point on the vulnerability curve (see below). The minimum observed water potential, Ψ_{min}, is often used as a point of comparison, but may not be directly applicable to the study of drought-related mortality unless it is paired with observations of actual mortality. That is, since observations of *in situ* woody plants dying from drought are relatively rare, Ψ_{min} may not be the lowest possible Ψ_l for a species. Therefore, we used published Ψ_l datasets to predict where Ψ_{md} would converge with Ψ_{pd}, a point we named $\Psi_{\Delta 0}$. We can describe $\Psi_{\Delta 0}$ in the context of Ohm's Law,

$$E = K\left(\Psi_{pd} - \Psi_{md}\right),$$

where E, transpiration, is the product of hydraulic conductance, K, and the pressure difference between the soil (represented by Ψ_{pd}) and the leaf (represented by Ψ_{md}). $\Psi_{\Delta 0}$ is the point of stomatal closure, where $\Psi_{md} = \Psi_{pd}$. Ψ_l could still drift lower than $\Psi_{\Delta 0}$ as the plant equilibrates with drying soil, but presumably that would happen in the absence the transpiration and carbon gain associated with stomatal opening.

To characterize the relationship between Ψ_l regulation strategies and observed drought-related mortality in angiosperms and gymnosperms, we 1) compiled water potential data from the literature, 2) evaluated these data against the definitions of isohydry and anisohydry, and 3) determined the relationship between Ψ_l and both measures of hydraulic safety and the risk of carbon starvation. Our hypotheses were that 1) few plants are truly isohydric, maintaining a constant Ψ_{md} regardless of Ψ_{pd}. Similarly, few plants are continuously anisohydric, lowering Ψ_{md} as Ψ_{pd} declines without ever a point of stomatal closure. 2) $\Psi_{\Delta 0}$ would be less negative than whatever critical water potential causes irreversible hydraulic failure, that is, plants would limit carbon gain before risking hydraulic failure; and 3) drought-related mortality would be more prevalent in species with either Ψ_{min} approaching Ψ_{crit} or Ψ_{pd} approaching $\Psi_{\Delta 0}$. Due to the aforementioned difficulty in determining Ψ_{crit} we used safety margins from Ψ_{50} and Ψ_{88} as indicators of hydraulic safety, and discuss the implications of this below.

Methods

Leaf water potential dataset

To characterize leaf water potential (Ψ_l; see Table 1 for a list of symbols used) regulation during drought stress for as many species as possible, we obtained published and unpublished datasets of leaf water potential, analyzed the Ψ_l regulation characteristics of each species, and, where possible, compared them to published values of xylem cavitation resistance and reports of drought-related mortality. We performed literature searches in the ISI Web of Science database and Google Scholar (http://scholar.google.com/) on the terms "'water potential' OR 'predawn' OR 'midday'"

and restricted the dataset to measurements of Ψ_l on ≥3 mature individuals of woody species at both predawn and midday on ≥3 dates. Data from cloudy days were excluded, as were points close to the limit of the pressure bomb used, when authors noted such detail. When multiple datasets were found for a species, they were combined to produce one record per species.

Minimum Ψ_{pd} and Ψ_{md} (termed Ψ_{min}) were obtained for each species. For each pair of Ψ points we calculated the diel drop in water potential as $\Delta\Psi = \Psi_{pd} - \Psi_{md}$. Thus, in cases where Ψ_{md} was more negative than Ψ_{pd}, $\Delta\Psi$ had a positive value (as in Fig. 1b). For each species, we generated regressions of Ψ_{md} on Ψ_{pd} and $\Delta\Psi$ on Ψ_{pd} (as in Fig. 1). Linear regressions were preferred, but if the relationship was clearly non-linear other equation forms were permitted. From these regressions we calculated $\Psi_{\Delta 0}$, the point where $\Psi_{pd} = \Psi_{md}$, equivalent to $\Delta\Psi = 0$, or the point at which there is no diel change in water potential due to constant stomatal closure. Several species displayed a clear "broken stick" relationship whereby Ψ_{md} dropped quickly at higher Ψ_{pd} and then tended to level off at lower Ψ_{pd}; in these cases a linear regression was fit to the more horizontal portion of the distribution. Another set of species did not appear to ever reach $\Delta\Psi = 0$ despite quite negative Ψ_{min} values; the regression line just paralleled the 1:1 line in Fig. 1a. These species were included in analyses and figures not involving $\Psi_{\Delta 0}$.

Cavitation vulnerability parameters

We characterized species vulnerability to cavitation by obtaining xylem cavitation vulnerability curves for as many species as possible. Because we did not have Weibull equation parameters for the majority species in the dataset, calculating Ψ_{crit} was not

practical. Therefore, cavitation vulnerability was represented by two parameters, Ψ_{50} and Ψ_{88}, the water potentials leading to 50% and 88% loss of conductance, respectively. Ψ_{50} was chosen because it is widely published even when full vulnerability curves are not. Ψ_{88} was chosen because a) it represents nearly-complete loss of conductance (Domec & Gartner 2001, Chen *et al.* 2009, Wortemann *et al.* 2011) and b) it occurs before the asymptotic portion of sigmoidal or Weibull-shaped vulnerability curves and can therefore be estimated with greater certainty than, say, 100% loss of conductance. We calculated Ψ_{50} and Ψ_{88} from the minority of cases where equations were published and otherwise used the program DataThief (Tummers 2006) to extract Ψ_{50} and Ψ_{88} values from published curve images. An immediate conclusion of this exercise is that published hydraulic vulnerability experiments will have potentially greater long-term use to science if the entire curves and all relevant parameters from those curves are included.

Data quality control

We did not want to include species in the dataset that had only been measured under well-watered conditions, but we did not have prior knowledge of the water potentials inducing drought stress for every species. Initially we set a threshold of a 0.5 MPa difference between minimum and maximum Ψ_{pd}, but species that clearly restricted Ψ_{md} over an even narrower range of Ψ_{pd} were included as well. The relationship between Ψ_{pd} and Ψ_{md} would be expected to have a slope of near-zero for isohydric species (Fig. 1a), resulting a low coefficient of variation, while the $\Delta\Psi$:Ψ_{pd} slope would be expected to have a slope closer to one (Fig. 1b) and a high coefficient of variation; the converse is the case for anisohydric species. Therefore, we excluded species for which Ψ_{pd} was not

predictive at all of either Ψ_{md} or $\Delta\Psi$, i.e. neither relationship shown in Fig. 1 had $r^2 > 0.3$. The species included had a mean $r^2 = 0.72$.

Two final literature searches were aimed at determining whether each species had been characterized as "isohydric" or "anisohydric" and whether current or historical drought-related mortality had been documented. We note that this an unsatisfying index of drought-related mortality since absence of documentation does not mean that mortality is not occurring. Further, it is important to note that only a few of the Ψ_l and mortality datasets overlap, i.e. there are few published Ψ_l datasets for mature woody species undergoing mortality attributable to drought (e.g. Breshears *et al.* 2009, Plaut *et al.* 2012). Our aim is to characterize the Ψ_l regulation of species susceptible to drought-related mortality, not to describe Ψ_l patterns immediately prior to such mortality.

Statistical analyses were performed in R (R Core Team 2012).

Results

The dataset consisted of 336 records representing 214 species (Appendix A). 61 species were excluded from the analysis due to poor relationships between Ψ_{pd} and both Ψ_{md} and $\Delta\Psi$, in most cases due to limited variation in Ψ_{pd}. The final dataset consisted of n = 157 species in 2 coniferous (n = 18 species) and 44 angiosperm (n = 139 species) families. For 42 species of the 157 we were unable to calculate $\Psi_{\Delta 0}$ due a nearly constant or increasing $\Delta\Psi$ over the range of Ψ_{pd} measured. These species were included in analyses of hydraulic limits but not in any analysis requiring $\Psi_{\Delta 0}$. Of the 157 species, we were able to obtain branch/stem vulnerability curves or equations for 63 species and point data (Ψ_{50}) for an additional 13 species. Of the 13 coniferous species for which we

obtained cavitation vulnerability data, only one had no reports of drought-related mortality. Thus, in the analyses of variance we first compared conifers to angiosperms (with and without interaction terms) and secondly compared angiosperms with and without reports of drought-related mortality.

Isohydry and anisohydry exist on a continuum

There were significant differences between species previously classified as either isohydric or anisohydric (Fig. 2). Isohydric species had less-negative Ψ_{min} ($P = 0.0153$) and minimum Ψ_{pd}, ($P = 0.000139$), and tended to have a shallower slope between Ψ_{pd} and Ψ_{md} ($P = 0.0683$). These labels appear to present a false dichotomy, however, after examination of the entire dataset. The range of Ψ_{md}:Ψ_{pd} slopes calculated for the dataset (Fig. 3) was much larger than the theoretical range of zero (isohydric) to one (anisohydric; Fig. 1a). The actual range was approximately -1 to 3, spanning species whose Ψ_{md} became *less* negative over the range measured to those for whom Ψ_{md} dropped faster than Ψ_{pd} over the range of Ψ_{pd} available. For species within the predicted 0-1 range, the lower limit of Ψ_{min} declined as the slope of the Ψ_{md}:Ψ_{pd} relationship increased (Fig. 3). The lack of species with very negative Ψ_{min} and shallow slopes is likely because under wet soil conditions associated with Ψ_{pd} close to zero, even very high transpiration rates would be unlikely to significantly lower Ψ_{md} into a range that would produce a shallow line.

Ψ_{min} and xylem cavitation vulnerability

Conifers maintained greater margins of safety from Ψ_{50} and Ψ_{88} compared to angiosperms (Fig. 4). The conifers, most of which have been reported to experience drought-related mortality, all had positive margins of safety from Ψ_{50} while angiosperms experienced Ψ_{min} close to or below Ψ_{50} (Fig. 4a). Both conifers and angiosperms maintained positive safety margins between Ψ_{min} and Ψ_{88} (Fig 4b). Angiosperms experiencing mortality had a more negative safety margin from Ψ_{50} at higher Ψ_{50}, as indicated by the significant difference in slope between the two angiosperm regressions (Fig. 4a). There was no relationship between safety margin from Ψ_{88} and drought-related mortality for angiosperms (Fig. 4b).

Minimum Ψ_{pd} and the point of stomatal closure

As predicted, Ψ_{pd} was largely constrained by the calculated $\Psi_{\Delta 0}$ (Fig. 5). Conifers and angiosperms behaved similarly, though the interaction term between $\Psi_{\Delta 0}$ and conifer/angiosperm group (which represents the slopes of the regressions) was marginally significant (P=0.0811; dashed line in Fig. 5). No significant differences were found between angiosperms with and without drought-related mortality. The points farthest from the 1:1 line (roughly $\Psi_{\Delta 0}$ < -10 MPa and minimum Ψ_{pd} > -10) represent species with Ψ_{md}:Ψ_{pd} slope and r^2 both close to one, i.e. anisohydric species.

Stomatal closure and vulnerability curve parameters

$\Psi_{\Delta 0}$ declined with indices of xylem cavitation, Ψ_{50} and Ψ_{88}, for both angiosperms and conifers (Fig. 6); conifer $\Psi_{\Delta 0}$ was significantly higher than angiosperms' in both cases. Conifers Ψ_{50} was always more negative than $\Psi_{\Delta 0}$, meaning that conifers would be

predicted to close their stomata before reaching 50% branch/stem xylem cavitation. Angiosperm Ψ_{50} was usually less-negative than $\Psi_{\Delta 0}$, indicating that they would likely lose >50% branch/stem conductance prior to stomatal closure. $\Psi_{\Delta 0}$ was also higher than Ψ_{88} for almost all species (Fig. 6b). There were no significant differences between angiosperms with and without reported drought-related mortality.

Estimated PLC at the point of stomatal closure

The estimated percent loss of conductance (PLC) at $\Psi_{\Delta 0}$ varied significantly between conifers and angiosperms (Fig. 7); overall conifers were predicted to experience lower PLC at the point of stomatal closure compared to angiosperms. Conifers had a wide range of estimated PLC at higher $\Psi_{\Delta 0}$, but lower $\Psi_{\Delta 0}$ was associated with minimal PLC in branches and stems. In other words, lower $\Psi_{\Delta 0}$ appeared to be associated with more cavitation-resistant xylem in conifers. In angiosperms, estimated PLC increased as $\Psi_{\Delta 0}$ decreased and there were no statistically significant differences between angiosperms with and without reported drought-related mortality.

Discussion

Based on the idea of Ψ_l as an integration of a plant's needs for carbon and a hydraulic connection to the soil, we proposed that Ψ_l regulation strategy would vary with xylem cavitation vulnerability and ultimately be reflected in a species' drought-related mortality. Our data supported our first hypothesis, namely, that few species regulate Ψ_l in a truly isohydric or anisohydric manner. Our second hypothesis was also supported; while we do not have estimates of Ψ_{crit} for all the species, the calculated water potential at

which stomata close and prevent further decline in plant water potential ($\Psi_{\Delta 0}$) was less-negative than Ψ_{88} for almost all the species in our database (Fig. 6b). We found mixed support for our third hypothesis, which was that susceptibility to drought-related mortality would be higher in species whose Ψ_{min} approached Ψ_{crit} (approximated here by Ψ_{88}) or whose minimum Ψ_{pd} approached $\Psi_{\Delta 0}$. Our results highlight the conservative Ψ_l regulation strategy of conifers, which contrasts to the more cavitation-tolerant one of angiosperms, and suggests that conifers may be at greater risk of mortality related to carbon starvation.

Conifers appear to regulate Ψ_l more conservatively than angiosperms

Conifers experience drought-related mortality despite maintaining a positive safety margin from Ψ_{50} (Fig. 4a). Angiosperms allow Ψ_{min} to decline below Ψ_{50} much more frequently, though having a lower Ψ_{min} relative to Ψ_{50} is only weakly correlated with drought-related mortality (Fig. 4a). Ψ_{88} appears to be more of a limit for Ψ_{min}, though conifers are more conservative than angiosperms with respect to that parameter as well (Fig. 4b). The overall relationship between Ψ_{min} and Ψ_{50}/Ψ_{88} is similar to that shown by Choat *et al.* (2012, Fig. 1). Conifers maintain Ψ_l above Ψ_{50} of branch xylem, while angiosperms appear to be less conservative with respect to Ψ_{50}. However, the overall margins of safety from Ψ_{50} and Ψ_{88} for conifers and angiosperms in our dataset are smaller than those calculated by Choat *et al.* (2012) because our dataset was restricted to observations of drought-stressed plants (see Methods). Interestingly, almost all of the conifer species with enough Ψ_l observations to be included in our dataset have experienced drought-related mortality (Fig. 5 shows all 157 species with sufficient Ψ_l

data). It is important to note that in almost every case the Ψ_l parameters, cavitation vulnerability curves, and observations of drought-related mortality were assembled from different studies and locations. Observations of Ψ_l from trees that have actually died from drought coupled with site-specific cavitation vulnerability curves remain the best way to assess the role of hydraulic failure in drought-related mortality.

Leaves are more vulnerable to cavitation than branches/stems in both angiosperms and conifers (Woodruff *et al.* 2007, Bucci *et al.* 2012), but the difference is greater for conifers (Johnson *et al.* 2012), which may be one reason that conifers maintain a larger safety margin from branch Ψ_{50}. Further, branch Ψ_{50} is highly correlated with both 95% loss of conductance in leaves and failure to recover from drought stress (Brodribb & Cochard 2009). Finally, extra-xylem components of leaves may be even more vulnerable to tension-induced dysfunction than leaf xylem (Charra-Vaskou *et al.* 2012). Rather than comparing Ψ_{min} to branch Ψ_{50}, estimating safety from hydraulic failure is probably best done in the context of a hydraulic model that allows parameterization of multiple xylem segments (e.g. Sperry *et al.* 1998, 2002). The advantage of using Ψ_{crit} (as in the Sperry model) is that there are clear consequences (i.e. hydraulic failure) of reaching it, and therefore a stronger basis for calculating safety margins from it.

Safety margins from stomatal closure are similar

Since $\Psi_{\Delta 0}$ represents the point of stomatal closure, such that $\Psi_{md} = \Psi_{pd}$, we expected plants to have evolved sufficiently cavitation-resistant xylem that Ψ_{pd} is less-negative than $\Psi_{\Delta 0}$. Thus, stomata open and allow gas exchange under most circumstances. Observations of Ψ_{pd} close to $\Psi_{\Delta 0}$ indicate that a plant is experiencing the

full range of Ψ_s over which stomatal regulation allows transpiration and gas exchange. Based on that, we would expect plants whose minimum Ψ_{pd} approaches $\Psi_{\Delta 0}$ to be at greater risk of drought-related mortality due to carbon limitation. However, while most plants operate with minimum Ψ_{pd} above $\Psi_{\Delta 0}$, the relationship between minimum Ψ_{pd} and calculated $\Psi_{\Delta 0}$ is not different among groups (Fig. 5). A methodological point to consider here is that the $\Psi_{\Delta 0}$ points with the greatest certainty are those equal to or less-negative than minimum Ψ_{pd}. That is, even with a highly significant regression between Ψ_{md} and Ψ_{pd}, if there are no observations close to the 1:1 line shown in Fig. 1a then we have low confidence in a calculated $\Psi_{\Delta 0}$. Thus, minimum Ψ_{pd} >> calculated $\Psi_{\Delta 0}$ may indicate that the Ψ_l data used do not represent sufficient drought stress to estimate $\Psi_{\Delta 0}$ for that species.

Conifer Ψ_l of stomatal closure is more conservative than angiosperms'

While conifers and angiosperms appear equally like to experience Ψ_{pd} close to $\Psi_{\Delta 0}$ (Fig. 5), $\Psi_{\Delta 0}$ is more conservative relative to cavitation vulnerability for conifers than for angiosperms (Fig. 6). $\Psi_{\Delta 0}$ is less-negative than Ψ_{50} for all the conifers, which effectively restricts the absolute range of soil water potentials over which conifers perform gas exchange. Because the majority of conifers here have experienced drought-related mortality, we can say that conifers that die from drought restrict Ψ_l and gas exchange before they reach 50% embolism. Angiosperms are much more tolerant of cavitation, as indicated by the majority of calculated $\Psi_{\Delta 0}$ points being more negative than Ψ_{50} (Fig. 6a), similar to the pattern of observed Ψ_{min} being more negative than Ψ_{50} (Fig. 4a). The similarity between angiosperms experiencing vs. not experiencing mortality

shown in Fig. 6 indicates that safety margins from Ψ_{50} and Ψ_{88} may not play an important role in drought-related mortality in angiosperms.

Loss of conductance at predicted stomatal closure point

Even if conifers regularly reach $\Psi_{\Delta 0}$, they are predicted to have low loss of conductance (PLC) relative to angiosperms (Fig. 7). Despite consistent predictions of low PLC, almost all the conifers in our dataset experienced drought-related mortality. This suggests that chronic limitation of carbon gain may be a side effect of this conservative Ψ_l regulation strategy. Based on the trend of more negative safety margins from Ψ_{50} (Fig. 4a) for angiosperms experiencing drought-related mortality, we expected that group to have higher estimated PLC at $\Psi_{\Delta 0}$, but this was not the case (Fig. 7). There are several possible explanations for why greater PLC is not associated with mortality in angiosperms. First, cavitation fatigue may change the relationship between Ψ_l and loss of conductance (Hacke *et al.* 2001). Thus, actual PLC may be greater for some of the angiosperms than would be estimated based on vulnerability curves. Second, refilling of embolized xylem (Bucci *et al.* 2003, Salleo *et al.* 2009, Zwieniecki & Holbrook 2009) may mitigate the consequences of cavitation, but the degree to which different species refill is not currently known. Further, the temporal dynamics of drought might interact with cavitation fatigue and refilling and either enhance or reduce drought-related mortality. Refilling is not fully understood but it appears to be a carbon-costly process that might become less likely as drought progresses and carbon reserves are drawn down. This time component is not captured in our analysis, and may explain the apparent lack of differentiation of angiosperms experiencing drought-related mortality. Finally, species for

which capacitance (Meinzer *et al.* 2009) represents a significant proportion of daily water use might have non-trivial estimated PLC *without* experiencing mortality.

Effects of plasticity in xylem cavitation vulnerability

Xylem cavitation vulnerability within a species can vary in space (e.g. Kavanagh *et al.* 1999, Pockman & Sperry 2000, Woodruff *et al.* 2007, Corcuera *et al.* 2011; also see Appendix A) and in time in response to different climate conditions (Fonti *et al.* 2009, Galle *et al.* 2010, Plavcova *et al.* 2012, Hudson *et al.* unpublished data). Given the considerable effort involved in measuring vulnerability curves, pairing published curves with other (i.e. Ψ_l) datasets remains the most tractable option for global analyses. However, estimating the error introduced by generalizing between datasets remains a challenge because the plasticity of hydraulic architecture almost certainly varies among the species included in this study.

On the usage of the terms "isohydry" and "anisohydry"

Our characterization of Ψ_l regulatory strategy (e.g. Fig. 3a) shows that isohydry and anisohydry exist on a continuum (Fig. 3), despite their historic presentation in the literature as distinct "types" (e.g., Fig. 1). Very few of the species in Fig. 3 appear truly isohydric, having both a slope close to zero and a high coefficient of variation (in the case of a shallow Ψ_{md}:Ψ_{pd} slope, a high coefficient of variation would be ascribed to the $\Delta\Psi$:Ψ_{pd} relationship shown in Fig. 1b). Similarly, the species in Fig. 3 with slopes > 1 appear to have higher Ψ_{min} compared to the entire range of values, suggesting that the relationship between Ψ_{md} and Ψ_{pd} might change if lower Ψ_{pd} were measured. This lack of

a clear delineation is not surprising, but as Fig. 2 shows, the terms are still used to describe fairly consistent suites of characteristics. Thus, isohydric and anisohydric remain useful terms for contrasting small numbers of species because of their connotations.

Acknowledgements

We are grateful to Laura Green for her efforts in data extraction, to Craig Allen for generously sharing his tree mortality literature library, and to Eric Hamerlynck and Jean-Marc Limousin for sharing Ψ_l datasets in spreadsheet format. J.A.P. was supported by the National Science Foundation's Graduate Research Fellowship Program. Water potential data were provided by the Sevilleta LTER (funded by NSF DEB 0620482), the Sevilleta Field Station at the University of New Mexico, and the US Fish and Wildlife Service, who provided access to the Sevilleta National Wildlife Refuge. Additionally, a large *Pinus edulis*/*Juniperus monosperma* dataset was utilized from a rainfall manipulation experiment within the Sevilleta LTER which was supported by an award to N.G.M. and W.T.P. from the Department of Energy's Office of Science (BER). We gratefully acknowledge the efforts of Robert Pangle, Jean-Marc Limousin, Nathan Gehres, Amanda Boutz, Patrick Hudson, Judson Hill, Enrico Yepez, Jennifer Johnson, Julie Glaser, Sam Markwell, Matt Spinelli, Greg Brittain, Jake Ring, Jim Elliot, Don Natvig, Renee Brown, Clif Meyer, and numerous undergraduate students in implementing that experiment and collecting much of the data.

References

Adams HD, Guardiola-Claramonte M, Barron-Gafford GA, Villegas JC, Breshears DD, Zou CB, Troch PA, Huxman TE. 2009. Temperature sensitivity of drought-induced tree mortality portends increased regional die-off under global-change-type drought. *Proceedings of the National Academy of Sciences USA* **106**: 7063–7066.

Allen CD, Macalady A, Chenchouni H, Bachelet D, McDowell N, Vennetier M, Gonzales P, Hogg T, Rigling A, Breshears D, *et al.* 2010. A global overview of drought and heat-induced tree mortality reveals emerging climate change risks for forests. *Forest Ecology and Management* **259**: 660–684.

Allison I, Bindoff NL, Bindschadler RA, Cox PM, de Noblet N, England MH, Francis JE, Gruber N, Haywood AM, Karoly DJ, *et al.* 2009. The Copenhagen Diagnosis, 2009: Updating the World on the Latest Climate Science. Sydney, Australia: The University of New South Wales Climate Change Research Centre

Barbour MM, Buckley TN. 2007. The stomatal response to evaporative demand persists at night in *Ricinus communis* plants with high nocturnal conductance. *Plant, Cell and Environment* **30**, 711–721

Bonan GB. 2008. Forests and climate change: forcings, feedbacks, and the climate benefits of forests. *Science* **320**: 1444-1449.

Brodribb TJ, Cochard H. 2009. Hydraulic failure defines the recovery and point of death in water-stressed conifers. *Plant Physiology* **149**: 575-584.

Bucci SJ, Scholz FG, Goldstein G, Meinzer FC, Sternberg LDSL. 2003. Dynamic changes in hydraulic conductivity in petioles of two savanna tree species: factors

and mechanisms contributing to the refilling of embolized vessels. *Plant, Cell & Environment* **26**: 1633–1645.

Bucci SJ, Scholz FG, Campanello PI, Montti L, Jimenez-Castillo M, Rockwell FA, La Manna L, Guerra P, Bernal PL, Troncoso O, *et al.* 2012. Hydraulic differences along the water transport system of South American *Nothofagus* species: do leaves protect the stem functionality? *Tree Physiology* **32**: 880-893.

Carminati A. Vetterlein D, Weller U, Vogel H-J, Oswald SE. 2009. When roots lose contact. *Vadose Zone Journal* **8**: 805-809.

Charra-Vaskou K, Badel E, Burlett R, Cochard H, Delzon S, Mayr S. 2012. Hydraulic efficiency and safety of vascular and non-vascular components in Pinus pinaster leaves. *Tree Physiology* **32**: 1161-1170.

Chen J-W, Zhang Q, Cao K-F. 2009. Inter-species variation of photosynthetic and xylem hydraulic traits in the deciduous and evergreen Euphorbiaceae tree species from a seasonally tropical forest in south-western China. *Ecological Research* **24**: 65-73.

Choat B, Jansen S, Brodribb TJ, Cochard H, Delzon S, Bhaskar R, Bucci SJ, Field TS, Gleason SM, Hacke UG, *et al.* 2012. Global convergence in the vulnerability of forests to drought. *Nature* doi:10.1038/nature11688

Corcuera L, Cochard H, Gil-Pelegrin E, Notivol E. 2011. Phenotypic plasticity in mesic populations of *Pinus pinaster* improves resistance to xylem embolism (P_{50}) under severe drought. *Trees – Structure and Function* **25**: 1033-1042.

Cowan IR, Farquhar GD. 1977. Stomatal function in relation to leaf metabolism and environment. In: Integration of Activity in the Higher Plant (ed. Jennings DH), pp. 471–505. Cambridge University Press, Cambridge.

Dawson TE. 1993. Hydraulic lift and water use by plants: implications for water balance, performance, and plant-plant interactions. *Oecologica* **95**: 565-574.

Domec J-C, Ogée J, Noormets A, Jouangy J, Gavazzi M, Treasure E, Sun G, McNulty SG, King JS. 2012. Interactive effects of nocturnal transpiration and climate change on the root hydraulic redistribution and carbon and water budgets of southern United States pine plantations. *Tree Physiology* **32**: 707-723.

Domec, J.C. and B.L. Gartner. 2001. Cavitation and water storage capacity in bole xylem segments of mature and young Douglas-fir trees. *Trees – Structure and Function* **15**: 204–214.

Donovan LA, Richard JH, Linton MJ. 2003. Magnitude and mechanisms of disequilibrium between predawn plant and soil water potentials. *Ecology* **84**: 463-470.

Farquhar GD, Sharkey TD. 1982. Stomatal conductance and photosynthesis. *Annual Review of Plant Physiology and Plant Molecular Biology* **33**: 317-345.

Fisher R, McDowell NG, Purves D, Moorcroft P, Sitch S, Cox P, Huntingford C, Meir P, Woodward FI. 2010. Assessing uncertainties in a second-generation dynamic vegetation model caused by ecological scale limitations. *New Phytologist* **187**:666-681.

Fonti P, von Arx G, García-González I, Eilmann B, Sass-Klaassen U, Gärtner H, Eckstein D. 2009. Studying global change through investigation of the plastic

responses of xylem anatomy in tree rings. *New Phytologist* **185**: 42-53. doi: 10.1111/j.1469-8137.2009.03030.x.

Galle A, Esper J, Feller U, Ribas-Carbo M, Fonti P. 2010. Responses of wood anatomy and carbon isotope composition of *Quercus pubescens* saplings subjected to two consecutive years of summer drought. *Annals of Forest Science* **67**: 809, doi: 10.1051/forest/2010045.

Jackson RB, Randerson JT, Canadell JG, Anderson RG, Avissar R, Baldocchi DD, Bonan GB, Caldeira K, Diffenbaugh NS, Field CB *et al.* 2008. Protecting climate with forests. *Environmental Research Letters* **3**: article number 044006, doi:10.1088/1748-9326/3/4/044006

Johnson DM, McCulloh KA, Woodruff DR, Meinzer FC. 2012. Hydraulic safety margins and embolism reversal in stems and leaves: Why are conifers and angiosperms so different? *Plant Science* **195**: 48-53.

Katul GG, Palmroth S, Oren R. 2009. Leaf stomatal responses to vapour pressure deficit under current and CO 2-enriched atmosphere explained by the economics of gas exchange. *Plant, Cell and Environment* **32**: 968-979. (POSSIBLY – need to check with Nate that this was the reference he meant)

Kavanagh K.L., Bond B.J., Aitken S.N., Gartner B.L. & Knowe S. (1999) Shoot and root vulnerability to xylem cavitation in four populations of Douglas-fir seedlings. Tree Physiology **19**, 31–37.

Kavanagh KL, Pangle R, Schotzko AD. 2007. Nocturnal transpiration causing disequilibrium between soil and stem predawn water potential in mixed conifer forests of Idaho. *Tree Physiology* **27**: 621-629.

Leuzinger S, Bigler C, Wolf A, Körner C. 2009. Poor methodology for predicting large-scale tree die-off. *Proceedings of the National Academy of Sciences USA* **106**: E106; author reply E107.

McDowell N, Pockman WT, Allen CD, Breshears DD, Cobb N, Kolb T, Plaut J, Sperry J, West A, Williams DG *et al.* 2008. Mechanisms of plant survival and mortality during drought: why do some plants survive while others succumb to drought? *New Phytologist* **178**, 719–739.

McDowell NG. 2011. Mechanisms linking drought, hydraulics, carbon metabolism, and vegetation mortality. *Plant Physiology* **155**: 1051-1059.

McDowell NG, Beerling D, Breshears D, Fisher R, Raffa K, Stitt M. 2011. Interdependence of mechanisms underlying climate-driven vegetation mortality. *Trends in Ecology and Evolution*, **26**: 523-532.

McDowell NG, Sevanto S. 2010. The mechanisms of carbon starvation: how, when, or does it even occur at all? *New Phytologist* **186**: 264-266.

Meinzer FC, Johnson DM, Lachenbruch B, McCulloh KA, Woodruff DR. 2009. Xylem hydraulic safety margins in woody plants: coordination of stomatal control of xylem tension with hydraulic capacitance. *Functional Ecology* **23**: 922–930.

Mildrexler DJ, Zhao M, Running SW. 2011 A global comparison between station air temperatures and MODIS land surface temperatures reveals the cooling role of forests. *Journal of Geophysical Research*, **116**: G03025, doi:10.1029/2010JG001486

Mott, K.A. (1988) Do stomata respond to CO, concentrations other than intercellular? *Plant Physiology,* **86**, 200-203.

Mott KA, Parkhurst DF. 1991. Stomatal responses to humidity in air and helox. Plant, Cell and Environment **14**: 509-515.

North GB, Nobel PS. 1992. Root-soil contact for the desert succulent *Agave deserti* in wet and drying soil. *New Phytologist* **135**: 21-29.

North, GB, Nobel PS. 1997 Drought-induced changes in soil contact and hydraulic conductivity for roots of *Opuntia ficus-indica* with and without rhizosheaths. *Plant and Soil* **191**: 249-258.

Oren R, Sperry JS, Ewers BE, Pataki DE, Phillips N, Megonigal JP. 2001. Sensitivity of mean canopy stomatal conductance to vapor pressure deficit in a flooded *Taxodium distichum* L. forest: hydraulic and non-hydraulic effects. *Oecologia* **126**: 21–29.

Pan Y, Birdsey RA, Fang J, Houghton R, Kauppi PE, Kurz WA, Phillips OL, Shvidenko A, Lewis SL, Canadell JG, *et al.* 2011. A large and persistent carbon sink in the World's forests. *Science* **333**: 988–993.

Plavcová L, Hacke UG. 2012. Phenotypic and developmental plasticity of xylem in hybrid poplar saplings subjected to experimental drought, nitrogen fertilization, and shading. Journal of Experimental Botany doi: 10.1093/jxb/ers303

R Core Team. 2012. R: A language and environment for statistical computing. Vienna, Austria. R Foundation for Statistical Computing.

Sala A, Piper F, Hoch G. 2010. Physiological mechanisms of drought-induced tree mortality are far from being resolved. *New Phytologist* **186**: 274–281

Sala A, Woodruff DR, Meinzer FC. 2012. Carbon dynamics in trees: feast or famine? *Tree Physiology* **32**: 764-775.

Saliendra NZ, Sperry JS, Comstock JP. 1995. Influence of leaf water status on stomatal response to humidity, hydraulic conductance, and soil drought in *Betula occidentalis*. *Planta* **196**: 357-366.

Salleo S, Nardini A, Pitt F, Lo Gullo MA. 2000. Xylem cavitation and hydraulic control of stomatal conductance in Laurel (*Laurus nobilis* L.). *Plant, Cell and Environment* **23**: 71-79.

Salleo S, Trifilo P, Esposito S, Nardini A, LoGullo M. 2009. Starch-to- sugar conversion in wood parenchyma of field-growing Laurus nobilis plants: a component of the signal pathway for embolism repair? *Functional Plant Biology* **36**: 815–825.

Sperry JS, Adler FR, Campbell GS, Comstock JP. 1998. Limitation of plant water use by rhizosphere and xylem conductance: results from a model. *Plant, Cell and Environment* **21:** 347– 359.

Sperry JS, Hacke UG, Oren R, Comstock JP. 2002. Water deficits and hydraulic limits to leaf water supply. *Plant, Cell & Environment* **25:** 251–263.

Tardieu F, Davies WJ. 1992. Stomatal response to abscisic acid is a function of current plant water status. *Plant Physiology* **98**: 540-545.

Tardieu F, Simonneau T. 1998. Variability among species of stomatal control under fluctuating soil water status and evaporative demand: modelling isohydric and anisohydric behaviours. *Journal of Experimental Botany* **49**: 419-432.

Tummers B. 2006. DataThief III. http://datathief.org/

van der Werf GR, Morton DC, DeFries RS, Olivier JGJ, Kasibhatla PS, Jackson RB, Collatz GJ, Randerson JT. 2009. CO_2 emissions from forests. *Nature Geoscience* **2**: 737-738.

Whitehead D. 1998. Regulation of stomatal conductance and transpiration in forest canopies. *Tree Physiology* **18**: 633-644.

Williams AP, Allen CD, Macalady AK, Griffin D, Woodhouse CA, Meko DM, Swetnam TW, Rauscher SA, Seager R, Grissino-Mayer HD *et al.* 2012. Temperature as a potent driver of regional forest drought stress and tree mortality. *Nature Climate Change*. doi:10.1038/nclimate1693

Woodruff DR, McCulloh KA, Warren JM, Meinzer FC, Lachenbruch B. 2007. Impacts of tree height on leaf hydraulic architecture and stomatal control in Douglas-fir. *Plant, Cell and Environment* **30**: 559-569.

Wortemann R, Herbette S, Barigah TS, Fumanal B, Alia R, Ducousso A, Gomory D, Roeckel-Drevet P, Cochard H. 2011. Genotypic variability and phenotypic plasticity of cavitation resistance in *Fagus sylvatica* L. across Europe. *Tree Physiology* **31**: 1175-1182.

Zwieniecki MA, Holbrook NM. 2009. Confronting Maxwell's demon: biophysics of xylem embolism repair. *Trends in Plant Science* **14**: 530–534.

Tables

Table 1. List of symbols used.

Symbol	*Description*	*Units*
Ψ_l	Leaf water potential	MPa
Ψ_{pd}	Predawn leaf water potential	MPa
Ψ_{md}	Midday leaf water potential	MPa
Ψ_{min}	Minimum midday leaf water potential	MPa
$\Delta\Psi$	Diel drop in Ψ_l, calculated as $\Psi_{pd} - \Psi_{md}$	MPa
$\Psi_{\Delta 0}$	Ψ_l at which $\Psi_{md} = \Psi_{pd}$ and $\Delta\Psi = 0$	MPa
Ψ_{50}	Water potential causing 50% loss of hydraulic conductance in xylem	MPa
Ψ_{88}	Water potential causing 88% loss of hydraulic conductance in xylem	MPa
Ψ_s	Soil water potential	MPa
Ψ_{crit}	Leaf water potential leading to hydraulic failure	MPa

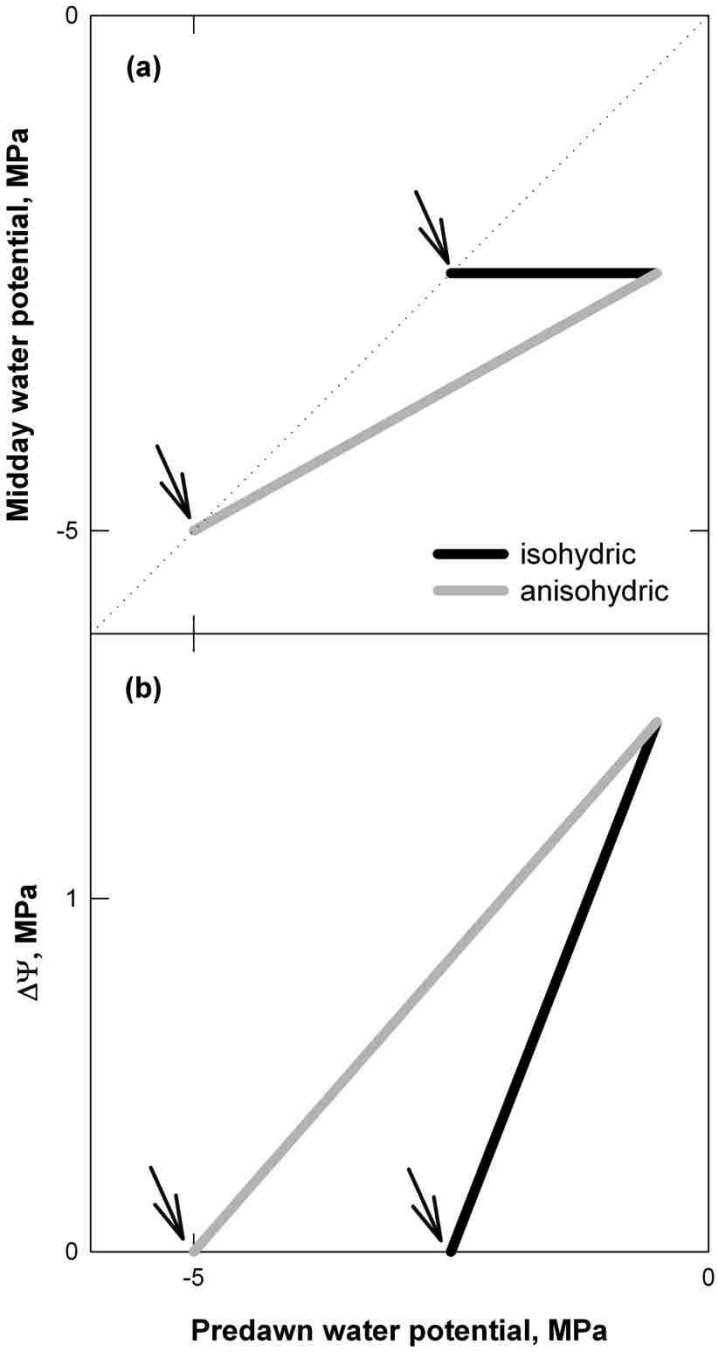

Figure 1. Theoretical leaf water potential regulation by isohydric (black) and anisohydric (gray) species showing (a) the relationship between predawn (Ψ_{pd}) and midday (Ψ_{md}) leaf water potential and (b) the relationship between Ψ_{pd} and $\Delta\Psi$, which is

calculated as Ψ_{pd} - Ψ_{md}. The Ψ at which gas exchange no longer occurs, $\Psi_{\Delta 0}$, is indicated with arrows in both panels; in (a) the 1:1 relationship is given by the dotted line.

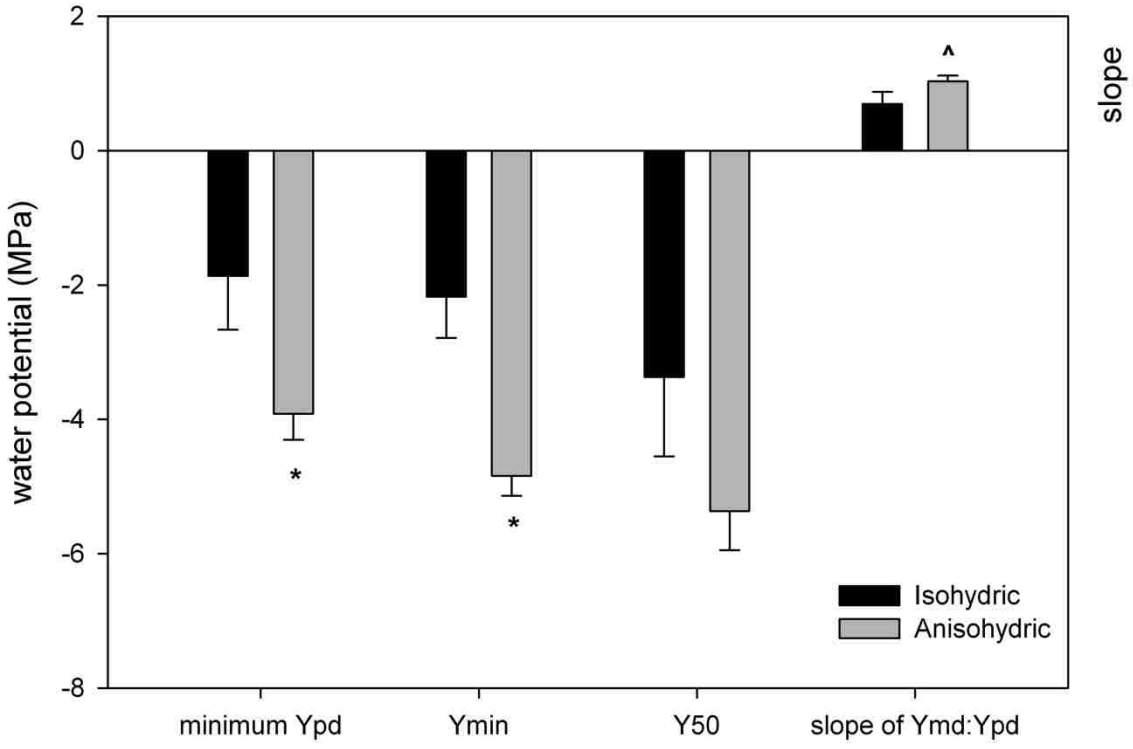

Figure 2. Comparison of parameters between species included in our dataset which have been classified as either isohydric (n=8) or anisohydric (n=26) in prior research. Parameters are the minimum predawn leaf water potential, minimum recorded leaf water potential, minimum published Ψ_{50}, and the calculated slope of the linear relationship between Ψ_{md} and Ψ_{pd} (as in Fig. 1a). Asterisks (*) indicate significant differences between isohydric and anisohydric means at the P<0.05 level; carat (^) indicates differences significant at the P<0.1 level.

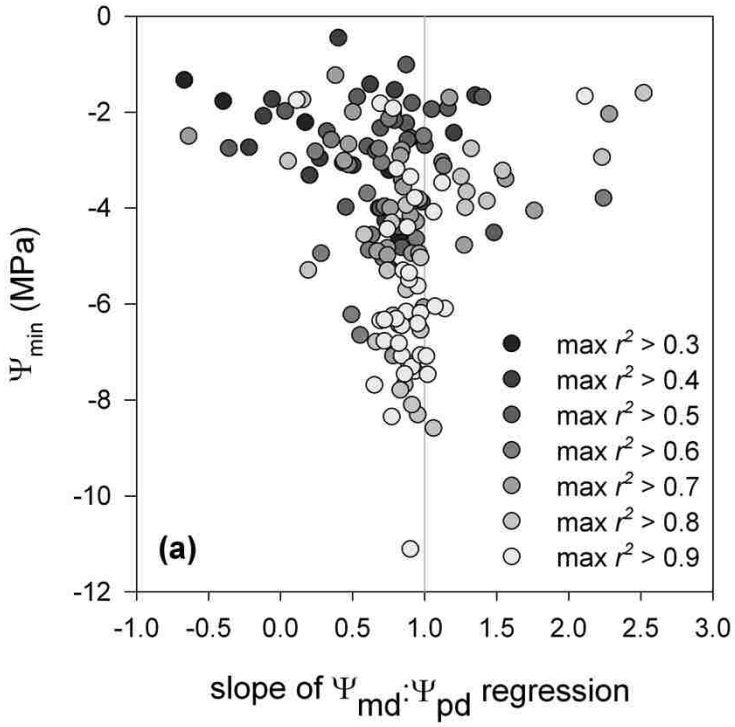

Figure 3. Relationship between Ψ_{min} and the slope of Ψ_{pd} vs Ψ_{md}. Symbol shading refers to the maximum coefficient of variation for the relationships for each species of Ψ_{md} to Ψ_{pd} or $\Delta\Psi$ to Ψ_{pd}.

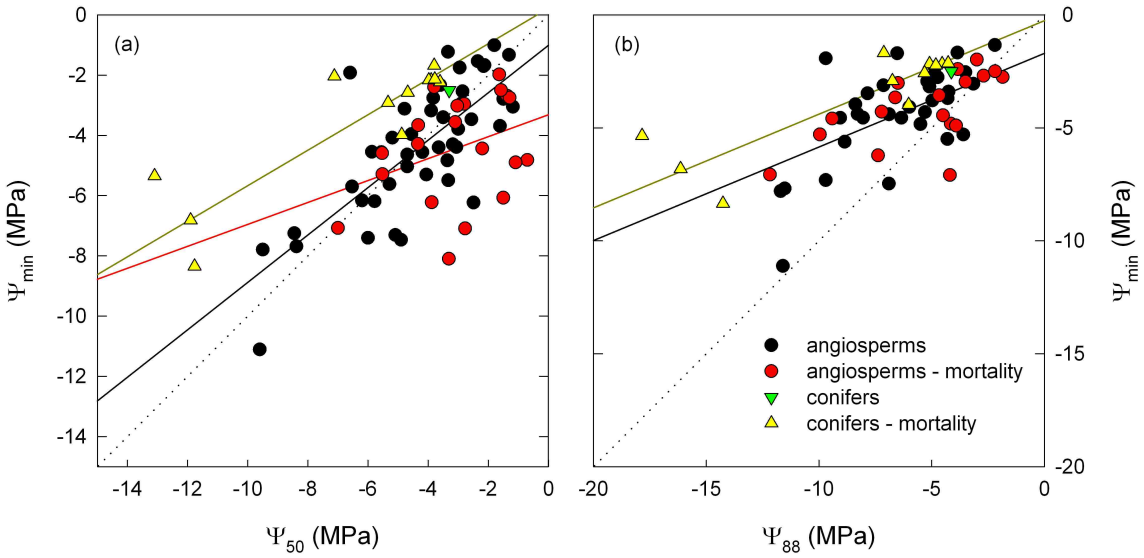

Figure 4. Relationship between Ψ_{min} and (a) Ψ_{50} and (b) Ψ_{88} for angiosperms (black circles), angiosperms with observed drought-related mortality (red circles), conifers (green downward triangles) and conifers with observed drought-related mortality (yellow upward triangles). The 1:1 relationship is shown as a dotted line. Regressions are shown as same-color solid lines. In (a) conifer regression significantly different from angiosperms ($P = 0.0000143$); angiosperm groups significantly different ($P = 0.0121$) with a nearly-significant interaction term ($P = 0.0769$). In (b) conifer and angiosperm regressions are significantly different ($P = 0.003696$) but angiosperm groups are not different.

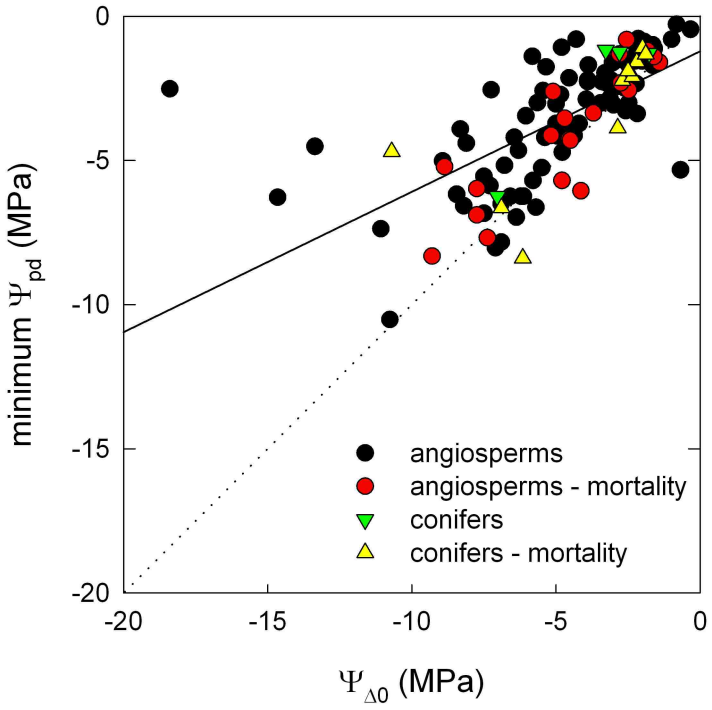

Figure 5. Relationship between $\Psi_{\Delta 0}$ and minimum observed Ψ_{pd} for angiosperms (black circles), angiosperms with observed drought-related mortality (red circles), conifers (green downward triangles) and conifers with observed drought-related mortality (yellow upward triangles). The 1:1 relationship is shown as a dotted line. No groups were different from the angiosperm regression (solid black line).

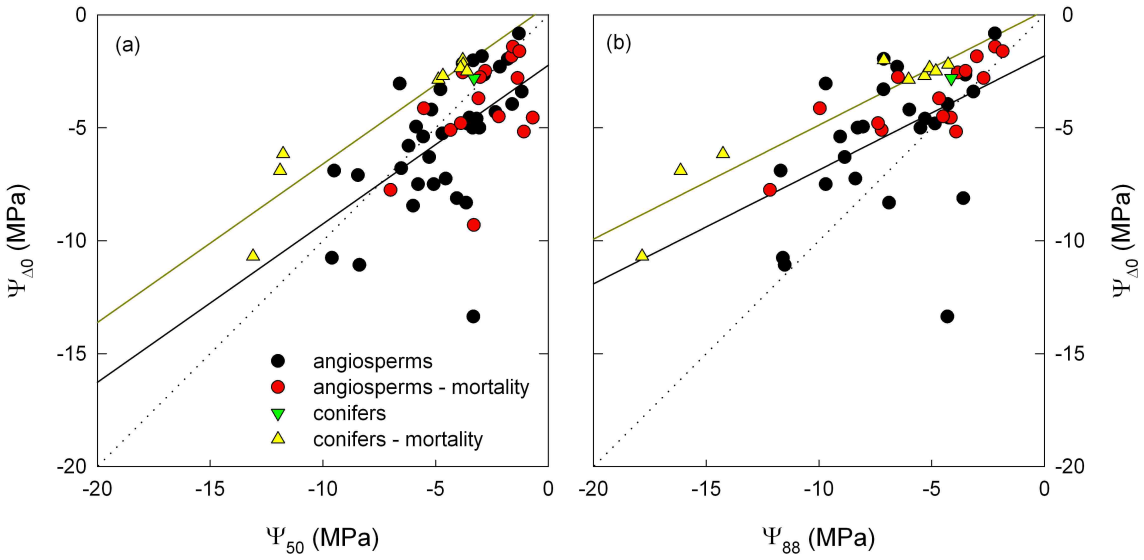

Figure 6. Relationship between $\Psi_{\Delta 0}$ and (a) Ψ_{50} and (b) Ψ_{88} for angiosperms (black circles), angiosperms with observed drought-related mortality (red circles), conifers (green downward triangles) and conifers with observed drought-related mortality (yellow upward triangles). The 1:1 relationship is shown as a dotted line. Regressions shown for angiosperms (solid black line) and conifers (solid dark yellow line) which were significantly different in (a) (P = 0.0009632) and (b) (P = 0.01467).

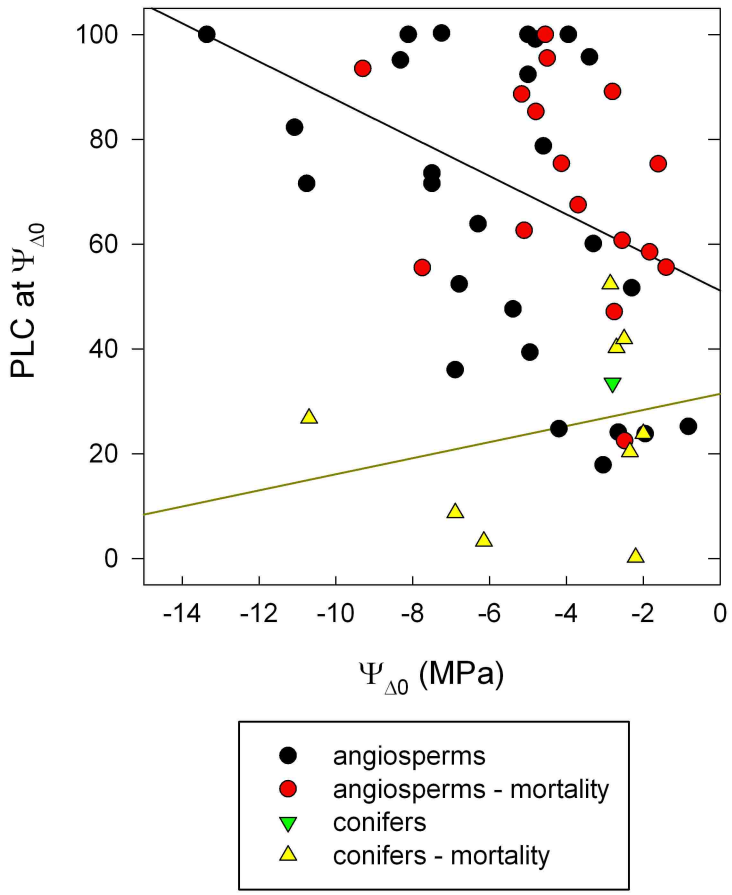

Figure 7. Relationship between $\Psi_{\Delta 0}$ and the estimated percent loss of conductance (PLC) at that Ψ_l for angiosperms (black circles), angiosperms with observed drought-related mortality (red circles), conifers (green downward triangles) and conifers with observed drought-related mortality (yellow upward triangles). Regressions shown for angiosperms (solid black line) and conifers (solid dark yellow line), which were significantly different (P = 7.14E-6).

Chapter 5

Conclusion

Global anthropogenic climate change, documented drought-related mortality, and the current inability to model such mortality all necessitate a better understanding of the processes and plant physiological characteristics that lead to mortality during drought. This dissertation addresses the hydraulic limits of trees prior to mortality (Chapter 2), the physiological function of trees experiencing prolonged drought (Chapter 3), and, more broadly, how strategies of Ψ_l regulation in conifers and angiosperms may contribute to risk of drought-related mortality (Chapter 4).

In Chapter 2 I applied the hydraulic model of Sperry *et al.* (1998) to a rainfall manipulation experiment in a piñon-juniper woodland in central New Mexico, USA. Neither piñon nor juniper exceeded their modeled hydraulic limits, but piñon that died experienced both chronically low hydraulic conductance and a seven-month period of near-zero gas exchange. It appears that a key effect of the drought treatment was to prevent recovery of hydraulic conductance following a very dry summer. Hydraulic conductance was also lower in droughted juniper, but not to the same extent and without resulting in mortality. It also highlights the confounding role of pests and pathogens in intact biological systems, since the piñon mortality documented in this chapter occurred concomitant with a bark beetle and *Ophiostoma* fungi outbreak (Gaylord *et al.* 2013).

In Chapter 3 I used mixed effect models to isolate the effects of prolonged drought from the effects of immediate conditions on piñon and juniper response to pulses of precipitation. I showed that prolonged drought reduces the ability of both species to

respond to precipitation pulses even after differences in soil moisture and pulse size between the drought and other treatments were taken into account. I hypothesized that chronic loss of conductance, modeled in Chapter 2 and measured by other members of our lab group, underlie this pattern of reduced sapflow and transpiration in the drought treatment. Structural shifts over the five-year period of study, such as reduced leaf area to sapwood/root area, may also be a factor, though they were not measured. One consequence of these changes is that trees under severe prolonged drought are unable to fully capitalize on soil moisture pulses to repair cavitated xylem or fix carbon for use during future drought. In a future characterized by more frequent or intense drought, these trees might be more likely to enter a downward spiral towards mortality, where even if pests did not materialize to kill them, they would be increasingly unable to recover from progressive loss of conductance and depletion of carbon reserves.

In Chapter 4 I used leaf water potential datasets collected for over one hundred species to assess how leaf water potential (Ψ_l) regulation strategies may predispose woody species to drought-related mortality. In agreement with other published studies (Choat *et al.* 2012, Manzoni *et al.* 2013), conifers maintained larger safety margins between minimum Ψ_l and the branch/stem water potential causing 50% loss of hydraulic conductance (Ψ_{50}) relative to angiosperms. The Ψ_l at which stomatal closure is predicted to occur is also more conservative relative to branch cavitation vulnerability in conifers than in angiosperms. Interestingly, the majority of conifers included in the dataset have been reported to experience drought-related mortality. These results suggest that while stomatal conductance in conifers is broadly protective of hydraulic integrity, this strategy confers a risk of non-hydraulic mechanisms of mortality, e.g. carbon starvation and

susceptibility to pests. What is not known currently is how the predicted Ψ_l of stomatal closure relates to Ψ_{crit} (as defined by Sperry *et al.* 1998), i.e. the minimum sustainable water potential of the most vulnerable segment of the soil-plant-atmosphere continuum. For conifers, the most vulnerable segment may be the needles/leaves (Johnson *et al.* 2012), in which case the Ψ_{50} commonly published for branches would overestimate the resistance of the entire pathway. Angiosperms appeared overall more tolerant of xylem cavitation, but there was no significant association between greater estimated loss of conductance and drought-related mortality. The lack of a clear link between loss of hydraulic conductance and mortality raises questions about the importance of the temporal aspects of drought stress, cavitation, refilling, and carbon dynamics.

Together, these chapters support the body of work showing that trees largely act to preserve the conducting ability of their vasculature via stomatal regulation of tissue water potentials. Thus, the limitation imposed by xylem cavitation vulnerability is intimately linked to the ability of trees to maintain positive carbon balance. Conifers appear more conservative in this regard than angiosperms, but might not appear so if their most vulnerable tissues were included in the analysis. The piñon-juniper woodland chapters demonstrate the importance of trophic interactions and cavitation-resistant xylem, but also the inevitability of mortality under certain climate conditions. Piñon is more vulnerable than juniper to cavitation, and is susceptible to several lethal insect and fungal pathogens. Ultimately, however, the observed juniper mortality shows that precipitation patterns too far outside the envelope of ambient conditions will cause mortality even in highly cavitation-resistant species.

References

Choat B, Jansen S, Brodribb TJ, Cochard H, Delzon S, Bhaskar R, Bucci SJ, Field TS, Gleason SM, Hacke UG, *et al.* 2012. Global convergence in the vulnerability of forests to drought. *Nature* doi:10.1038/nature11688

Gaylord ML, Kolb TE, Pockman WT, Plaut JA, Yepez EA, Macalady AK, Pangle RE, McDowell NG. 2013. Drought predisposes piñon–juniper woodlands to insect attacks and mortality. *New Phytologist*, doi: 10.1111/nph.12174

Johnson DM, McCulloh KA, Woodruff DR, Meinzer FC. 2011. Hydraulic safety margins and embolism reversal in stems and leaves: Why are conifers and angiosperms so different? *Plant Science* **195**: 48-53.

Manzoni S, Vico G, Katul G, Palmroth S, Jackson RB, Porporato A. 2013. Hydraulic limits on maximum plant transpiration and the emergence of the safety-efficiency trade-off. *New Phytologist* **198**: 169-178.

Sperry JS, Adler FR, Campbell GS, Comstock JP. 1998. Limitation of plant water use by rhizosphere and xylem conductance: results from a model. *Plant, Cell and Environment* **21**: 347– 359.

Appendix A

Supporting Information - A supplementary file, available via the LoboVault repository (http://repository.unm.edu/), provides the dataset used in Chapter 4. The following data are included in the table; a second worksheet within the file includes the complete references.

Column title	*Definition*
Species	Species
authority	authority
code	Within-dataset species code
Iso/Anisohydric	Classification in the literature, if any
Family	Family
Porosity	D = diffuse-porous, I – intermediate, R = ring-porous, T = tracheid-bearing, U = unknown
Angiosperm/Gymnosperm	A = Angiosperm, G = Gymnosperm
mortality	Y = reported mortality due to drought, N = no reports of drought-related mortality found
slope of Ψ_{md}:Ψ_{pd}	Slope of linear regression of Ψ_{md} on Ψ_{pd}, as in Fig. 1a
Ψ_{pd}_max	Maximum observed Ψ_{pd}
Ψ_{pd}_min	Minimum observed Ψ_{pd}
Ψ_{md}_min	Minimum observed Ψ_{md}; also Ψ_{min}
x-intercept ($\Psi\Delta0$)	$\Psi_{\Delta0}$ calculated from linear regression
max_linear_r2	The greater of the r^2 values from the Ψ_{md}:Ψ_{pd} and $\Delta\Psi$:Ψ_{pd} regressions
max_r2	Maximum r^2 for linear and non-linear regressions
Fig34	Species was used only in Figure 3 & 4
Fig567	Species was used in Figures 3-7
$\Psi_{\Delta0}$	$\Psi_{\Delta0}$ that was used in analysis (either from linear or non-linear regression)
branch PLC at $\Psi_{\Delta0}$ (max)	branch percent loss of conductance (PLC) at $\Psi_{\Delta0}$, estimated from most vulnerable curve
branch PLC at $\Psi_{\Delta0}$ (min)	branch percent loss of conductance (PLC) at $\Psi_{\Delta0}$, estimated from least vulnerable curve
P50min	Minimum branch Ψ_{50}
P50max	Maximum branch Ψ_{50}
P88min	Minimum branch Ψ_{88}
P88max	Maximum branch Ψ_{88}
Ψ_{leaf} citation	Source(s) for Ψ_l data
vulnerability curve citation	Source(s) for vulnerability curves
mortality citation	Source(s) for drought-related mortality observations